2000-05-08

Analysis of the Two Isoforms of the Human Alkyl Adenine DNA Glycosylase (HAAG) Gene: A Comparative Study of its Isoforms, its Protein and its Resistance to DNA Damage Agents

Kenneth C. Bonanno
Worcester Polytechnic Institute

Registration # BBT-DSA-2532

ANALYSIS OF THE TWO ISOFORMS OF THE HUMAN ALKYL ADENINE DNA GLYCOSYLASE (HAAG) GENE: A COMPARATIVE STUDY OF ITS ISOFORMS, ITS PROTEIN AND ITS RESISTANCE TO DNA DAMAGE DRUGS

A Masters Thesis

submitted to the Faculty of

WORCESTER POLYTECHNIC INSTITUTE

in partial fulfillment of the requirements for the

Degree of Master of Science

in Biotechnology

by

Kenneth C. Bonanno
May, 2000

APPROVED:

Michael Volkert, PhD.
University of Massachusetts Medical Center
Major Advisor

David S. Adams, PhD.
WPI Project Advisor

Daniel Gibson III, PhD.
WPI Project Co-Advisor

Ronald Cheetham, PhD.
Biology and Biotechnology Dept. Head

ABSTRACT

This study was conducted at the University of Massachusetts Medical Center in the Volkert laboratory. Human alkyl adenine DNA glycosylase (hAAG) is a DNA repair enzyme that repairs alkylated DNA bases. hAAG was cloned in 1991 and a second isoform was classified in 1994. The difference between the two isoforms of hAAG is an alternate spliced first exon.

Both isoforms of the hAAG gene were present in the Volkert laboratory collection, however the second isoform (hAAG-2) was phenotypically different than the first and became the first focus of this study. Using the improperly functioning isoform as a template, and constructing a 5' primer with the identical upstream sequence as the functioning isoform (hAAG-1), a phenotypically similar gene was constructed by PCR. The new isoform (hAAG-2) was cloned into an expression vector and its activity as a DNA repair agent was studied. A second version of hAAG-2 was also constructed, incorporating a histidine tag for protein purification and identification purposes.

Efforts included using the ability of hAAG to complement glycosylase deficient *alk*A *tag*A *E. coli* double mutant strains to assess and to compare the ability of the two isoforms of hAAG and to determine if the histidine tag affected function. The ability of hAAG to rescue cells from exposure to a variety of DNA damaging agents was studied by inducing each isoform and analyzing the sensitivity of the cells to increased doses of DNA damaging agents. Both hAAG-1 and hAAG-2 were able to restore the wild type resistance of the *alk*A and *tag* genes when exposed to the alkylating agents MNNG and MMS.

In order to study the ability of hAAG to repair alkyl lesions larger than methyl groups, it was necessary to inactivate the *uvr*A dependent nucleotide excision repair gene. In *E. coli,* methyl lesions are repaired primarily by glycosylases, while nucleotide excision repairs bulky lesions. Thus, in order to detect hAAG activity on these types of damage, it was necessary to inactivate the bacterial *uvr*A gene. Each isoform of hAAG was transformed into a triple mutant strain deficient in *alk*A *tag*A and *uvr*A, then exposed to CNU, BCNU, and Mitomycin C. Each of these DNA damaging agent caused increased toxicity in the presence of hAAG. hAAG-1 expressed in the *alk*A *tag* double mutant strain was exposed to Mitomycin C and showed greater resistance than hAAG-1 expressed in the *alk*A *tag uvr*A triple mutant. In fact, in the nucleotide excision proficient strain, expression increased Mitomycin C resistance above that seen in the control, suggesting that glycosylase activity may function in a partnership with nucleotide excision repair and that the two isoforms of hAAG have subtle differences.

An *omp*T protease knockout host strain was constructed using P1-transduction and used to examine protein products. hAAG-2 was inserted into the pBlueScript plasmid so that the gene could be regulated by the T7 promoter for use beyond the scope of this thesis. A protein synthesis time course assay was conducted to determine the expression levels of hAAG-1 and hAAG-2 when induced by IPTG. Immunoblot detection of the histidine tag was used to measure expression levels of each isoform.

ACKNOWLEDGMENTS

I cannot believe I am able to type this page. Barely one year ago, I began to finalize my MQP and thought that that was the most scientific document I would be able to write. Today, I look at that report as a learning process to create this thesis. In order for me to have come so far in such a short amount of time, I needed some guidance, direction, and friendships along the way. My time at WPI and in the Volkert laboratory at U Mass Medical Center provided me all three. To these people, I owe my sincere gratitude.

First, I would like to thank Dr. Volkert for his excitement, leadership, persistence, and motivation to drive me towards the completion of this study. At times when this project may have gone in any direction, Dr. Volkert was there to provide advice and guidance to help steer this project in the correct direction. When I was in need of encouragement, Mike became my cheerleader. For these reasons and more, thank you.

Dr. Adams continued to assist me at WPI, whether it be with my classes, logistics, or in an effort to improve my project. Your availability and enthusiasm were greatly appreciated. Dr. Gibson had proved to be a great addition as the third member of my committee. Thank you for your availability and interest in my study.

Dr. Ludlum deserves my thanks for initially providing me an avenue at U Mass Medical Center to perform my undergraduate thesis work and for introducing me to Dr. Volkert.

Dr. Matijasevic assisted me both directly and indirectly with this study. As a member of the Ludlum team, Zdenka researches a different story to that of this study. However, her expertise with science not only helped me to devise some feasible protocols, but allowed me to learn to develop scientific conversation. I was able to take a great amount of Zdenka's time to discuss the progress of this study and to attempt to reach conclusions based on the results. Zdenka also did a great job critiquing and editting this very draft. She was the final link in helping me become both confident and comfortable in all of the aspects of my study. For these intangible reasons and for the loan of chemicals and supplies, I thank you.

I would like to thank the members of the Volkert lab—Nate, Jennifer, Jen-Yeu, Dadbeh, Anne, and Lin—for putting up with me in lab and for making time spent in lab with them enjoyable. I trouble-shot many experiments with Nate and also sought his advice on many of the theories behind the applications I used. Scientific topics or just daily conversation with Nate were both insightful and entertaining. Jen-Yeu joined the lab at an ideal time, as his background in protein applications, other biological techniques were exploited at the conclusion of this study. His overall personality also provided some laughter and educational insight.

Jennifer and Dadbeh were with me throughout the entire year and deserve thanks simply for putting up with me on a daily basis. My individual conversations with each of them were very enjoyable as the year progressed, and for their friendships I thank them. Anne and Lin were newcomers to the Volkert lab, however both have worked elsewhere in the department. I would like to thank them for their day-to-day support and conversation. Special thanks must be given to the Yellow Guy with Knunchucks, for providing an ongoing topic of conversation throughout lab.

The members of the Leong lab helped me throughout the past few years with their knowledge, their equipment, and their friendships. Special consideration must be given to Nikhat, Ken, Padhma, Doug, Lorranne, Tom, and especially Kishore.

Dr. Joanne Whitefleet –Smith deserves thanks for allowing me to assist her in her lab modules during the academic year. I was able to learn a great amount from Joanne and was happy that she was accommodating to my hectic schedule. For all that you taught me, both directly and indirectly, about TAing a lab module, thank you.

I would like to thank my Mom and Dad for their love and encouragement throughout the past year. Their willingness to listen to me talk about the status of my project, even though we all knew that they had no clue about what I was talking about, was very rewarding to me. Not only did it show that they both cared greatly about my success, but it also allowed me to try to discuss the aspects of this study to those without a biological background. My parents deserve all my gratitude in the world for many reasons, but especially for their assistance in motivating me to achieve my academic goals.

I would like to thank the rest of my family, including my sister Jill, my Nana, Grandma and Grandpa, and all my other Aunts, Uncles, and cousins who constantly inquired about the status of my project and showed overall concern about my progress.

Stacy also deserves a great amount of gratitude. Not only did you listen to my frustrations along the way, but you served as my audience for my practice presentations and provided me encouragement and motivation to settle for nothing less than the best.

I would like to thank Peytra for making me a plethora of LB Amp[100] "#52" plates for use during the data collection period of this project. Her assistance allowed me to expediate many of the experiments conducted in this study.

To other professors and collegues who have asssisted me during the year, especially Dr. Julia Kruskal, thank you for your ongoing support.

Finally, to my friends, especially Chris, Brian, and Dan; the brothers of Lambda Chi Alpha, especially Craig, James, Stew, Jesse, Chad, Carl, Justin, Pag, Shane, Karl and Matt; and the Squires of St. Raphael's K of C, thank you for adding to the enjoyment of the past year, and for providing resources to allow me to take breaks from my studies.

Table of Contents

Table of Figures

Table of Tables

INTRODUCTION

The Importance of Deoxyribose Nucleic Acid

One of the most extensively studied materials of biology during the past half-century, deoxyribose nucleic acid, DNA, is an essential component within the cell. With the exception of some viruses, DNA is the genetic material or "blueprint" of all cells and organisms. Genes encoded from the DNA of bacteria and eukaryotic cells ranging from a simple yeast cell to complex mammalian cells command many of the cellular functions and activities.

The central dogma of molecular biology is a model that describes the transcription and replication of DNA. It is replicated in a semi conservative manner or transcribed into RNA, ribose nucleic acid, which is used in the creation of protein (Figure 1). Without a specific protein, a cell may lose some specific function(s). Therefore, the accuracy of this transcription process is vital for cell function. The correct transcription of DNA to RNA must occur so that the RNA can either undergo translation into protein (mRNA) or assist in the production of proteins (rRNA, tRNA).

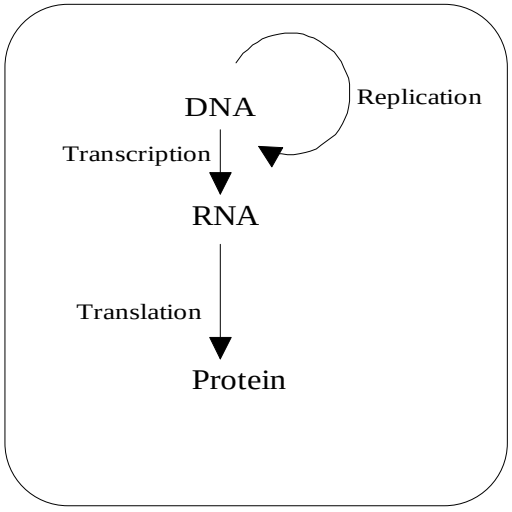

Figure 1: Model of the Central Dogma of Molecular Biology. DNA is either replicated in a semiconservative manner or transcribed into RNA, which is then further translated into protein.

The structure of DNA consists of a ring sugar connected to a nucleoside base at its C1' and a phosphate at its C3' and C5' (Figure 2). There are four nucleoside bases in DNA: adenine, thymine, cytosine, and guanine. These bases are further categorized into two groups, the purines and pyrimidines.

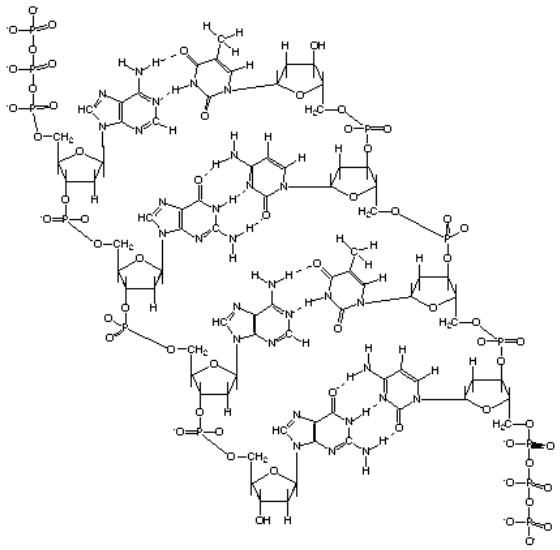

Figure 2: The Structure of DNA. Note the location of the base and that the phosophdiester bonds are created to join nucleotides together at the 5' and 3' carbon of the deoxyribose. Adapted from the URL: http://esg-www.mit.edu:8001/esgbio/lm/nucleicacids/dna.html

The purines consist of adenine and guanine and the pyrimidines contain cytosine and thymine. Adenine binds to thymine and guanine binds to cytosine (Figure 3).

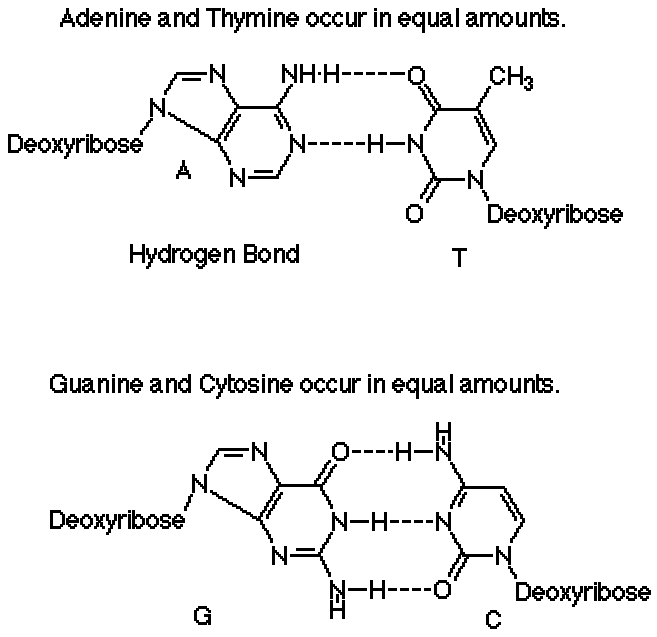

Figure 3: The two bases classifications and their binding partners. The pyrimidines are located on the left of this figure and the purines on the right. Please note that there is a third pyrimidine, Uracil, but it is not shown because it is only present in RNA, not DNA. Adapted from the URL: http://www.chem.wsu.edu/Chem102/102-DNAStruct.html

Damage to DNA

"DNA damage causes a temporary arrest of cell-cycle progression" (Krokan et al, 1997), and DNA repair is essential before replication so that the correct DNA sequences are synthesized. For this reason, DNA repair mechanisms are highly conserved throughout evolution. DNA is susceptible to various types of damages that alter the sequence of the genetic code. These damages occur either spontaneously or may be induced by external environmental factors (Friedberg et al, 1995). This section will describe these two classes of DNA damge.

Spontaneous DNA Damage

Spontaneous DNA damage occurs when the genetic sequence of DNA becomes altered due to either the activity or failure of a cellular mechanism. Such spontaneous damage or mutation to DNA includes the mispairing of bases in DNA synthesis and chemical alterations of the nucleoside base structures. Mismatched bases are very

common in the replication of DNA, thus DNA polymerase scrutinizes the dNTP's as they are inserted along a replicating strand of DNA (see below). In addition, DNA polymerases have proofreading tools that remove and replace improperly paired bases (Kunkel, 1992). Other mismatch errors include frameshift mutations. A frameshift mutation occurs when the sequence of DNA is altered due to template misalignment, thus altering the triplet amino acid sequence code from being replicated as intended. In addition to the proofreading activity of polymerase, a second mismatch correction system scans newly synthesized DNA for frameshift and mismatch errors. The mismatch DNA repair system provides additional support to protect the fidelity of newly synthesized DNA. In those instances where proofreading and mismatch repair fail, mutations arise. These types of mutations include missense mutations, in which an incorrect amino acid is translated; deletions and insertions due to slippage or dislocation; and miscoding followed by realignment (Kunkel, 1992, Figure 4).

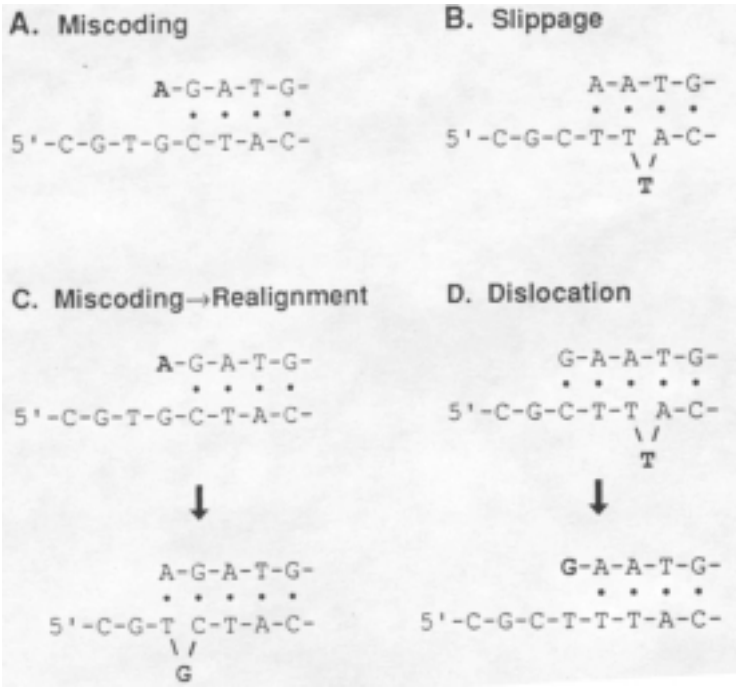

Figure 4: Mutational intermediates for substitution and frameshift errors. Adapted from Kunkel, 1992.

Other types of spontaneous mutations occur by altering the chemistry of the DNA bases. Sometimes, an isomer of a nucleoside base may arrange itself so that it does not bond to its traditional Watson-Crick partner. These spontaneous mutations are named

tautomeric shifts. Deamination is the conversion of an amino group to a double bonded oxygen [oxide] ($-NH_2 \rightarrow =O$). Adenine or guanine may undergo a deamination of their exocyclic amino group, converting them to purine analogs. Cytosine may also undergo deamination, which converts it to a uracil nucleoside. Errors in replication, recombination, and repair processes may also lead to spontaneous DNA damage (Friedberg et al, 1995). There are several other functions that lead to spontaneous mutations including transposon activity, translocations, transitions, inversions, and duplication of genetic material (Lewin, 1997). An additional source of mutation results from spontaneous chemical modification of DNA bases and nucleotides. The most common form of spontaneous damage leading to mutation occurs when an oxygen radical creates an oxidation product by damaging a nucleoside. The most frequent oxidation product is 8-oxo-guanine, or GO.

These examples of spontaneous mutations provide a source of internal DNA damage. This type of damage occurs naturally, without the influence of environmental factors. There is a second category of DNA damage, however, which is influenced by environmental toxins.

Environmental DNA Damage

Environmental damage occurs when physical and chemical environmental factors interact with DNA. The physical agents that damage DNA include both ionizing and ultraviolet radiation. Ionizing radiation affects the bases and sugar–phosphate backbone of DNA. Often, a free radical (-OH) attacks a base and creates a lethal or mutagenic lesion. The N-glycosylic bond, the bond that connects the base to the deoxyribose, also suffers destabilization from ionizing radiation. Nicks can also form in the DNA backbone (Friedberg et al, 1995). The base, the glycosylic bond, and the sugar-phosphate backbone of the DNA molecule are left vulnerable to ionizing agents, thus providing evidence that ionizing radiation strongly attacks all components of DNA.

Ultraviolet radiation is also a physical environmental toxin. Exposure to this wavelength spectrum of light (400 to 100 nm) creates dimerization of pyrimidines due to the formation of bonds between adjacent pyrimidines (Friedberg et al, 1995). This bond formation varies among the wavelength intensities. Cyclobutane pyrimidine dimers, for

example, form additional bonds by saturating the 5,6 double bonds of each nucleoside whereas the pyrimidine-pyrimidone photoproduct forms a new bond between the 6,4 postions of adjacent pyrimidines (Friedberg et al, 1995).

In addition to these two physical environmental avenues of DNA damage, there are many chemicals that damage DNA. Some of these chemicals can be classified into groups such as Psoralens, Alkylating Agents, and Cross-Linking Agents. Psoralens, a crosslinking agent that forms covalent adducts to thymine and cytosine in the presence of UV light, intercalates into the DNA (Friedberg et al, 1995). The function of the latter two chemical categories will be described in more detail in the section below discussing the drugs used in this study.

DNA Excision Repair Pathways

The most relevant DNA repair to this study consists of the excision repair processes. These repair mechanisms include nucleotide excision repair (NER) and base excision repair (BER). Since hAAG is a base excision repair enzyme, this process will be explained in greater detail than nucleotide excision repair.

The Nucleotide Excision Repair System

Nucleotide excision repair consists of excising a series of bases surrounding a bulky lesion such as a pyrimidine dimer resulting in removal of an oligonucleotide surrounding and including the lesion. The uvrABC complex completes this process with the help of the UvrD helicase, DNA polymerase, and DNA ligase. The *uvrA+* and *uvrB+* genes of the NER process are susceptible to regulation by the LexA protein (Friedberg et al, 1995). The LexA protein also controls the SOS Response system, so it has been suggested that increased damage induces *uvrA* and *uvrB* to increase their levels of production.

In the excision process, UvrA dimerizes and binds to UvrB. Once this complex forms, it patrols the DNA searching for irregularities and bulky adducts. Once an error is found, the UvrAB complex binds to the DNA in need of repair. The DNA gets kinked, UvrA recruits UvrC, and subsequently gets released so that UvrC may bind. The UvrBC complex on the DNA creates nicks approximately 12 base pairs apart from each other.

UvrD, an enzyme with helicase activity, releases the damaged fragment and UvrC, however UvrB remains bound to the gapped DNA and is released only when the DNA polymerase I enzyme is ready to resynthesize the missing fragment. Finally, DNA ligase joins the fragment to the rest of the strand (Figure 5, Friedberg et al, 1995).

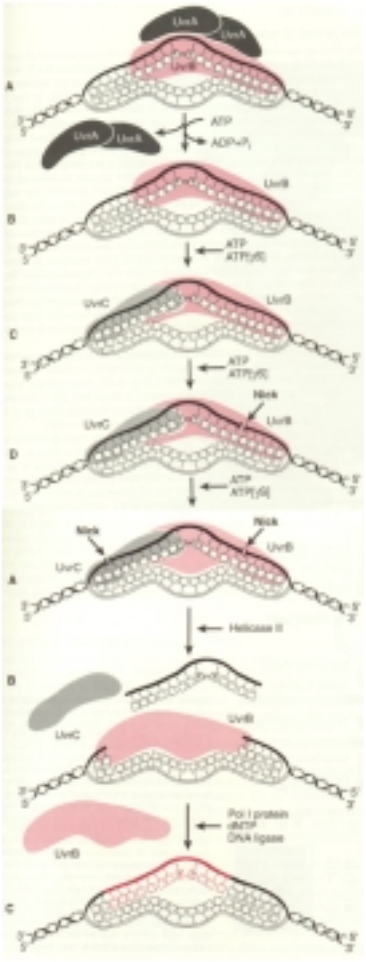

Figure 5: Mechanism of action of the UvrABC complex in NER.
Adapted from Friedberg et al, 1995.

This process is both fundamental and important to this study. Survival Assays were conducted in a *uvrA*- background. These strains were not able to conduct NER because without *uvrA*, the UvrAB complex cannot be formed, thus UvrB would not be able to bind to the DNA. Therefore, it is important to understand the significance of the presence of the *uvrA*+ gene.

The uvrA protein is recruited by other proteins to sites of damage. One such protein, called transcription repair coupling factor (TRCF) recruits UvrA. This process,

named transcription coupled repair, involves the RNA polymerase enzyme pausing at a pyrimidine dimer adduct (Figure 6). TRCF binds to a paused RNA polymerase, removes it and its mRNA from the site of DNA damage. At this point it recruits UvrA, which dimerizes and forms its complex with UvrB. UvrB binds to the DNA and continues the repair process above. UvrA is removed along with the TRCF (Selby and Sancar, 1993; Friedberg et al, 1995).

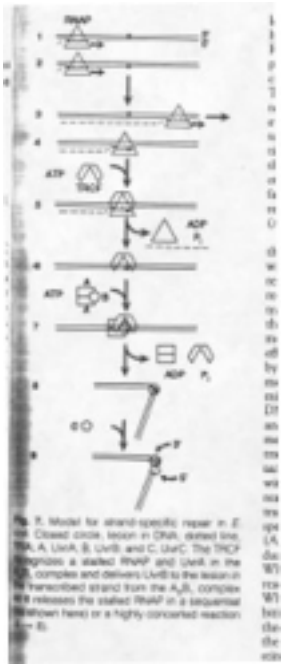

Figure 6: Model for recruitment of UvrA by TRCF at a pyrimidine dimer adduct. Adapted from Selby and Sancar, 1993.

Base Excision Repair

The base excision repair pathway is a biochemical method for correcting a single erronous base. The activity of this process hinges on the ability of a glycosylase such as hAAG to catalyze the first reaction initiating this pathway. BER is a DNA repair mechanism that uses a glycosylase such as hAAG to remove a damaged base from DNA (Krokan et al., 1997; Wilson III and Thompson, 1997; Singer and Hang, 1997). Once hAAG performs its task, other enzymes of the base excision repair pathway are able to perform their function.

There are several different classes of glycosylases; only three systems will be considered in this review: the Alkyl Adenine DNA Glycosylases, Uracil- DNA Glycosylase, and the Mut M, Mut T, Mut Y Glycosylases. However, prior to specific discussion of each glycosylase, the discovery of glycosylase activity can be attributed to Dr. Thomas Lindahl in 1976.

The Discovery of Glycosylase Activity

A glycosylase is very specific in nature and is an enzyme that carries out the first step in the base excision repair process. It recognizes one or more particular kinds of damaged bases and then cleaves the glycosylic bond that attaches the base to the phosphate sugar backbone (Volkert, 1988). The activity of glycosylases were first analyzed and studied by Thomas Lindahl in 1976 (Lindahl, 1976). He describes a new class of repair enzymes that remove and replace damaged nucleotides in nonreplicating DNA strands. This study indicated that the hydrolysis of N-glycosidic bonds of damaged nucleotides occurred rather than cleavage of the phosphodiester bonds as in other repair pathways. He also distinguished and isolated the functions of three separate enzymes – Ura-DNA Glycosidase, 3-MeAde-DNA Glycosidase, and endonuclease II – by examining the inactivation of purified enzyme products (Lindahl, 1976). The glycosolase model proposed by this study (Figure 7) corresponds closely to that generally accepted today.

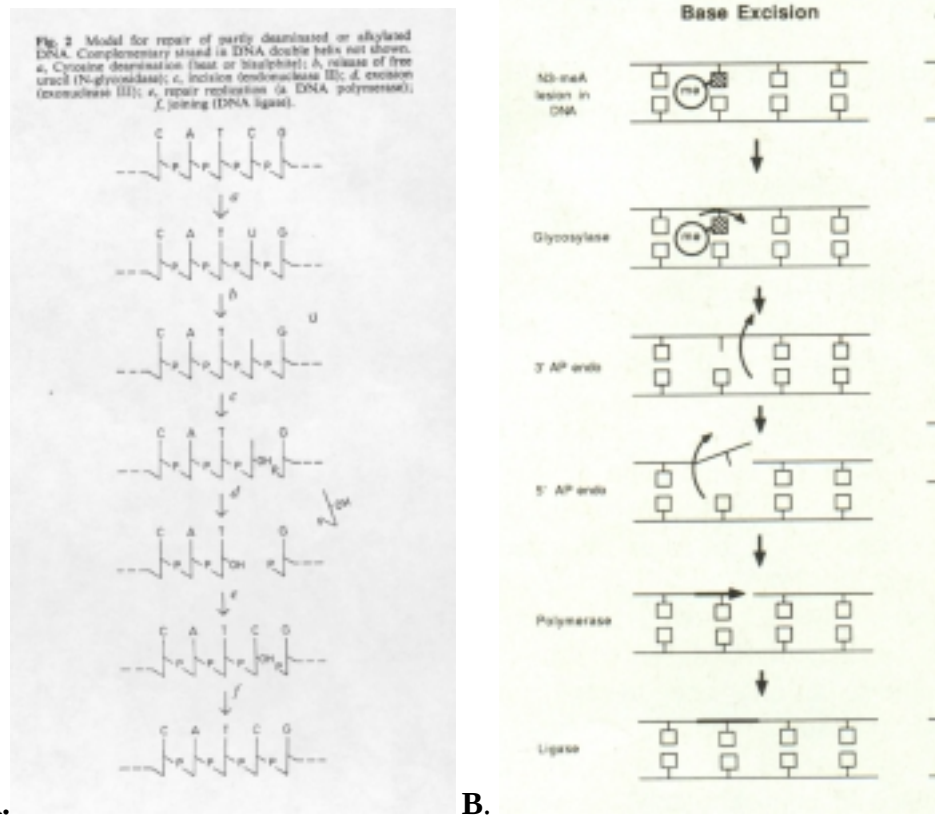

A. **B.**

Figure 7: A).Glycosylase model proposed by Lindahl in this landamark *Nature* paper. Reproduction of Lindahl, 1976. B). The modern model of glycosylase activity (Volkert collection).

The base excision repair mechanism consists of a cascade of enzymes each performing one single task. A summary of the pathway (figure 7b) involves the following:

A glycosylase cleaves the damaged or incorrect nucleoside at its glycosidic bond. This creates an abasic site. A 5'AP endonuclease excises the abasic site of DNA on the 5' side of the abasic site. A 3'AP lyase or deoxyribophosphodiesterase (dRpase) then cleaves the abasic site from the strand of DNA to prepare the site for synthesis by DNA polymerase I by setting up the correct orientation of 3'-OH and 5'dNTP. This is the step in which base excision repair received its name, as only a single base is excised in the repair process. To complete this pathway, DNA polymerase inserts the correct base and DNA ligase seals the nick.

The most relevant base excision repair enzyme to this study is the human alkyl adenine DNA glycosylase. Therefore, a brief history of its discovery, function, and structure must be examined in order to see its homology with its bacterial counterparts.

The human Alkyl Adenine DNA Glycosylase (hAAG) gene

The hAAG gene is one of the many DNA repair mechanisms in the human body. This gene is an important repair glycosylase that removes many base damages including 3MeA (3-methyl adenine), 3-methylguanine, 7-methylguanine, 1,N^6-ethenoadenine, hypoxanthine, cyclic etheno adducts of adenine and guanine, 8-oxoguanine, 8-oxo-7,8-dihydroguanine and various adducts of nitrogen mustards used in cancer chemotherapy (Wilson III and Thompson, 1997; Lau et. al, 1998).

The Samson laboratory cloned hAAG in 1991 and mapped the gene to chromosome 16 (Samson et al., 1991). This team isolated hAAG using an *E. coli alkA-tag-* mutant system similar to that which they used to clone the yeast homolog (MAG). They screened random cDNA clones versus control plasmids for MMS resistance. Those plasmids that showed resistance were digested with BamHII and then placed in human hamster hybrids to determine the chromosome location. The hybridization of hamster and human glycosylases varied substantially to allow differentiation (Samson, 1991). Human-mouse hybrids were used to confirm the findings of the human-hamster experiments linking hAAG to chromosome 16. Samson's protein had a calculated weight of 32.8 kDa and released 3-meA. This clone showed no homology to the 3-meA DNA glycosylases of bacteria or lower eukaryotes, however showed 85% homology to that of rat (Samson et al, 1991).

More laboratories became involved in the study of hAAG after the Samson cloning. Two years later, Vickers et al directly mapped the gene to the short arm of chromosome 16, confirming the Samson data (Figure 8).

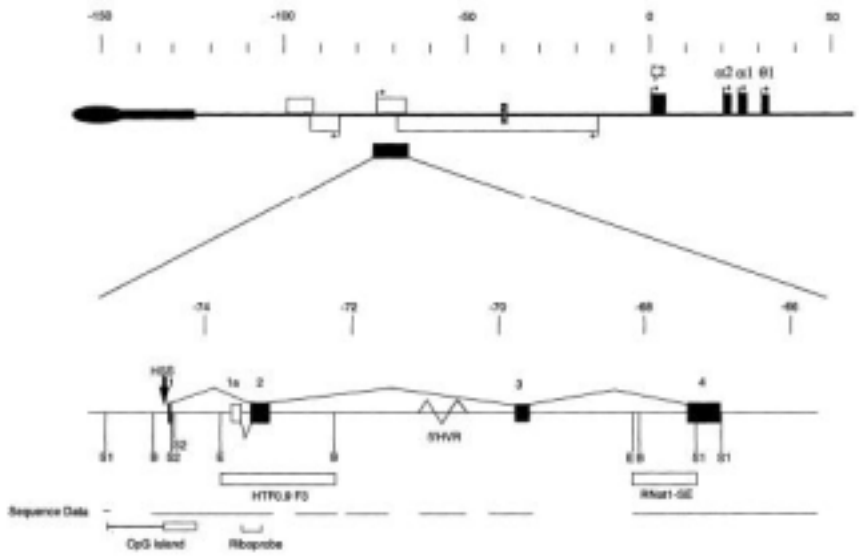

Figure 8: Short arm of Chromosome 16 mapped with hAAG shown in detail.

This team made a curious finding in that there was an alternative first exon to the one Samson cloned in their clone. They speculated that this could be due to use of alternative promoters. The mapping done in this study was very important to the future experiments of hAAG. First, it proved that the Samson sequence was valid, even though they obtained a different exon 1, they proved that the sequence of the Samson exon 1 was located in the genome as a part of an intron to their clone (Vickers et al, 1993). In addition, they prove that the point of divergence between the Samson exon 1 and their exon 1 was exactly at the boundary between exons 1 and 2 (Vickers et al, 1993). However, it was not until the work of Pendlebury et al that it was proven that the difference in the first exon was a result of alternative splicing (Pendlebury et al, 1994). This team used RT-PCR reactions to prove that both the alternative splice events occur simultaneously in all types of cells and tissue and that both forms of hAAG are produced in all cell types (Pendlebury et al, 1994). Therefore, each of these separate versions of the hAAG gene is a product of alternative splicing, or the process of a single gene giving rise to more than one mRNA product. Splicing is the process of removing the introns from the DNA strand and combining only the exons to make the mature RNA sequence. In creating the mRNA for the hAAG gene, one of two known routes can be taken. Changing the splice site can do many things to the gene such as vary the reading frame

(which in turn alters the protein) to introducing new termination codons. Thus, in many genes that are alternatively spliced, a part of an exon in one isoform of the gene can be a part of an intron in another isoform (see Voet and Voet, 1995). The hAAG gene has two known isoforms because of alternative splicing. Each isoform has four exons, however the first is different in each case. Currently, it is not clear why hAAG has an alternative splice mechanism, as each isoform is present in all cells at similar levels (Vickers et al, 1993, Pendlebury et al, 1994).

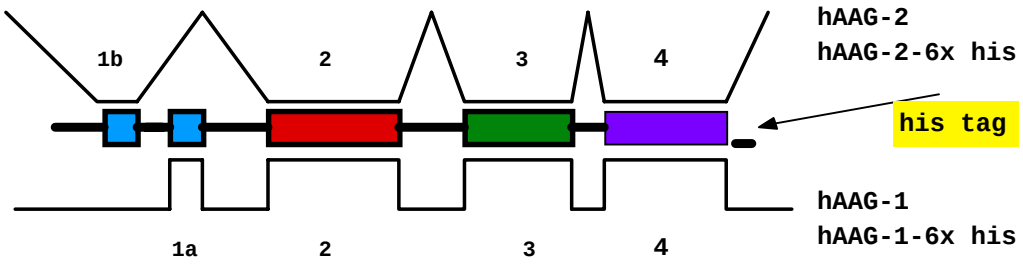

Figure 9: Representation of the alternative splice sites of hAAG

Dr. Ludlum's Research

Dr. David Ludlum, a chemist in the Pharmacology Department at the University of Massachusetts Medical Center, has dedicated his life to finding chemical methods to battle cancer cells. His career entailed two main areas of interest: the improvement of cancer chemotherapy and the understanding of chemical carcinogenesis. Dr. Ludlum provided the world of science with great insights on the functions of Nitrogen Mustards and other chemical agents involved in controlling the spread of cancer cells. However, the scope of this study entails chemical carcinogenesis. The hAAG gene is involved in DNA repair. Since Dr. Ludlum is interested in repair mechanisms that work on alkylated DNA, his lab has worked in cooperation with the Volkert lab over the past few years. Through a collaborative effort between the Volkert and Ludlum laboratories, the functions of the hAAG gene have been explored.

Dr. Volkert's Research

Dr. Volkert has long been interested in the molecular biology of *E.coli* and the regulation and the function of DNA repair genes in *E. coli*. More recently, however his lab has shifted towards human DNA repair and, as he coined, "damage avoidance" genes. Dr. Volkert's lab has been comparing bacterial repair genes and human repair genes in *E. coli*. He is also interested in human DNA repair genes that are active on oxidative damage.

Dr. Volkert has assisted Dr. Ludlum in his research by cloning the hAAG gene into a stable vector and by creating a his_6 tagged version of the gene to simplify purification of its product (Volkert, unpublished results). Dr. Volkert performed experiments involving the comparison between the wild type and his_6 tag form of the hAAG-1 gene and found that both hAAG-1 and its his tagged form complemented the *alk*A, *tag* mutant (MV2157) strain, restoring near wild type levels of alkylation resistance in a strain that lacks its own alkyl specific DNA glycosylases (Volkert, unpublished results). Therefore, similar testing was needed to compare the second isoform of hAAG to determine if this form of the gene behaves in a similar manner to its alternatively spliced gene product.

Structure of hAAG

hAAG is a single domain protein with 7 alpha helices and 8 beta- pleated sheets (Lau et. al, 1998). Figure 8 displays a crystallized representation of the AAG protein and its active site.

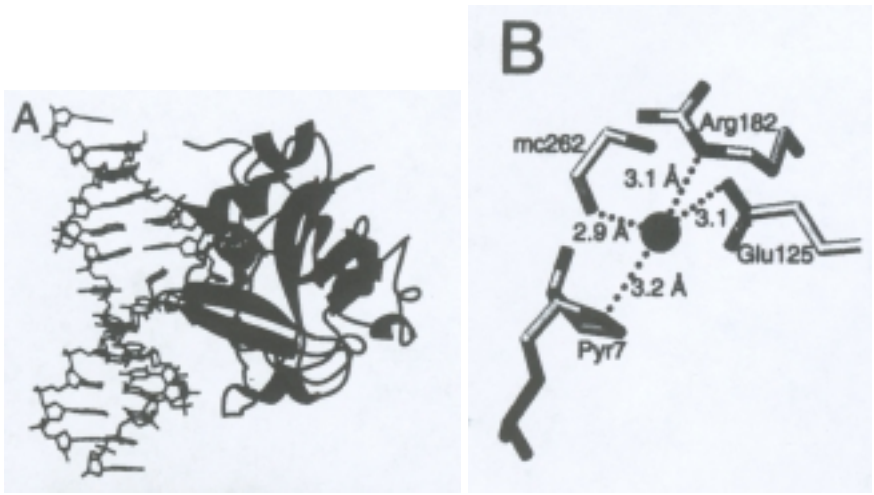

Figure 10: (A) The Crystal structure of the AAG complexed to DNA AAG binds in the minor groove of DNA and expels the pyrrolidine into the enzyme active site. (B) In the active site, water forms hydrogen bonds (dotted lines) with Glu-125, Arg-182, the main chain carbonyl of Val-262, and N4' of the pyrrolidine abasic nucleotide (Pyr7) (Lau et. al, 1998).

hAAG has been studied extensively in the past 8 years. In this time, a few knockout mice have been created to analyze the in vivo function of hAAG in a mammalian system. hAAG has great homology with many of its mammalian homologs, including the mouse and rat glycosylase (Engleward et al, 1993).

The Different Repair Mechanisms of Genetic Damage in *E. coli*

As discussed above, there are several situations in which DNA finds itself vulnerable to damage. Since DNA is the genetic material of an organism, it is vital that a working sequence is preserved. Therefore, a series of repair mechanisms have evolved to protect the fidelity of the DNA sequence. These repair systems are quite sophisticated in function. Similar systems are present in prokaryotic and eukaryotic cells; the bacterial repair systems have often served as models of study for their eukaryotic homologs.

There are two broad categories of DNA repair of damage and mutations. The first consists of rectifying the damage by reversal. In this system, the DNA damage is repaired at the site of the lesion. The second category of DNA repair consists of

removing a section of DNA from the heteroduplex strand. This category, named excision repair, involves a wide range of machinery to perform the repair process. An additional response to DNA damage is termed "tolerance of DNA damage" (Friedberg et al, 1995). This mechanism neither removes nor reverses the primary lesions or adducts, however allows cells "to tolerate" them. Recombination tools often respond to DNA damage in this manner. Unfortunately, permanent genomic mutations frequently arise because this mechanism does not fix the damage to the DNA.

In this section, the reversal of DNA damage will be explored in *E. coli,* followed by the tolerance of DNA damage.

The First Line of Defense: The DNA Polymerase Complexes

As described above, DNA replication machinery provides the first line of defense against DNA replication errors. The replication machinery consists of DNA polymerase enzymes with accessory proteins. The DNA polymerases are highly selective in their ability to insert nucleotides into the daughter strand of DNA, showing selectivity during both the dNTP binding and chemical steps (Kunkel, 1992). However, when an error does occur, the proofreading machinery, specifically the 3' → 5' exonuclease activity excises the newly inserted incorrect base.

Mismatch Repair: The MutH, MutL, MutS Repair System

Mismatch repair in *E. coli* relies on the methylation of a sequence in its own genome to detect mismatched base errors. The MutS protein detects any mismatches that slip through the DNA polymerase machinery or arise due to chemical alternations such as deamination events. A complex is formed with the assistance of MutL. This complex consists of a DNA loop forming in the opposite direction of the mismatch that MutS has bound. MutH then cleaves the complex at the GATC site, destroying the entire strand. DNA polymerase III must then begin synthesis of that strand again.

Since the potentially erroneous base lies in the newly synthesized strand, this system must be able to discriminate between parental and newly synthesized DNA. This occurs by the scanning for the placement of a methyl group on the adenine of GATC sequences. The importance of the GATC site relies on the activity of dam methylation.

The dam complex, called the dam methylase, follows downstream from polymerase I and methylates the adenine of the sequence GATC. The mismatch repair genes must function prior to the activity of the dam methylase in order to distinguish between the methylated parental and unmethylated daughter strands. Therefore, MutS scans the region of newly synthesized DNA between the DNA polymerase and the dam methylase for base errors due to mismatches. In order to determine which strand to cleave, the MutH protein examines the GATC sequence and cleaves the unmethylated strand. MutH then nicks the DNA strand with the unmethylated GATC site. The complex formed by the MutL protein breaks down and the daughter strand undergoes synthesis again (Figure 11). Once the dam methylase adds a methyl group to the adenine of the GATC site, this repair mechanism has no means to distinguish between parental and newly synthesized strand, thus potential mutations may occur to the genome if MutS does not function in the area between DNA polymerase and the dam methylase (Gilman, 1996).

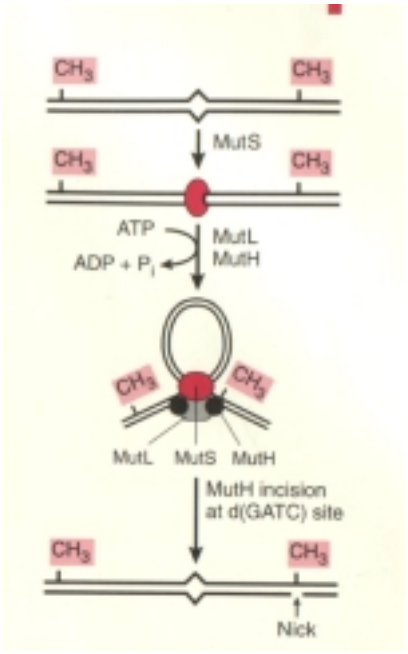

Figure 11: The Activity of the dam methylase and the MutH, MutL, MutS Proteins. Adapted from Friedberg et al, 1995.

Enzymatic Photoreactivation

Pyrimidine dimers form as a result of UV radiation. Neither DNA replication nor transcription can function properly in the presence of a pyrimidine dimer because the bulky adduct kinks the DNA in an abnormal manner and the dimerized bases fail to properly pair with their partners in the complementary strand. Photoreactivation (PR) is one DNA repair mechanism for such lesions. An enzyme called photolyase uses the energy of white light (300-500nm) to bind to pyrimidine dimers and break the bonds, thus restoring the DNA to its normal state (Friedberg et al, 1995).

DNA Repair Mechanisms Active on Alkyl Lesions

Considering that DNA is the genetic blueprint of all existence, it is left quite vulnerable to methylation by both internal and external toxins. Therefore, cells have evolved a series of mechanisms that protect against unwanted methylation. Alkylation damage is repaired via two main processes. One pathway is regulated by the adaptive response regulon. The other consists of constituitively expressed alkyl repair genes (Figure 12). The genes of each pathway display many overlapping features and some genes are active in both repair processes.

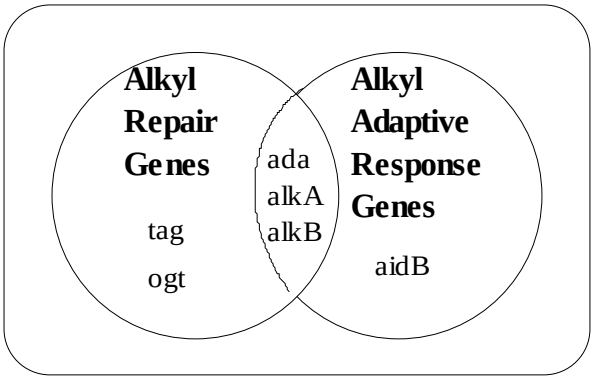

Figure 12: The two mechanism in which alkylation damage may be repaired. Note the overlapping functions of *ada*, *alkA*, and *alkB*.

The alkylation of DNA is both helpful and harmful to survival. As stated in the section above, the addition of a methyl group to a GATC sequence assists the DNA to distinguish itself as the true genomic code. However, while these types of methylation assist the fidelity of DNA replication, there are several different methyl damages that occur to DNA as well. These damages usually occur at specific sites on the bases, but

also may occur to the oxygen double bonded to the phosphodiester backbone. A few places in which the DNA undergoes unwanted alkylation include the O6 of guanine, O4 of thymine, 3rd and 7th positions of guanine , and the 3rd position of adenine. Many of these lesions may become lethal if left untreated.

The system that the *E.coli* has devised is very efficient at repairing the methyl lesions that are lethal to DNA. This sytem involves the use of the genes within the adaptive response scheme and other alkylation repair genes such as *ogt* and *tag*. The sections below detail the processes in which methyl damage is removed from DNA.

The Adaptive Response System

The function of the Ada protein, which senses alkylation damage in cells, is two-fold: it controls the processes of the adaptive response system and directly repairs specific DNA lesions. Thus, it is the controller of the adaptive response system, which is a regulon that includes the *ada* gene itself, *aid*B, *alkB*, and *alkA* genes (Lindahl, 1988). The adaptive response system repairs alkylation damage to DNA replication. When Ada senses that there is a need for additional repair processes or excessive lesions are created, it activates the transcription of itself and the other three genes of its regulon (Figure 13, Friedberg et al, 1995, Lindahl 1998). Thus, the Ada protein has a much larger role in the *E. coli* than just the repair of some alkylated lesions.

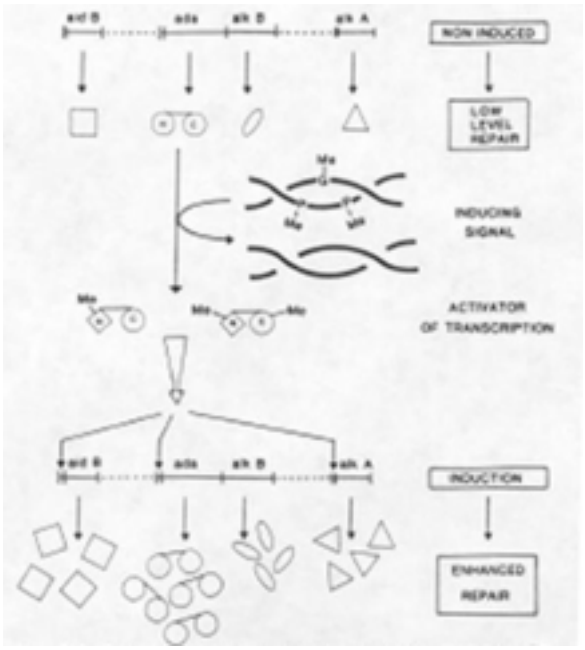

Figure 13: The Adaptive Response Regulon controlled by Ada. Adapted from Lindahl, 1988.

DNA Alkyltransferases: the Repair of O^6-Guanine and O^4- Thymine Alkylations and Phosphotriesters in DNA

In *E.* coli, two genes encode proteins that function together in the process of removing O–alkylation lesions to guanine and thymine—Ada and Ogt. These proteins repair O—alkylation lesions to guanine and thymine, thus preventing the mutant bases from pairing with the incorrect base in replication. O^6—methyl guanine pairs with thymine if not corrected and O^4—methyl thymine pairs incorrectly with cytosine (Friedberg et al, 1995). Therefore, this repair system is vital to ensure the fidelity of the genetic material is kept intact.

The sites of base alkylation that Ada acts on are specific; these sites include only the oxygen atoms of the nitrogenous bases carrying alkyl groups (Friedberg et al, 1995). As mentoioned above, Ada helps with the correction of O^6—meG and O^4—meT. In addition, Ada recognizes the alkylation at phosphotriester bonds as well, which are lesions found in the DNA backbone.

Ada is a suicide enzyme, which means that it terminates its own function when it repairs the DNA. It does so by fixing the alkylated lesion using the side chain of two

cysteine residues, one at the N-terminal end and the other at the C-terminal end (Figure 14, Friedberg et al, 1995, Lindahl et al, 1988, Meyers et al, 1993).

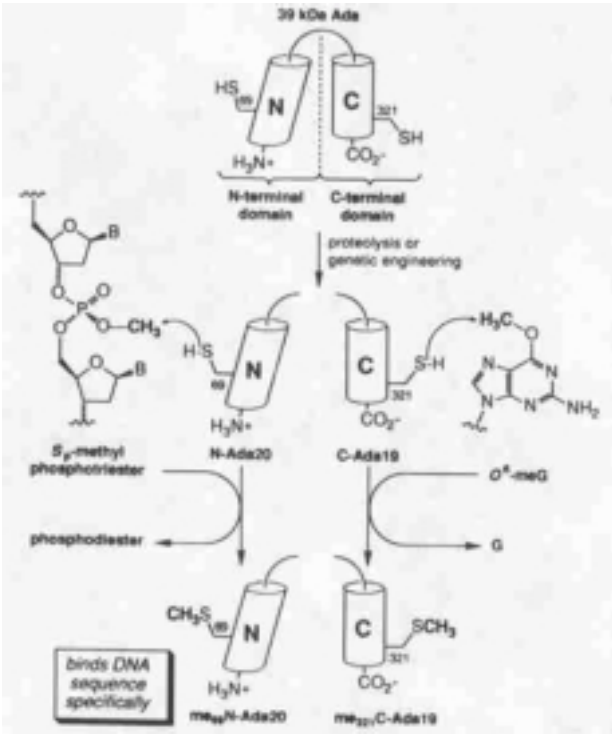

Figure 14: The activity of the Ada protein. Note the two cysteine residues at amino acid locations 69 and 321. Once the cysteine residues accept methyl groups, the enzyme can no longer function.

The second DNA alkyltransferase in *E. coli*, Ogt, differs from Ada in many aspects. This second DNA alkyltransferase protects cells from the damage of alkylation while the adaptive response system produces an optimal level of the repair genes under its regulatory control. This allows the cell to make moderate repair to alkylation damage while the adaptive response genes transcribe (Friedberg et al, 1995). Ogt differs from Ada in that it only works on alkylated bases and not on the alkylated phosphotriester bonds (Friedberg et al, 1995). The extra protection against alkylated base damages suggests that alkylated base damage is more lethal than that of the DNA backbone. Ogt is the primary alkyltransferase in cells which have not yet been induced by *ada*. Upon induction of the adaptive response system, *ada* assumes control of methyl transferase activity (Volkert, personal communication). While the *ogt+* gene product does not act exactly the same as the *ada* gene product, it does perform one similar function:

transferring the methyl lesions of bases away from the base thus restoring its correct chemical structure.

3-meA DNA Glycosylases: The Repair of 3meA, 3meG, and 7meG lesions in DNA

E. coli has two 3-meA DNA glycosylase enzymes in its genome. These two enzymes function in conjunction with the alkyltransferases to remove a methyl lesion from the genome. However, their mechanism and the types of alkylated bases they repair, are quite different from that of the alkyltransferases.

The first 3-meA DNA glycosylase in *E. coli* is encoded by the *tag* gene and is about 21 kDa in size. This enzymne has a narrow substrate specificity. 3-meA DNA glycosylase I fully releases 3-meAdenine lesions from DNA and catalyses the release of 3-meG at lower levels (Friedberg et al, 1995). It is constituitively expressed and is not regulated as part of the adaptive response process (Samson, 1991).

The second 3-meA DNA glycosylase in *E. coli* is encoded by the *alkA* gene. This gene is part of the *ada* regulon and is quite different from the first glycosylase. It is possible that this enzyme recognizes positively charged residues rather than methylated lesions as its broad specificity includes those lesions listed in Table 1 (Friedberg et al, 1995).

Table 1: The lesions recognized by the DNA glycosylase encoded by *alkA+*.

3-meA DNA glycosylase II catalyses	the exision of these residues on DNA
1. 3-meA	5. N1-carboxyethyladenine
2. 3-meG	6. N7-carboxyethylguanine
3. 7-meA	7. O2-meT
4. 7meG	8. O2-meC

Similarities and differences between alkA *and* tag

For enzymes that perform very similar functions, *alkA* and *tag* are quite different from one another. The protein products show very little homology to each other

(Friedberg et al, 1995), possibly suggesting that they function in a different manner. Also, while the *alkA* gene is a member of the adaptive response regulon (Figure 13 above), *tag* is not. This means that the *alkA* gene is inducible by the alkylation adaptation response of the cell whereas *tag* is constituitive by alkylation adaptation (Friedberg et al, 1995). The *tag* gene has a narrow, but efficient substrate specificity, as it removes 3-meA in a quick and efficient manner. The *alkA* gene catalyzes the release of a greater range of lesions (Table 1). Since *tag* is expressed constituitively in cells, it is able to repair 3-meA lesions immediately. The *ada* gene must be induced before it is able to repair alkyl lesions. Therefore, while the ada regulon induces a multitude of *alkA* gene products to assist with the methyl repair processes, the enzyme encoded by *tag* repairs the 3-meA lesions of methylated DNA (Friedberg et al, 1995).

The function of both 3-meA DNA glycosylases is to remove alkylated damage from DNA. As the cells progress from prokaryotes to eukaryotes to mammalian, it becomes curious to observe the similarities and differences of the repair processes that are analogous to this *E. coli* repair system. The enzymes from other species function in the *E. coli* cell in mutant strains lacking both *alk*- and *tag*- (Samson, 1991).

The adaptive response system and the *ogt*+ and *tag*+ genes provide a series of mechanisms to repair methylated DNA lesions.

Other DNA Repair Mechanisms in *E. coli*

While the focus of this study primarily involves the bacterial genes *alk*A and *tag*, and their role in the removal of methylated DNA damage, one should also note some of the additional repair pathways that the *E. coli* (as well as other organisms) have evolved to combat DNA damage.

Ligation of DNA Strand Breaks

Single strand breaks and nicks in the DNA often undergo repair by the enzyme DNA ligase (Friedberg et al, 1995). This enzyme directly rejoins the 3’ hydroxyl group to a 5’ dNTP to create a phosphodiester bond. While this enzyme works alone, it also assists in some of the latter steps of the excision repair cascades.

Repair by Recombination

This system of repair functions when DNA containing bulky lesions such as pyrimidine dimers are replicated prior to repair of the lesion. It involves the function of a series of *rec* genes. These rec genes invade the daughter strand by forming a holliday junction opposite a site of damage such as a pyrimidine dimer in order to fill in a gap across. This leaves a gap opposite an undamaged template and allows for the replication or resynthesis across the gap (Figure 15, Friedberg et al, 1995). Basically, RecA interacts with other proteins to create a holliday junction between the parent strand without the DNA damage and the stalled daugther strand at the point in which a DNA polymerase is stalled by the presence of a pyrimidine dimer. The parent strand without DNA damage now serves to fill the gap across from the pyrimidine dimer with the correct sequence. The daughter strand continues to be synthesized using the opposite daughter strand as its template. Once the area containing the bulky lesion is successfully replicated, the Holliday junction is resolved and the DNA continues synthesis to completion. While this method does not fix the bulky lesion on the parental strand, it "tolerates" its presence by using recombination machinery to continue synthesis. The cell preserves DNA fildelity by further diluting the damage as future replications occur.

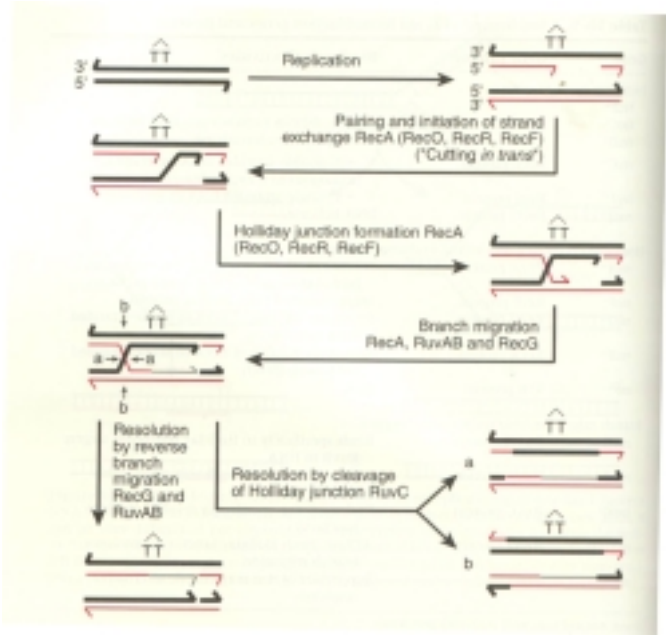

Figure 15: Recombinational Repair of DNA

The SOS Response

The SOS repair system assists cellular survival when exposed to extremely poor environmental conditions. DNA may undergo excessive radiation damage, which creates a number of lesions. Many of these lesions may not be repairable by either the nucleotide excision repair or recombination repair mechanisms because they may occur across from each other on double stranded DNA. Thus, DNA polymerase III stalls when it approaches a base across from a site on the opposite strand of DNA containing excessive damage. The SOS response system begins to function at the point DNA pol III is stalled. The LexA protein becomes inactivated and the genes under LexA repression, *umuD* and *umuC,* are induced (Opperman et al, 1999). These UmuD and UmuC proteins form a complex and function with RecA and SSB (single strand binding protein) to replicate translesion areas of damaged DNA (Reuven et al, 1999). Thus, UmuD and UmuC form the complex that constitutes the fifth DNA polymerase (Reuven et al, 1999; Tang et al, 1999).

The SOS response does not necessarily correct the DNA damage, however it "tolerates" its presence by using recombination machinery to permit DNA synthesis to continue, thus keeping the cell alive. DNA polymerase V is very mutagenic, however the cell uses it because it is efficient at replicating the nucleotides across from abasic sites or UV pyrimidine dimer sites. Polymerase V synthesizes DNA across from these damaged sites according to the "A-rule," as dAMP is preferentially incorporated opposite the lesion (Tang et al, 1999).

Other Glycosylase Repair Systems

There are other glycosylase activities in a cell other than those of hAAG and its homologs such as 3-meA DNA glycosylase in *E. coli*. This section examines a two of the other major glycosylases.

The MutM, MutT, MutY Repair System for Oxidative Damage

MutM, MutT, and MutY for a repair system for oxidative damage in DNA. Specifically, this system protects DNA from the lethality of 8-oxoG. Each enzyme functions independently; however, it is the product of one enzyme that is used as a substrate by another (Figure 16).

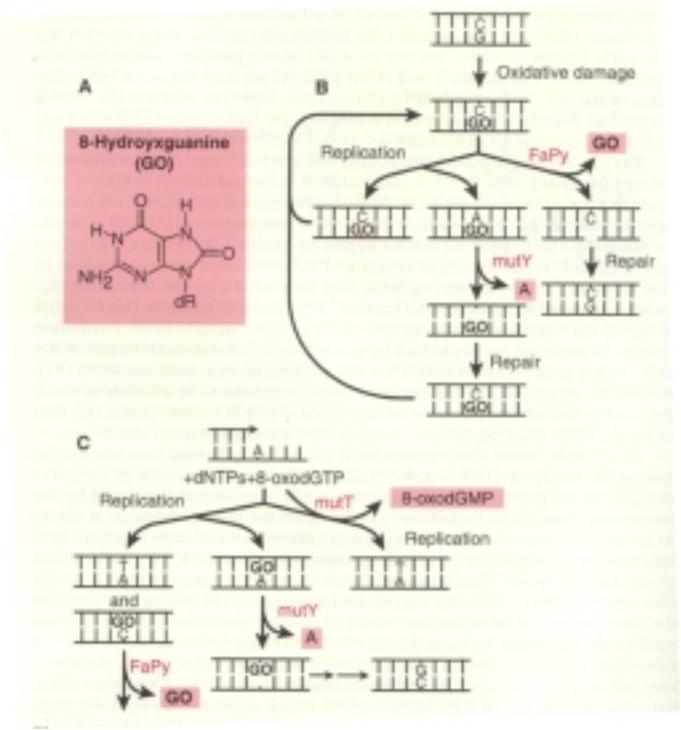

Figure 16: The MutM, MutT, MutY Glycosylase pathway. Adapted from Friedberg et al., 1995.

Panel A from Figure 16 is a representation of 8 oxo-guanine, commonly referred to as GO. A double strand of DNA that is susceptible to oxidative damage may incur such damage on some of its guanine nucleotides. If a guanine incurs oxidative damage, MutM, also referred to as FaPy, excises the 8-oxoG base and prepares the DNA for synthesis and repair. If replication should occur prior to being fixed by MutM, the 8-oxo-guanine may mispair with adenine. Should this happen, mutY is able to detect the GO-A mispair and excise the adenine. This recycles the GO damage for either another round of replication or for mutM to fix (Figure 16, panel B). The function of mutT is to prevent 8-oxodGTP from entering the deoxynucleotide triphosphate pool that DNA polymerase

uses to synthesize new DNA. MutT phosphorylates 8-oxodGTP to 8-oxodGMP (Figure 16, Panel C).

Uracil DNA Glycosylase

The Uracil DNA Glycosylase removes deaminated cytosine (chemically uracil) residues from DNA. These structures may appear in the DNA as either misincorporated Uracil nucleotides or deamination damage to cytosine. Ura-DNA Glycosylase selects for deoxyUridine, therefore it does not repair RNA molecules. This glycosylase phosphorylates the region 5' to the Uracil base (Friedberg et al, 1995). Its importance is to preserve the fidelity of DNA by safeguarding the misincorporation of a uracil base.

Description of Drugs used in this Study

The Alkylating Agents

Alkylating agents are a group of compounds that modify DNA upon contact thus providing a therapeutic effect (Ludlum, 1997). The nitrogen mustard, an early alkylating agent that selectively killed tumor cells, was first used in classified clinical trials 1942, thus beginning modern cancer chemotherapy treatments (Ludlum, 1997). After World War II, the United States government declassified the nitrogen mustard work and modern cancer chemotherapy began (Dittami, 1997).

Alkylating agents have been used in the chemotherapy of cancer and other neoplastic diseases. These chemical compounds have strong electrophile properties, thus they undergo Sn1 reactions to release a negative charged ion and convert from a tertiary amine to a quaternary compound (Goodman and Gilman, 1996). Then, to attach to a base pair of a DNA molecule, the mustard undergoes an Sn2 nucleophilic substitution (Figure 17).

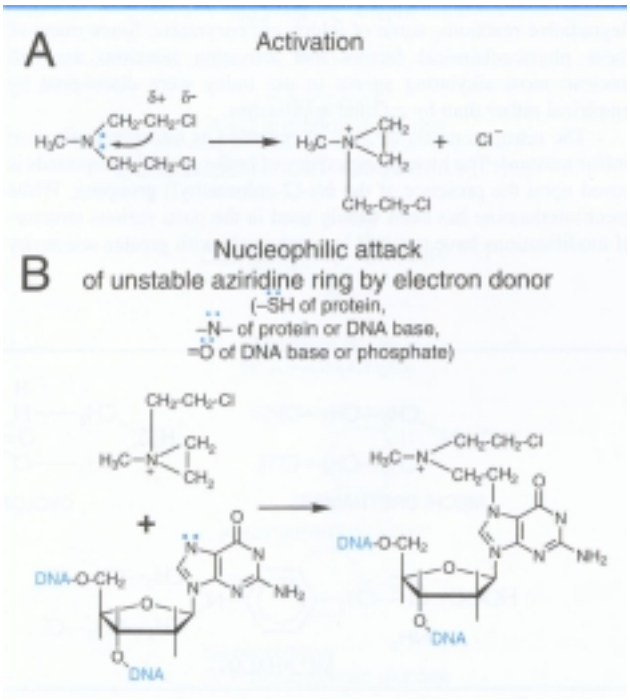

Figure 17: The Mechanism of action of the Nitrogen Mustard Mechlorethamine. Other alkylating agents follow a similar mechanism. Based on figure 51-1 from Goodman and Gilmann, 1996.

Nitrogen mustards attract DNA's guanine at the number 7 position (Figure 18).

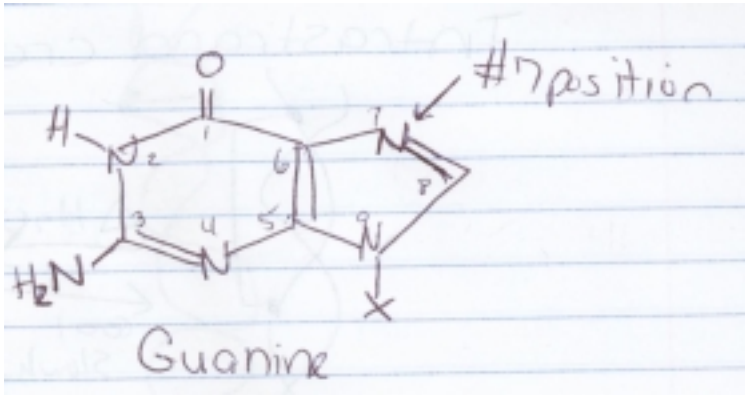

Figure 18: Sketch of the seventh position where a Nitrogen Mustard attracts Guanine

Within minutes after a person ingests an N-Mustard, it has completely reacted in the body. This drug kills the cell by linking to a nucleotide and preventing DNA synthesis. Once DNA is alkylated; however, it often repairs itself using base or

nucleotide excision repair systems described above prior to the next cell cycle or division. In this case, the damage is repaired and the alkylating agent is not lethal.

An interesting atribute to cancer therapy is the role of the oncogene p53, which is essential for normal control of cell growth as it provides a pathway for apoptosis. The p53 gene responds to DNA damage by arresting the cell cycle, thereby allowing repair to be completed before replication is allowed to resume (Oren, 1999). If the damage is beyond cellular repair, p53 triggers cell suicide or apoptosis to occur. Normal cellular arrest and apoptosis functions of p53 limit tumorgenesis; however, if a mutation occurs to the p53 gene, it is very likely that a tumor cell may be created (Sheikh and Fornance, 2000). The mutation of this p53 gene occurs in nearly half of all human tumors, making the mutant gene a likely candidate for cancerous genetic alternations (Sheikh and Fornace, 2000; Oren, 1999). Therefore, tumor cells fail to arrest the cell cycle when DNA damage occurs and proceed directly to replication. The p53 gene, thus, is a target for several cancer therapies, such as treatment of Nitrogen Mustards, because treatment leads to preferential killing of p53 deficient tumor cells (Sellers and Fisher, 1999). Cancer cells, therefore, display optimum toxicity due to their erroneous rapid growth in the absence of wild type p53.

The Nitrosoguanidines: N-methyl-N'-Nitro-N-Nitrosoguanidine (MNNG) and N-ethyl-N'-Nitro-N-Nitrosoguanidine (ENNG)

N-methyl-N'-nitro-N-nitrosoguanidine (MNNG) was synthetically created by Green and Greenberg in 1960 after it was shown to function as an effective agent against L1210 cells injected in mice (see: Ludlum, 1997a; Ludlum, 1997b). Unstable in water, MNNG provides a high yield of N-methyl-N'-nitroguanidine and nitroso radicals, which quickly get converted to nitrous acid, upon decomposition (Gichner and Veleminsky, 1982). MNNG alkylates nucleic acids best in the acidic pH range of 5.0-5.5 (Gichner and Veleminsky, 1982). MNNG reacts with the nucleophilic centers in DNA such as the highly attacked N7 position of guanine and the N3 postion of adenine. MNNG is more reactive than other alkylating agents such as MMS as it methylates the DNA at more sites than MMS. For example, MNNG reacts with oxygen residues that have lower

nucleophilicity. These sites include the O6 position of guanine, the O4 and O2 positions of thymine, the O2 position of cytosine, the oxygen located in the ribose ring, and the oxygen residues of the phosphates (Gichner and Veleminsky, 1982). MNNG methylates adenine at the third position of its structure, thus preventing base pairing (Gichner and Veleminsky, 1982). The 3 meA-DNA glycosylases I and II repair this lesion to correct the DNA sequence in *E. coli* and hAAG repair this lesion in mammalian cells (Engleward et al, 1996).

A. 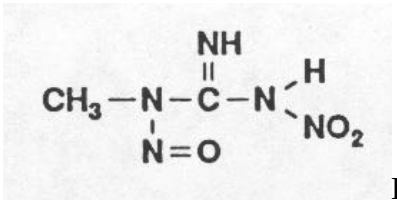 B. 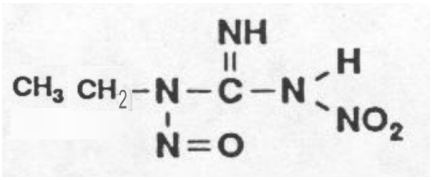

Figure 19: Chemical Structure of A). MNNG and B). ENNG

MNNG is not found in the natural environment, however its use as a model alkylator in research laboratories has assisted scientists study the adaptive response DNA repair system (Gichner and Veleminsky, 1982) and the alkylation of genetic material. An ethyl homolog of MNNG, N-Ethyl-N'-nitro-N-nitrosoguanidine (ENNG), was also used to some extent in this study. It behaves in a similar manner to MNNG, but produces ethyl rather than methyl lesions.

Methyl Methanesulfonate (MMS)

Methyl methanesulfonate (MMS) is a methylating agent. It is less reactive than other alkylating agents used in this study such as the nitrosoureas and MNNG, yet it yields various methyl lesions on the DNA (Sakumi and Sekiguchi, 1990). Unlike MNNG, MMS undergoes an Sn2 reaction.

MMS produces various methylation adducts to the DNA, however it preferentially forms adducts to nitrogen atoms of the nucleotide rather than oxygen (Samsom et al, 1986, Sakumi and Sekiguchi, 1990). MMS selectively damages N-guanine residues, so the great majority of adducts formed by MMS in vivo are N-methylated guanines (Roy et al, 1996).

MMS also differs from the other methylating agents in the damage it creates. Whereas MNNG produces toxicity to the cell by preventing chromosome replication during S phase of cell division, MMS produces toxicity mainly by damaging cell membranes (Smith and Grisham, 1983). MMS can form genetic mutations, just as the other alkylating agents, however it is not as reactive as the other alkylating agents and it does not have a broad specificity for selecting alkylation sites in DNA.

The Cross-Linking Agents

Mitomycin C (MMC)

Mitomycin C is an antibiotic that was isloated in Japan in 1958 during a screening of soil samples. The structural chemistry of Mitomycin C (Fig. 20) involves an aziridine group, a quinone group, and a mitosane ring that assist in the alkylation of DNA (Goodman and Gilman,1996; Silverman,1992). Mitomycin C inhibits DNA synthesis by cross-linking the DNA at the N^6 position of the adenine and at the O^6 and N^7 positions of guanine (Goodman and Gilman, 1996; Verweij et al, 1995).

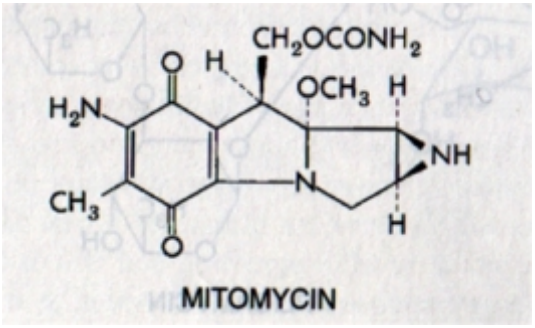

Figure 20: Mitomycin C Structure (Reproduction, Goodman & Gilman, 1996)

Mitomycin C is a bioreductive alkylating agent which is reduced via electron pushing. This reduction occurs either spontaneously or with the assistance of enzymes (Goodman and Gilman, 1996). Bioreductive activation is a prodrug strategy in which an inactive compound is metabolically reduced to an alkylating agent (Silverman, 1992). Mitomycin C has three potential sites for alkylation, however none of these sites is preferentially reactive (Goodman and Gilman, 1996). Two of the alkylation sites are

located on the aziridine group and the other is located at one of the side chains of the mitosane ring (--CH_2OCONH_2).

Mitomycin C can be reduced by one or two electrons. One electron reductions, performed by enzymes such as cytochrome p-450 reductase, enhance toxicity under hypoxic conditions. These reductions reduce mitomycin C to its semiquinone form, which is reversible by the addition of O_2.

Double electron transfer reduces mitomycin C to its hydroquinone form. This reduction, performed by enzymes such as DT-diaphorase, creates the opening of the aziridine ring and loss of the carbamyl group. The new configuration creates DNA reactive sites at the 1 and 10 positions (Goodman and Gilman, 1996; Rauth et al, 1998). The molecules NADH or NADPH play a role in each reduction as either can assist as a cofactor (Rauth et al, 1998). Figure 21 describes the mechanism of action of mitomycin C. In step 8.83, R represents an electron if the reaction involved the reduction of only one electron, converting the quinone to the semiquinone stage, or a hydrogen if the reaction involved the reduction of two electrons, reducing the quinone to the hydroquinone stage (see: Silverman, 1992).

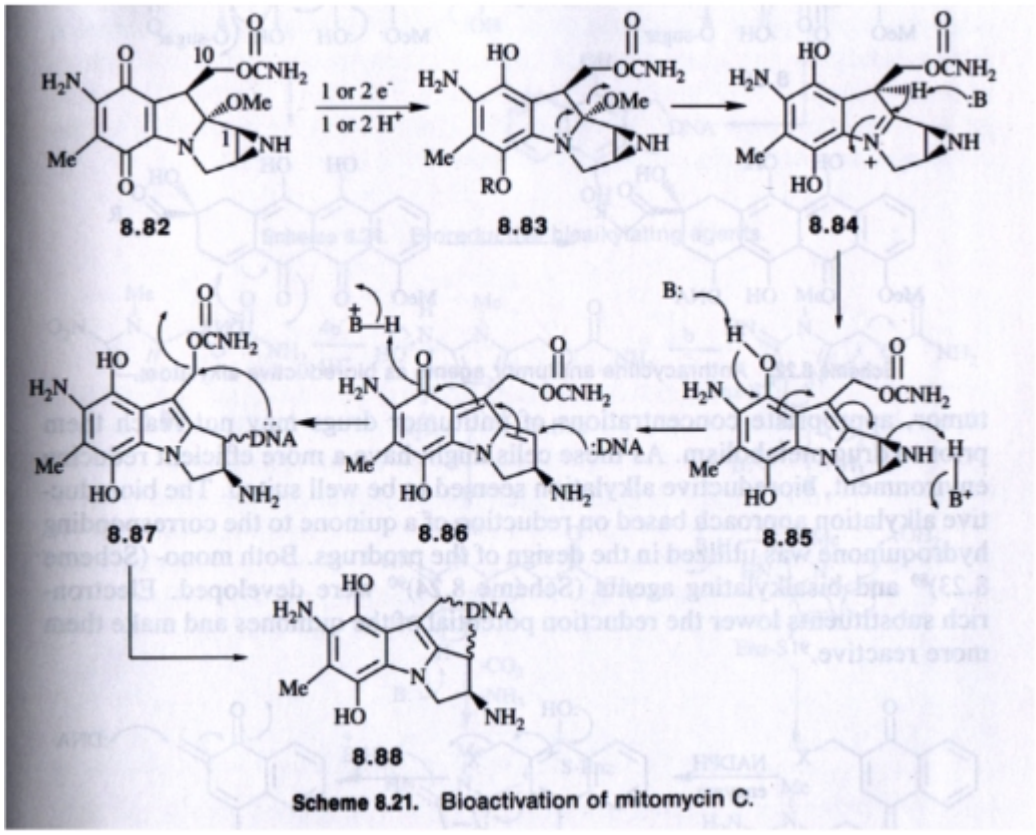

Figure 21: Mechanism of Action of Mitomycin C. (Reproduction, Silverman, 1992)

Shortly after the discovery of mitomycin C in 1958, Iyer and Szybalski proved that mitomycin C could crosslink DNA strands (Rauth et al, 1998; see: Silverman, 1992). Mitomycin C crosslinks DNA at the N^6 position of adenine or at either the O^6 and N^7 positions of guanine (Goodman and Gilman, 1996; Verweij et al, 1995). By crosslinking the DNA, mitomycin prevents additional synthesis, thus the cell will not be able to reproduce and subsequently dies.

The United States FDA approved the use of mitomycin C for anticancer treatment in 1974 to fight solid tumors (Rauth et al, 1998).

The Nitrosoureas

Nitrosoureas differ from other alkylating agents in that they decompose very rapidly in aqueous solutions and in addition to alkylating DNA, these compounds have

the ability to carbamoylate proteins (see: Ludlum, 1997). This category of compounds was created following the discovery that MNNG is effective in slowing the growth of tumor cells in mice (Green and Greenberg, 1960). MNU (Figure 22) exhibited even more activity than MNNG. Thus, an entire new class of compounds was derived from MNNG named the nitrosoureas.

Chloroethyl derivatives of MNU were created and developed due to their greater activity and lower toxicity as therapeutics. Chloroethylnitrosoureas (CENUs) have the ability to form a cytosine-guanine crosslink DNA thereby denaturing the DNA (Ludlum, 1997, Eisenbrand et al, 1986). This study used 2-chloroethyl-N-nitrosourea (CNU) and N,N'-bis(2-chloroethyl-N-nitrosourea (BCNU), members of the chloroethylnitrosourea (CENU) family (Figure 22).

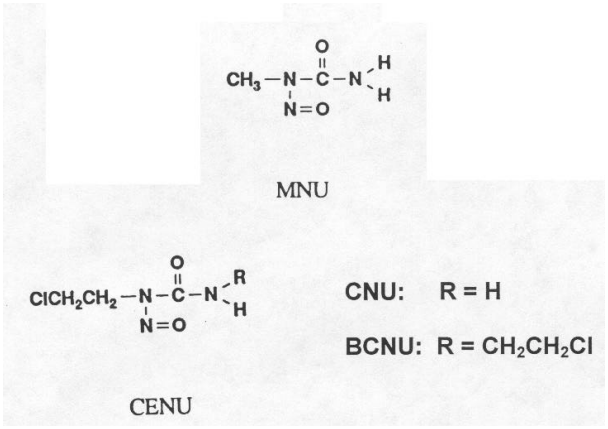

Figure 22: The Molecular Structure of MNU and the CENUs

CNUs are very potent yet very toxic alkylating agents and anticancer drugs (Eisenbrand et al, 1986; Erickson et al., 1980). CNU is lipid soluble thus enters the tumor cells by passive diffusion (Ludlum, 1997b). Therefore, CNU and other nitrosoureas are useful for the treatment of malignant diseases such as brain tumors and lymphomas (Weinkam and Dolan, 1983). This attribute, however, is countered by the highly toxic qualities that nitrosoureas also possess.

The mechanism of alkylation by CENU has not yet been fully determined, however it is known that DNA crosslinking occurs in a two step reaction. The first step involves the addition of a chloroethyl group to a guanine-O^6 DNA position. CNU also

attacks the N^6 ring of adenine, N^4 ring of cytosine and either the N^1or N^7 of guanine. In a clinical setting, the second step occurs hours after the first. The molecule forms an interstrand crosslink using the bound chloroethyl group to react slowly with a nucleophilic site on the opposite strand of DNA (Erickson et al.,1980). Figure 23 demonstrates this proposed mechanism of CNU described above. In this reaction, R = CH_2CH_2Cl, which is used to react with DNA to produce an interstrand crosslink between a guanine molecule from one strand and a cytosine from the opposite strand (see: Silverman, 1992).

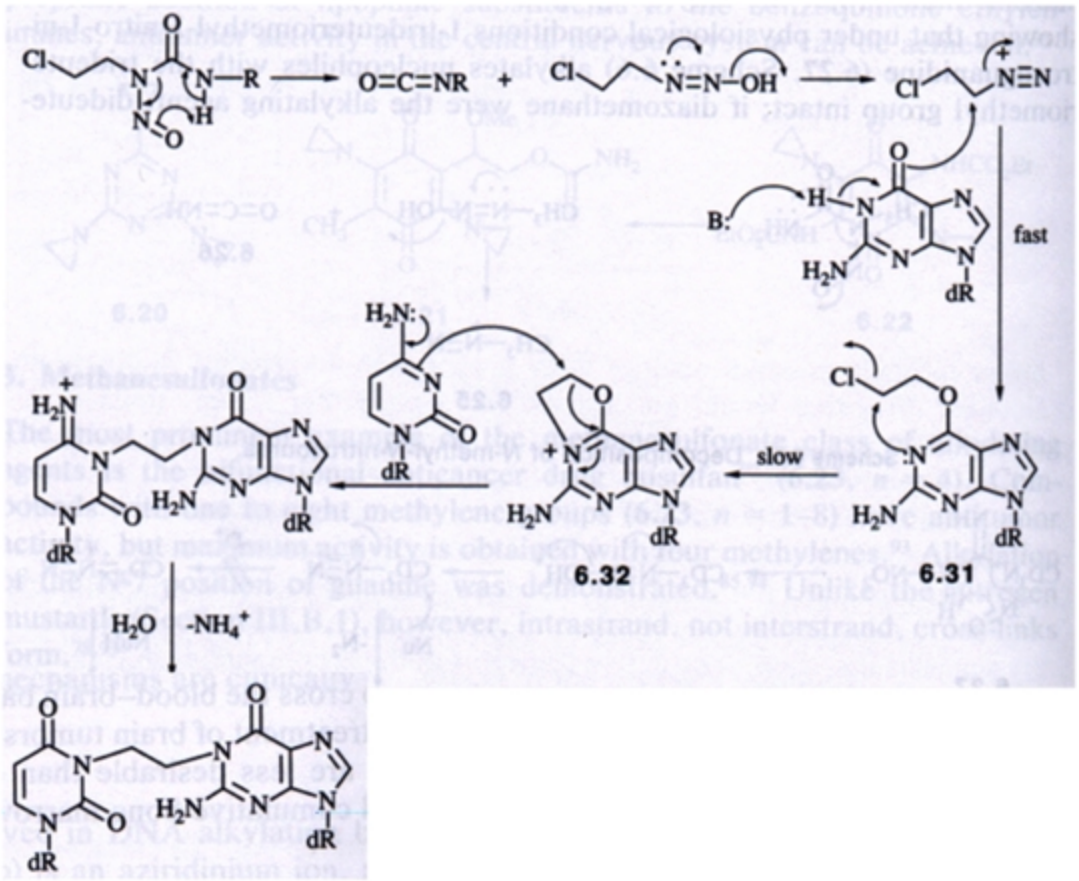

Figure 23: The Mechanism proposed for crosslinking of DNA by CNU (Reproduction, Silverman, 1992)

There are three major pathways that lead to the decomposition of CNU (Fig. 24, Eisenbrand et al, 1986).

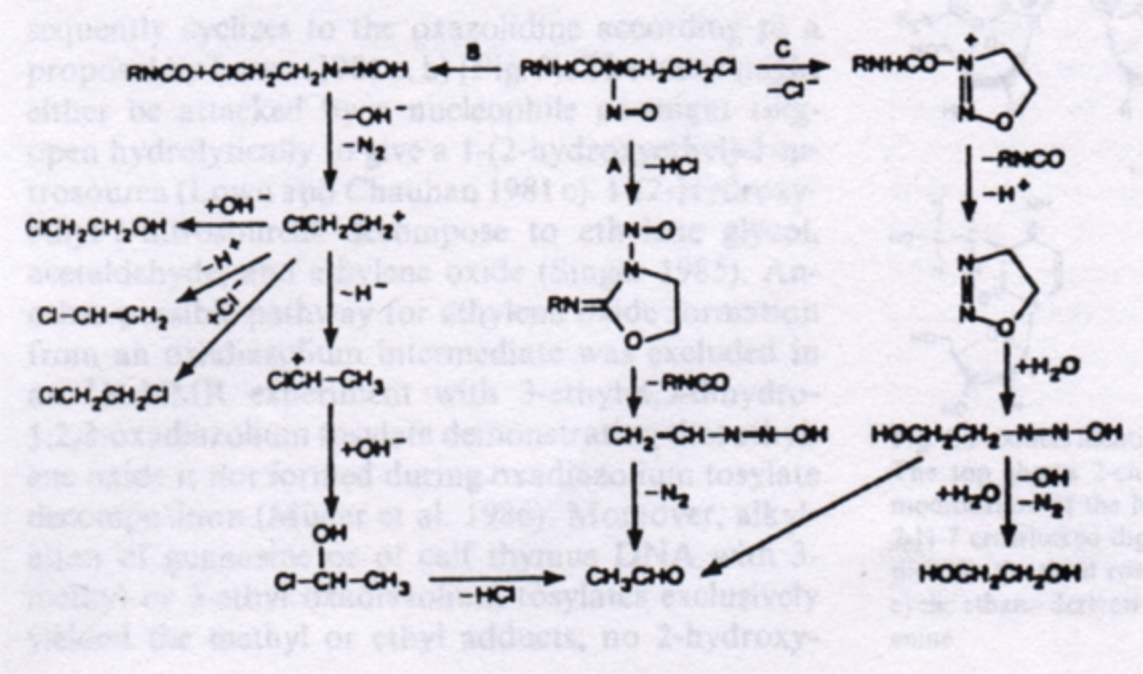

Figure 24: Three Decomposition Pathways for CNU
(Reproduction, Eisenbrand et al, 1986)

In pathway A, the CNU forms a ring. Pathway B is the major pathway for CNU decomposition. It involves the formation of a bifunctional electrophile and isocyanate (Eisenbrand et al, 1986). Pathway C also involves a ring formation intermediate stage. These three pathways determine the decomposition of CNU which in turn determines the ability of the drug to work on the DNA.

N,N'-bis(2-chloroethyl-N-nitrosourea (BCNU) proved to be very active in curing mice that had been injected with a lethal dose of L1210 cells (Ludlum, 1997). BCNU differs from CNU structurally because of the addition of another chloroethyl group. BCNU was the first of the nitrosoureas to be submitted for clinical trials and is one of the few drugs that are capable of passing through the blood brain barrier. Since it is able to do so, BCNU is used as a treatment for brain tumors.

CENUs create intra and interstrand crosslinks in the DNA (Figure 25).

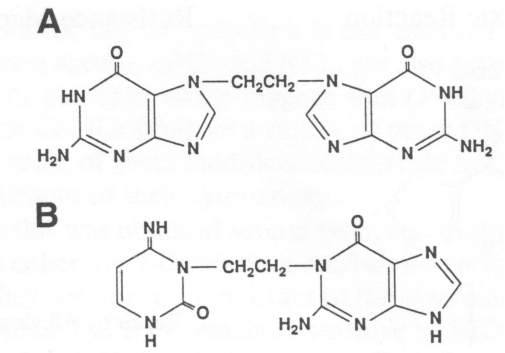

Figure 25: DNA crosslinks formed by CENU. A. 1,2-bis(7-guanyl)-ethane; B. 1-(3-cytosinyl),2-(1-guanyl)ethane. Adapted from Ludlum, 1997.

The multistep reaction shown in Figure 26 was proposed to explain both the formation of the C-G crosslink and the role of alkyltransferase in conferring resistance to CENUs (Tong et al, 1982). The first step in the reaction is a transfer of a chloroethyl group from the CENU to the O^6-position of the guanine in DNA. This is followed by an intramolecular cyclization reaction to form the intermediate, 1, O^6-ethanoguanine, which reacts with the N-3-position of cytosine to form the C-G crosslink. Alkyltransferase can remove the chloroethyl group from the O^6-position guanine before crosslinking occurs, restoring O^6-(2-chloroethyl) guanine to its original unmodified form and protecting the cell from toxicity (Figure 26; Ludlum, 1997).

Figure 26: Reaction of CNUor BCNU with guanine in DNA. When a chloroethyl group is attached to the O^{6+} position of guanine, a DNA crosslink can occur. However, alkyltransferase activity can repair the guanine residue by removing the chloroethyl group before the crosslinking occurs. R denotes the deoxyribose of DNA. Adapted from Ludlum, 1997.

The *E. coli* 3-meA-DNA Glycosylase II (*alkA*) has been shown to excise some of the modified bases from the CNU-treated DNA (Figure 27, Ludlum 1997).

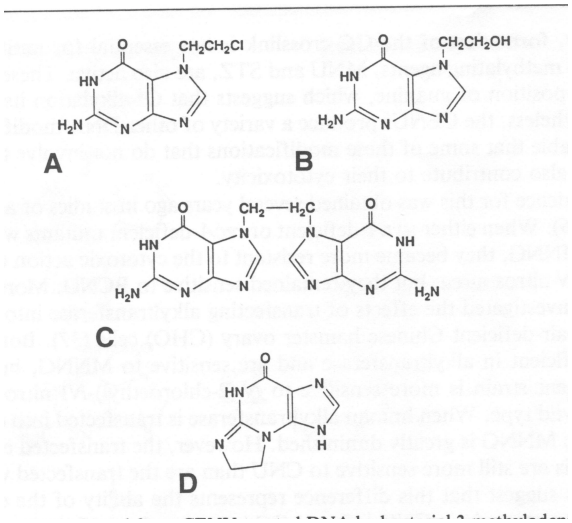

Figure 27: Modified base release from N-(2-chloroethyl)-N^1-alkyl-N-nitrosourea treated DNA by bacterial 3-methyladenine DNA glycosylase II (*alk*A). A. 7-(2-chloroethyl)guanine; B. 7-(2-hydroxyethyl)guanine; C. 1,2-bis(7-guanyl)ethane; D. N^2, 3-ethanoguanine. Adapted from Ludlum, 1997.

Histidine Tag

One of the goals of this study was to use the histidine (his) tag to assist in the detection of glycosylase protein product. A histidine tag is a polyhisdine tail usually consisting of a series of six histidine amino acids attached to the end of a gene, which encodes an identifiable marker. This marker can be especially useful for identifying protein production. Anti-his antibodies can be used in experiments such as the Western blot to attract and collect the his-tag labeled protein. This serves as a method for identifying the level of protein produced.

Prior to this study, a his-tagged version of hAAG-1 was constructed. As a part of this study, the PCR product of the hAAG-2 gene was incorporated into the vector containing the hAAG-1-his_6. This provided the laboratory with a his–tagged version of each isoform.

Previous SDS-PAGE analysis performed on purified protein from hAAG-1-bearing *E. coli* cells revealed the presence of truncated form of hAAG (Ludlum, personal communication). It was believed that this truncation was due to the OmpT protease located on the outer membrane of the *E. coli* cells.

The OmpT Protease

The outer membrane protein *Omp*T is a protease that catalyzes protein degradation by cleaving between dibasic sites, preferentially Arg-Arg linkages (Sugimura and Higashi, 1988). O*mp*T proteolysis may also occur after lysine or arginine residues (Cavard and Lazdunski, 1990). *Omp*T is also responsible for protamine inactivation by degradation of the toxic peptide at the external face of the cell envelope, thus protecting the cell from antimicrobial cationic proteins in the environment (Stumpe, et al, 1998). Protamine causes membrane permeability.

OmpT is known to cleave secreted fusion proteins and thereby allows harvesting of the mature products from the culture supernatant (Maurer et al, 1997). Interestingly, if a cell is permeablilized or broken to allow the *ompT* gene product to interact with intracellular proteins, it can cleave these even though they normally would not have come

into contact with each other (Henderson et al, 1994). The *Omp*T protease also has specific functions such as cleavage of the HlyA transport signal secreted through the outer membrane, cleaving of fusion proteins which causes the extracellular release of toxin B subunit, and the degradation of a B-lactamase protein A in the periplasmic space. These functions suggest that *OmpT* processes precursor polypeptides and degrades membrane proteins (White et al, 1994).

Relevance to the Study of hAAG

DNA repair enzymes are vital for the transfer of correct genetic information from parent to daughter cells. Therefore, it is important to understand their basic functions. Once this is known, scientists can apply therapies for diseases based on the strengths of the repair enzymes. Studying hAAG, thus, allows scientists to further understand how base excision repair enzymes function. This is important for multiple reasons, one of which is to attempt to selectively treat cancer cells instead of normal cells.

An important item to cancer chemotherapy is the status of DNA repair. Therefore, by studying a gene that repairs DNA, indirectly, possible cancer therapies are being researched. Since cancer is generally results from mutations in DNA, understanding these repair genes is essential in the fight against cancer. From a cancer formation perspective, maximizing the activity of repair enzymes such as hAAG prevents inherited mutations. However, from a cancer therapeutic perspective, minimizing these repair activities in cancer cells would be a benefit. So in this study, while not directly working with cancerous cells, a DNA repair gene whose function may assist in cancer therapy in one of the two approaches was explored.

What can be Learned Using a Bacterial System

This study uses a human gene cloned into a plasmid transformed into *E. coli* cells. The choice for using a bacterial system instead of a mammalian system involves many benefits. First, one is able to compare the relationship of hAAG to its bacterial homologs, products of the *alkA* and *tagA* genes. In this manner, one can study the overlapping functions of the 3-meA DNA Glycosylases of bacteria versus that of man. Another asset to using a bacterial system is the ability to observe and analyze if hAAG

function deviates between mammalian and bacterial cells. Scientific literature has proven some mammalian cell reisistance to different types of DNA damage in the presence of hAAG (Engleward, 1997). Finally, bacteria have the quickest growth rate, thus providing an expedient approach for conducting daily studies.

The Purpose of Thesis

This Master Thesis involved several areas of emphasis, thus it had multiple purposes. One purpose of this Masters thesis was to construct the alternative form of the hAAG gene (hAAG-2 and its his-tagged derivative) and to compare the properties of the hAAG-1 and hAAG-2 isoforms. The hAAG-2 isoform is very similar in function to hAAG-1, as seen in this study and prior work (Pendlebury et al, 1994). With the help of Dr. Volkert and his previous work, analysis of the similarities and differences between the two forms of the hAAG gene was an important aspect of this study.

A second purpose was to use the constructed genes in mutant *E. coli* systems to determine the function of each gene against DNA alkylating agents and crosslinkers. The purpose for this aspect of the study was to determine if the results obtained in an *E. coli* system were consistent with those obtained in a mammalian system. In addition, it would further suggest the precise function of hAAG and if it acted alone or with additional enzymes.

The third purpose of this study was to obtain information about the hAAG protein production of each isoform. This will allow one to observe if there are different levels of production between each isoform.

Experimental Strategy

The strategy for the experiments in this project was very precise and clear. The first objective was to produce the second isoform of the hAAG gene. Once this was completed the strategy was to use it in a series of survival tests in which the human hAAG gene was expressed in bacteria genetically engineered to lack their own genes homologous to that of hAAG. The strategy behind performing the survival tests was to compare the ability of the two isoforms of the hAAG gene to enhance the survival of the DNA repair deficient bacteria. While these studies occurred, a knockout mutant *omp*T *E.*

coli strain was constructed. This strain made it possible to purify intact, full-length hAAG protein from bacteria.

The three themes of this project, therefore, were to produce the second isoform of the hAAG gene, to test that gene's ability to rescue cells from specific chemical lesions and compare its action to that of its alternative isoform, and to create a knockout *omp*T *E. coli* mutant strain in order to produce the intact proteins in order to perform various protein analyses efficiently.

MATERIALS AND METHODS

This section describes the materials and methods used in this study. It is divided into five main sections. The bacterial strains section discusses the relevant bacteria strains and plasmids used and created in this study. The Recombinant DNA techniques section discusses the experiments performed on such strains. The survival curve section involves testing the resistance of strains expressing different isoforms of the human alkyl adenine DNA glycosylase gene (hAAG). The *omp*T section involves the microbial genetics of creating a strain carrying a mutant form of this gene. The Protein Analysis section discusses the experiments performed in the *omp*T mutant background.

Bacterial Strains

The bacterial strains used or created in this study are listed in Table 2. All strains are derived from *E. coli. K12.* Key strains have mutations inactivating *alk*A1 and *tag*A1, two bacterial DNA glycosylase genes required for repair of alkylated DNA. The bacterium *E. coli* is rod-shaped and has a 4500 kilobase circular genome (Davis et. al, 1997).

Table 2: *E. coli* Strains used or created in this study, unique characteristics of each strain relevant to this study, and the source or reference of the strain.

Strain	Relevant Characteristics and Properties	Source
Q	High Efficiency Transforming Strain	Lab Collection
MV1161	Derivative of AB1157	Lab Collection
MV1176	*uvr*A deficient strain. Tranductant derived from HK19R of JC3912	Lab Collection
MV2157	*alk*A1 *tag*A1 mutant of transductant of MV1174 x P1 GC4800	Lab Collection
MV3855	MV2157 *alk*A1 *tag*A1 *uvr*A mutant.	Lab Collection
MV4122	MV2157 transformed with pMV509 (hAAG-1)	Lab Collection
MV4126	MV2157 transformed with pMV513 (hAAG-1-His_6)	Lab Collection
MV4135	pMV518 hAAG-2-$(his)_6$ reconstructed in MV2157	Lab Collection
MV4136	pMV519 hAAG-2-$(his)_6$ reconstructed in MV2157	Lab Collection
MV4137	pMV513 transformation of AD202 (*omp*T)	Lab Collection

MV4138	pMV513 transformation of WA834 (*omp*T *E.coli*:B)	Lab Collection
MV4139	MV4137 x P1 * CAG12171 linked to OmpT::Kan	This Study
MV4140	MV4137 x P1 * CAG12171 linked to OmpT::Kan	This Study
MV4147	pMV536 in Q	This Study
MV4148	pMV537 in Q	This Study
MV4210	MV2157 transduced to ompT P1-4139. *alk*A1 *tag*A1 *omp*T::Kan mutant	This Study
MV4211	MV4210 transformed with hAAG-1-his-6 (pMV513). *alk*A1 *tag*A1 *omp*T::Kan mutant	This Study
MV4212	MV4210 transformed with hAAG-1-his-6 (pMV513). *alk*A1 *tag*A1 *omp*T::Kan mutant.	This Study
MV4213	MV4210 transformed with hAAG-2-his-6 (pMV536). *alk*A1 *tag*A1 *omp*T::Kan mutant.	This Study
MV4214	MV4210 transformed with hAAG-2-his-6 (pMV536). *alk*A1 *tag*A1 *omp*T::Kan mutant.	This Study
MV4215	MV4210 transformed with hAAG-2-his-6 (pMV537). *alk*A1 *tag*A1 *omp*T::Kan mutant.	This Study
MV4216	MV4210 transformed with hAAG-2-his-6 (pMV537). *alk*A1 *tag*A1 *omp*T::Kan mutant.	This Study
MV4217	Q transformed with hAAG-2 (pMV543)	This Study
MV4218	Q transformed with hAAG-2 (pMV543)	This Study
MV4219	Q transformed with hAAG-2 (pMV544)	This Study
MV4220	Q transformed with hAAG-2 (pMV544)	This Study
MV4221	Q transformed with hAAG-2 (pMV545)	This Study
MV4222	Q transformed with hAAG-2 (pMV546)	This Study
MV4223	Q transformed with hAAG-2 (pMV546)	This Study
MV4224	wt. hAAG-1(pMV509) in MV4210	This Study
MV4225	wt. hAAG-1 (pMV509) in MV4210	This Study
MV4226	pMV545 transformed in MV4210	This Study
MV4227	pMV546 transformed in MV4210	This Study
MV4228	pTRC99a vector in MV4210	This Study
MV4229	pTRC99a vector in MV4210	This Study
MV4230	wt. hAAG-1(pMV509) in MV4210	This Study
MV4231	wt. hAAG-1 (pMV509) in MV4210	This Study
MV4232	pMV509 vector with pMV536 EcoRI-Sal I insert (pMV550) in MV4210	This Study
MV4233	pMV509 vector with pMV536 EcoRI-Sal I insert (pMV551) in MV4210	This Study
MV4234	pBS KS- with pMV536 EcoRI-Hind III insert (pMV552) in Q	This Study
MV4235	pBS KS- with pMV536 EcoRI-Hind III insert (pMV552) in Q	This Study

	(pMV553) in Q	
MV4236	pTRC99a vector in MV3855 *alk*A1 *tag*A1 *uvr*A mutant.	This Study
MV4237	wt. hAAG-1 (pMV509) in MV3855 *alk*A1 *tag*A1 *uvr*A mutant.	This Study
MV4238	hAAG-1-his-6 (pMV513) in MV3855 *alk*A1 *tag*A1 *uvr*A mutant.	This Study
MV4239	wt. hAAG-2 (pMV550) in MV3855 *alk*A1 *tag*A1 *uvr*A mutant.	This Study
MV4240	hAAG-2-his-6 (pMV536) in MV3855 *alk*A1 *tag*A1 *uvr*A mutant.	This Study
MV4241	pBS KS- with pMV536 EcoRI-Hind III insert (pMV552) in MV4210	This Study
MV4242	pBS KS- with pMV536 EcoRI-Hind III insert (pMV553) in MV4210	This Study
MV4243	plasmid from MV4218 in MV4210 *alk*A1 *tag*A1 *omp*T::Kan mutant.	This Study
MV4244	plasmid from MV4218 in MV4210 *alk*A1 *tag*A1 *omp*T::Kan mutant.	This Study
MV4245	plasmid from MV4220 in MV4210 *alk*A1 *tag*A1 *omp*T::Kan mutant.	This Study
MV4246	plasmid from MV4220 in MV4210 *alk*A1 *tag*A1 *omp*T::Kan mutant.	This Study
MV4247	plasmid from MV4221 in MV4210 *alk*A1 *tag*A1 *omp*T::Kan mutant.	This Study
MV4248	plasmid from MV4222 in MV4210 *alk*A1 *tag*A1 *omp*T::Kan mutant.	This Study
MV4249	plasmid from MV4223 in MV4210 *alk*A1 *tag*A1 *omp*T::Kan mutant.	This Study
MV4250	pMV543 in MV3855 *alk*A1 *tag*A1 *uvr*A mutant.	This Study
MV4251	pMV544 in MV3855 *alk*A1 *tag*A1 *uvr*A mutant.	This Study
MV4252	pMV545 in MV3855 *alk*A1 *tag*A1 *uvr*A mutant.	This Study
MV4253	pMV546 (from MV4223) in MV3855 *alk*A1 *tag*A1 *uvr*A mutant.	This Study
MV4254	wt hAAG-2 (pMV551) in MV3855 *alk*A1 *tag*A1 *uvr*A mutant.	This Study

Bacterial Plasmids

The plasmids used in this study were either obtained from the lab collection or were created using genetic techniques. Each plasmid is carried by one of the strains listed in table 2. Table 3 describes the plasmids used and created in this study.

Table 3: List of plasmids used in this study, the strain each plasmid is stored, the unique characteristics of each plasmid, and the original source of the plasmid.

Plasmid	Strain Hosting Plasmid	Relevant Characteristics	Source
pMV509	MV4224	wt hAAG-1 clone	Lab collection
pMV513	MV4211	hAAG-1(his)$_6$. pMV509 cut with Cel II and HindIII- Then religated using his tagging oligos MV3 and MV4 that contain CelII Hind III compatible ends.	Lab collection
pMV518	MV4135	hAAG-2(his)$_6$ original plasmid	Lab collection
pMV519	MV4136	Original plasmid with hAAG-2-His$_6$	Lab collection
pMV536	MV4213	hAAG-2(his)$_6$ in pMV513. MV20 and MV21 primers used. PCR produced using pMV518 as template. EcoRI-HindIII fragment cut.	This Study
pMV537	MV4148	hAAG-2(his)$_6$ in pMV513. MV20 and MV21 primers used. PCR produced using pMV518 as template. EcoRI-HindIII fragment cut.	This Study
pMV541	MV4206	EcoRI-HindIII fragment from pMV513 (hAAG-1) inserted into pBS vector	Lab Collection
pMV542	MV4207	EcoRI-HindIII fragment from pMV513 (hAAG-1) inserted into pBS vector	Lab Collection
pMV543	MV4217	hAAG-2 EcoRI-AfeII fragment from pMV536 into EcoRI-AfeII cut pMV509 backbone	This Study
pMV544	MV4219	hAAG-2 EcoRI-AfeII fragment from pMV537 into EcoRI-AfeII cut pMV509 backbone	This Study
pMV545	MV4221	hAAG-2-his-6 EcoRI-AfeII fragment from pMV536 into EcoRI-AfeII cut pMV513	This Study
pMV546	MV4222	hAAG-2-his-6 EcoRI-AfeII fragment from pMV537 into EcoRI-AfeII cut pMV513	This Study
pMV550	MV4232	pMV509 vector with pMV536 EcoRI-Sal I insert (pN1)	This Study
pMV551	MV4233	pMV509 vector with pMV536 EcoRI-Sal I insert (pN2)	This Study
pMV552	MV4234	pBS KS- with pMV536 (hAAG-2) EcoRI-Hind III insert	This Study
pMV553	MV4235	pBS KS- with pMV536 (hAAG-2) EcoRI-Hind III insert	This Study

Culture Media and Growth Conditions

The bacterial strains were commonly grown in liquid Luria-Bertani (LB) medium. The antibiotic Ampicillin was often added because the strains carrying the plasmids were resistant to Ampicillin. If another strain of bacteria were present in the LB, it would die because it was not Ampicillin resistant, rather it was sensitive to Ampicillin. Therefore, this antibiotic was used to select for the plasmid bearing cells.

Cells were grown in 6 mL liquid LB-Amp broth oscillated overnight in a 37 degree Celsius incubator. To obtain a pure colony from this cell stock, a toothpick was used to streak colonies on LB-Amp media plates. These plates were also placed in the 37 degree Celsius incubator overnight. A pure clone from these plates was then inoculated in LB-Amp broth, incubated overnight, and then frozen at -80 degrees Celsius in LB + 10% DMSO as a permanent stock.

Recombinant DNA Techniques

The following techniques were used to manipulate the DNA as a pure plasmid and within host cells. They were each essential for the biotechnological aspects of this study.

Plasmid Purification

Isolation of plasmid DNA was performed using the Qiagen QIAprep Spin Miniprep Kit. The cells were lysed using a method based on the alkaline lysis method of Birnboim and Doly, 1981 (Qiagen, Inc.). A buffer containing RNAase was used to remove any RNA present. Excess material such as the cell membranes, components, and chromosomal DNA were removed by centrifugation at 14,000 rpm for 10 minutes. The plasmid was recovered in the supernatant and was allowed to bind to the Qiagen spin column. Bound DNA was washed to remove endonucleases and salts in the buffers PB and PE respectively. The DNA was then eluted from the QIAprep column with 50 uL low concentration TE buffer and centrifugation. The DNA yield was then determined using a spectrophotometer to measure absorbance at a wavelength of 260 nm.

Polymerase Chain Reaction (PCR)

PCR was used to isolate and amplify a specific DNA segment. Using an enzyme stable at high temperatures, this procedure acts as a photocopier for a DNA template (Davis et al, 1994). In this experiment, oligonucleotide primers, MV20 and MV21 were used to amplify the 980 base pair fragment (Table 4). The source of the DNA template was the plasmid pMV518. The PCR basically is a cyclic three-step reaction. The first step is the heat denaturation step. This step separates the double stranded DNA into two single strands. The primers are then allowed to bind to the DNA single strands. The Ampli Taq enzyme and dNTPs elongate a complementary strand to each template DNA strand in the third step. Then, the cycle is repeated twenty-nine times, using sufficient primers so that each cycle doubles the number of DNA fragment produced. At the completion of this reaction, an extended elongation time provided extra time for the completion of the synthesis of new strands of DNA. In each cycle, the number of strands doubled to create an exponential increase in the amount of DNA fragment.

Table 4: Description of oligonucleotide primers used for the PCR reaction to create hAAG-2.

PCR Primers	Sequences	Tm (C)	Description of Use
MV6	5'- CTG TAT CAG GCT GAA AAT C -3'	56	First primer used to amplify the lagging strand. Discarded due to diverse Tm compared to MV20.
MV20	5'- CAT GGA ATT CTA AGG AGG TAT CTA ATG CCC GCG CGC AGC GGG GCC CAG TTT TGC –3'	79	Used to amplify 5' leading strand of hAAG-2 sequence. Has identical upstream of hAAG-1 incorporated, including site for ribosome binding and EcoRI restriction site.
MV21	5'- GTC AGG TGG GAC CAC CGC GCT ACT GCC GCC –3'	78	New primer constructed for amplification of lagging strand. Designed with comparable Tm to that of MV20.

The goal of the PCR was to amplify an isoform of the human Alkyl Adenine DNA Glycosylase (hAAG) gene using primers MV20 and MV21, and a DNA template pMV518. The template was the fragment of DNA amplified and the primers were the small chains of nucleic acids that complemented a certain region

downstream of the fragment of interest. One primer attached to the 5' end of one strand of the template in the second step of the PCR cycle, the other primer attached to the 5' end of the opposite strand of the template to a flanking sequence downstream from the end of the fragment of interest. In the first step of the PCR, the DNA template separated into two single DNA strands. In the annealing step, the primers attached to each strand of DNA. In the elongation stage, DNA polymerase then copied each strand of DNA to make the complementary strand. In the next cycle, all four of these strands were again duplicated to produce eight copies. This continued for a total of thirty cycles.

There were five different conditions used in the PCR experiment for this study because the DMSO concentration was varied. Following the PCR, the products from each reaction were analyzed on a 1% TAE gel. The reaction that generated the best yield of DNA of interest was then run on a second gel using multiple lanes so that all of the DNA product could be excised for further study.

Purification of DNA Fragments

To purify a DNA fragment from an agarose gel, the Gene Clean Kit (Bio101, Inc.) was used. The basic Gene Clean procedure was to dissolve the agarose, to bind the DNA to silica beads, centrifuge the mix to concentrate the DNA, wash it, and then elute it to release DNA from the beads. If a specific band of DNA was needed for further analysis, the Gene Clean Kit was a quick method to purify a DNA fragment from an agarose gel. First, a piece of 1% TAE agarose gel slice containing the DNA fragment was excised and NaI was added to the gel excision containing the desired DNA fragment. Then, GLASSMILK, a chemical with a silica matrix component, was added to bind to the DNA. Centrifugation precipitated the DNA-silica complex and NaI was removed in the supernatant. The GLASSMILK with DNA attached to it was washed a series of times with an alcohol containing Wash Solution (Bio101, Inc.). The DNA was then released from the GLASSMILK with low salt concentration TE buffer and after centrifugation, the supernatant contained clean, pure DNA.

Restriction Digests

Following the purification of the DNA fragment of interest, a restriction digest involving the EcoRI and HindIII restriction sites was performed. By combining these

enzymes in their appropriate buffer with the DNA, the DNA was cut at specific sequences forming sticky or blunt ends. Typically 3 to 10 ug of plasmid DNA was cut in a 10 uL reaction containing salt buffer and the EcoRI and Hind III restriction enzymes. These fragments were then used to perform a ligation. Restriction digests were also helpful to determine the size of a piece of DNA and to determine if it was likely to contain the correct sequence, based on the location of specific restriction sites.

Cell Preparation and Transformation

Transformation is the introduction of a plasmid into a competent cell. A competent cell is a cell that is chemically treated to allow its membrane to be permeated by plasmids. Two strains were made into competent cells for this study, Q and 4210. The cell preparation and transformation experiment is done as the first step in creating a new bacterial strain.

A cell is prepared for a transformation by growing to Klett 50, which is an absorbance level that indicates that the cells are in the log phase and corresponds to approximately 3×10^8 cells per mL. Following growth, the cells were centrifuged and resuspended in a mix of 0.1 M Pipes, pH 6.8 and 2.5 M $CaCl_2$. These chemicals treat the cell to induce competency.

These cells, once competent, were very receptive to plasmids in a transformation. In this study, small scale transformations were used. Two hundred microliters of cells were mixed with 5-10 ug purified DNA in a solution containing 0.1 M Pipes, pH 6.8, 1 M $CaCl_2$, 1 M $MgCl_2$, and dH_2O. Following an extended incubation (30 minutes to 48 hours) on ice, the cells were heat shocked at room temperature for two minutes and incubated with aeration in LB to allow growth. Then, the cells were streaked on LB plates and incubated at 37 degrees Celsius overnight.

Ligation

A ligation joins together two DNA fragments using an enzyme from bacteriophage T4 called T4 DNA ligase. The DNA fragment purified from the PCR (90 ug/mL) and the vectors pMV513 (110 ug/mL) and pMV509 115 ug/mL) linearized with EcoRI and Hind III enzymes were joined together using this enzyme

after digestion with the appropriate restriction enzymes. The ligation reaction created certain plasmids relevant to this study. Those plasmids were subsequently used in the transformation protocol to create new strains.

DNA Sequencing

The Nucleic Acids Core facility at the University of Massachusetts Medical Center and the DNA sequencing services of Iowa State University performed DNA sequencing to verify the nucleotide sequence of the engineered plasmids. The UMMC Nucleic Acids Core facility used a computer analysis program ABI Prism Model version 2.1.1.

Cell Survival Assays

Survival curves were performed to test the function of the hAAG-2-$(his)_6$ gene with respect to that of the hAAG-1-$(his)_6$ isoform. Additional experiments included testing the function of the hAAG-1 gene with respect to that of hAAG-2, and observing the effect of the histidine tag on each gene. Each curve involved a series of carefully timed actions in order to provide an accurate measurement of the survival of the cells.

For survival measurements, bacteria were grown in LB medium to Klett 30, which is approximately 10^8 cells per mL. Cells were then dispersed into two tubes, one induced with 0.1 M IPTG to turn on the hAAG gene, the other uninduced, and were incubated at 37 degrees Celsius for 90 minutes. Following incubation, cells were supplemented a dose of an alkylating agent or cross-linking agent and incubated for an additional half-hour. One of the tubes from each set served as an untreated control. Aliquots were then removed, diluted in 1 x E buffer components plus 4% NaS_2O_3 to inactivate residual chemical, and spread on LB-Amp plates to estimate cell survival (Volkert, 1984). Results are estimated by calculating the titer and the fraction survival. The survival was expressed as a percent of the colony titer divided by that of the untreated control for each dose. All experiments were performed from two to seven times for each strain. Figures represent the Mean ± the Standard Error. In those instances where error bars are not seen, the Standard Error is too small and masked by the symbol.

Protein Analyses

Transferring hAAG-2-his$_6$ into pBluscript KS-

The his-tagged isoforms of hAAG were genetically engineered into the plasmid pBluescript. Construction of hAAG-2-6x-his into pBluescript consisted of performing restriction digests at the EcoRI and HindIII sites of the hAAG-2-6x his gene from plasmid pMV536. The reciprocal sites of pBluscript were also cut. A ligation occurred to produce the plasmid pMV552 (Table 2). Correct ligation was confirmed in further restriction analyses.

Protein Synthesis and Concentration Time Point Analyses

Cultures are grown overnight on a roller at 37 degrees Celsius. The plasmid containing cells were grown in the presence of ampicillin. Addition of 0.2 mM IPTG when the cultures reach an OD_{600} of 0.61(Klett 80) induces the synthetic lac promoter to produce RNA polymerase, which in turn initiates high-level expression of hAAG-1-his6 or hAAG-2-his6 inside the plasmid. An initial sample of 100 ul culture is collected immediately prior to IPTG induction to serve as time point zero. Cells were harvested at 1.5, 2, 6, and 12 hours after induction. Once harvested, cells were centrifuged and the supernatant removed. Cells were then suspended in1x SDS gel sample buffer, boiled for 5 minutes, and frozen at –20 degrees Celsius for later use.

Western Blot Analysis

The samples from the time course assay were electrophoresed in a 7.5% polyacrylamide gel in the presence of SDS and electrotransferred to a nitrocellulose membrane at 30 volts overnight. The blot was incubated with 0.3 ug/ml penta-his (Qiagen, Inc.) for 2 hours, then with anti-mouse IgG conjugated with horseradish peroxidase (NEB). The blot was visualized using a chemiluminescence detection kit (Amersham Pharmacia Biotech, Inc).

P1-Mediated Transduction and the Genetics of Strain Construction

Transduction is a bacteriophage mediated recombinational process in which a phage injects erroneously packaged bacterial DNA fragments from one strain of bacteria into another. This transferred chromosomal segment then recombines with homologous portions of the bacterium's chromosome to incorporate itself into the bacterium's chromosome (Voet and Voet, 1995). The bacteriophage P1 transduces very nicely into *E. coli*, the bacteria that we have used to host our gene. Therefore, alterations to the strain were constructed in order to create specific conditions. One genetic alteration made in this study was to create the *alk*A1, *tag*A1, *omp*T triple mutant strain MV4210.

Results

Introduction

The results of this study can be separated into five sections. The first consists of the preparation of the hAAG-2 and hAAG-2-his$_6$ forms of the gene. The second involves the biology of the two isoforms and the comparison of each isoform to its histidine tagged counterpart. The third section includes the creation of the *alkA1 tagA1 omp*T mutant strain. Preparation of the hAAG-2-his$_6$ gene inserted into pBluescript is the fourth major section of this report. Finally, protein analysis is presented.

Cloning and sequencing of the Alternative hAAG Gene

The cloning and sequencing of the secondary exon sequence of the hAAG-1 gene involved the amplification of the hAAG-2-his$_6$ gene fragment from pMV518 using the polymerase chain reaction (PCR), ligation of the amplified fragment into a pMV513 plasmid backbone, and transformation of this new plasmid into a competent cell to produce a new strain.

Construction of hAAG-2 by PCR

A previous version of hAAG-2-his$_6$ failed to exhibit an alkylating agent resistance phenotype, like that seen when induced hAAG-1-his$_6$ is expressed in an *alk*A1 *tag*A1 *E. coli* mutant strain (Volkert, unpublished observation). It was unclear if this was due to faulty expression, or a functional difference between the hAAG-1 and hAAG-2 isoforms. In order to eliminate expression differences, the hAAG-2 gene was reconstructed to produce a version that had the identical upstream sequence as hAAG-1 using PCR. These constructs were named pMV536 and pMV537, and contained the hAAG-2 gene sequence attached to a polyhistidine tail.

For the construction of these plasmids, a 980 base pair (bp) fragment amplified from plasmid pMV518, which carries the original non-functional hAAG-2 sequence, was

inserted between the EcoRI and HindIII sites of the pMV513 plasmid. Several attempts to amplify the correct fragment failed due to the difference in melting temperature between the two initial primers used. The MV20 primer contained an EcoRI site, the identical upstream sequence as hAAG-1, and a region that hybridized to Exon 1 of hAAG-2. Two downstream primers were used in separate reactions, MV6 and MV21. The two initial primers were MV20 (melting temperature 78 degrees) and MV6 (melting temperature 66 degrees). In this PCR, although a band in the 980 base pair region was observable, it was not the band of interest. Curiously, a second band also appeared in the 2,000 base pair region. Restriction analysis led to the prediction that this additional band might be a dimer, however several tests using restriction enzymes to cut this dimer failed to confirm this (Figure 28).

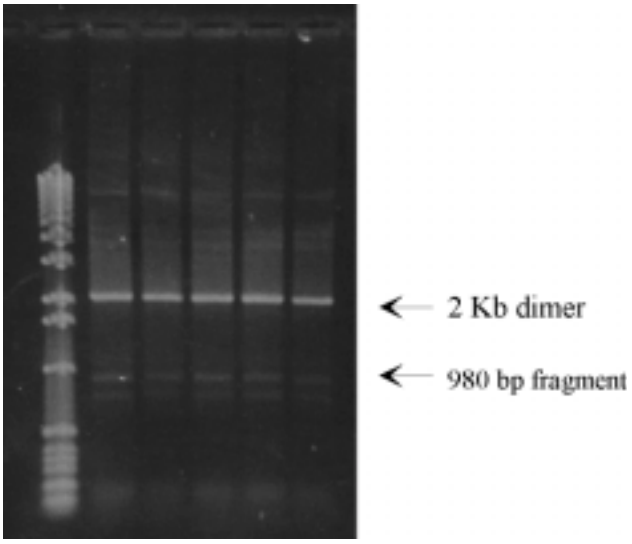

Figure 28: PCR reaction involving MV20 and MV6 primers. Note the band at 2 Kb and also two bands between 900bp and 1 Kb. The expected fragment size was 980bp.

Therefore, a new primer MV21 was designed to match the melting temperature of primer MV20. The use of primers MV20 and MV21 allowed successful amplification of the hAAG-2 form of the gene from the pMV518 template. Several PCR reactions were run simultaneously, differing in the amount of DMSO, which modifies the annealing temperature of the PCR reaction. Small aliquots of all PCR reactions were run on a 1% agarose TAE gel to determine which conditions yielded the highest levels of specific

fragment amplification (figure 29). A larger volume of the 980 bp band produced in reactions 1 and 2 (Figure 29, lanes 1 + 2) was repurified on a 1% TAE agarose gel. These products were purified using a gene clean kit (Bio101, Inc.), then, cleaved with the appropriate restriction enzymes, used in the ligation reactions described below.

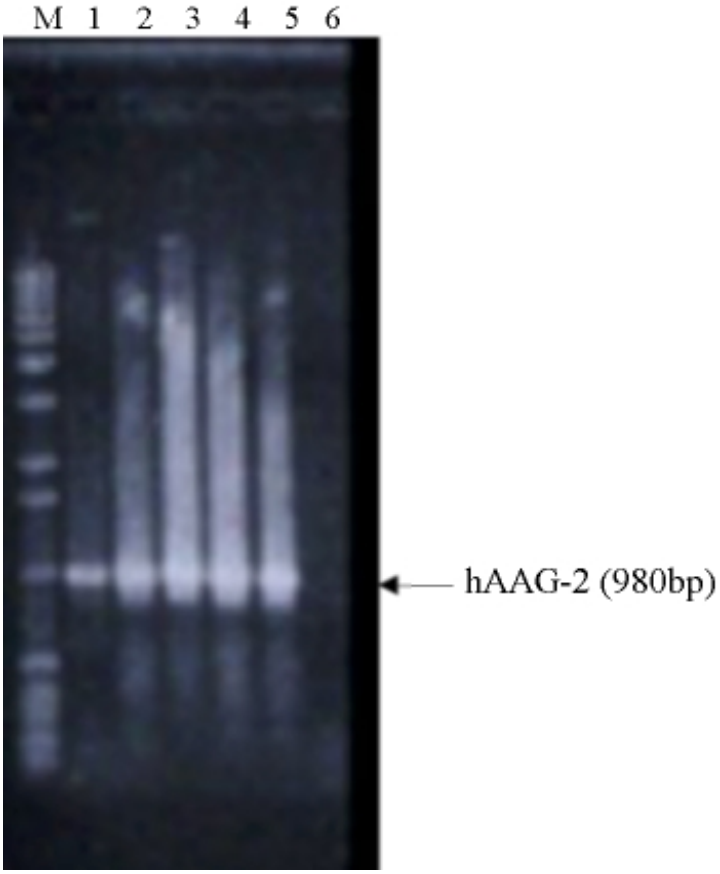

Figure 29: PCR of 980 bp fragment of hAAG-2 gene. The only variable between the lanes was the amount of DMSO, ranging from 0 uL in lane 1 to 10 uL in lane 5. Lane 6 was the negative control, using the same conditions as lane 3 with no DNA template.

Ligation of PCR fragment into pMV513 backbone

The PCR fragment was inserted into the plasmid vector by ligating the EcoRI and Hind III sites. The plasmid carrying hAAG-1-his_6, pMV513, was used as the vector because simple restriction digests allow discrimination between exon 1 of hAAG-1 and hAAG-2 (Figure 30).

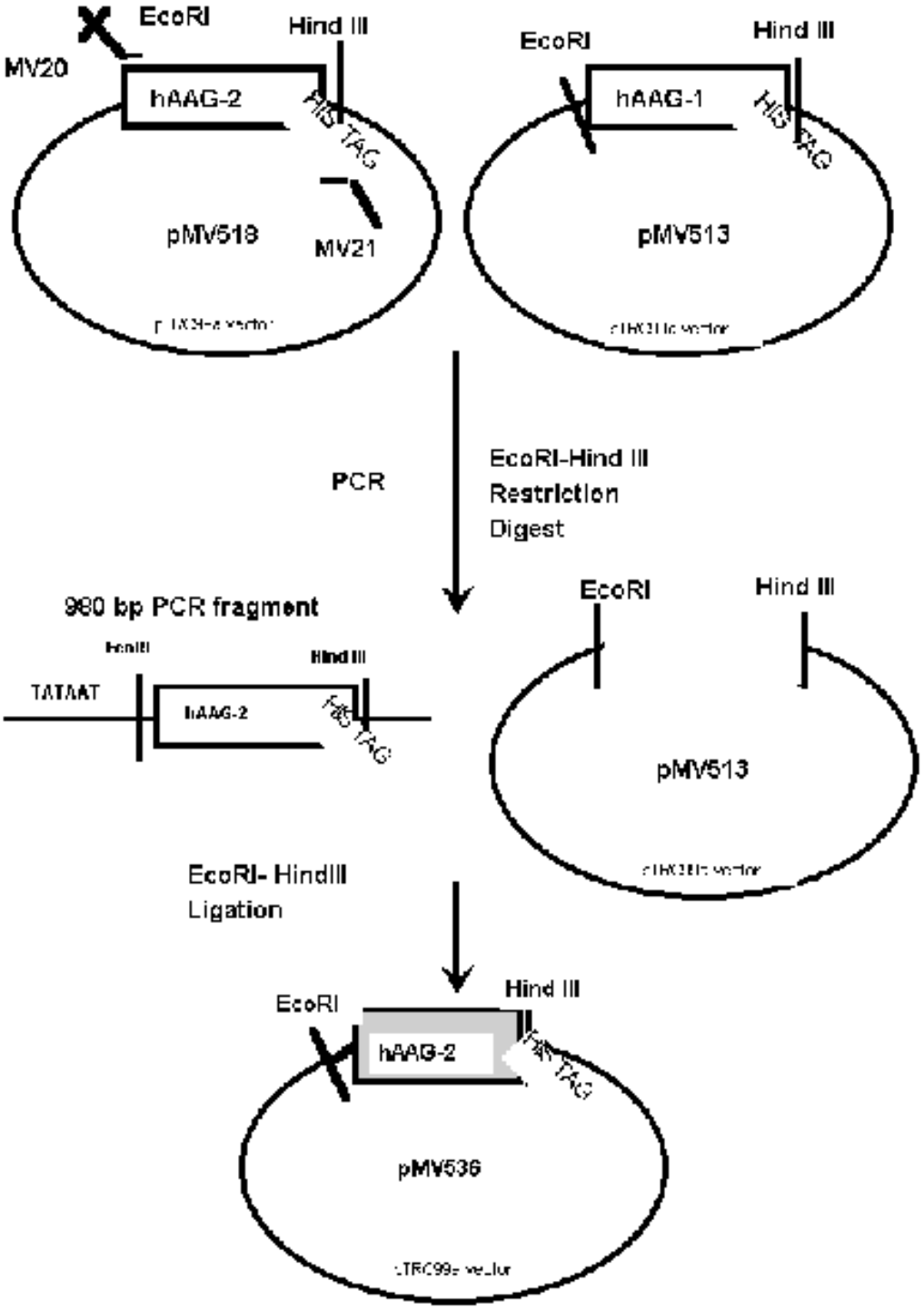

Figure 30: Plasmid creation. The EcoRI-HindIII site of pMV518 was amplified using PCR and then ligated into the pMV513 vector between its EcoRI-HindIII sites to create hAAG-2-his$_6$.

Transformation of Ligation Product into Competent Cell Q

The strain W3110 lacIq, referred to as Q, is a high efficiency transforming strain used to recover ligation products. Competent Q cells were transformed with the ligation products of the hAAG-2 PCR fragment and the pMV513 vector backbone. After transforming these ligation products into competent Q cells, six individual amp^r colonies were transferred from the transformation plate and were streaked on individual LB-Amp plates to purify them. Then, a single clone from each of these plates was inoculated in 5 mL of LB-Amp broth and grown overnight. Once the cells grew, the Qiagen mini-prep kit was used to purify the plasmids from the Q cells for analysis and transformation into glycosylase deficient cells.

Strain Numbers MV4147 and MV4148

After the plasmids were purified with the Qiagen mini-prep kit, several experiments were performed to confirm the accuracy of the sequence. First, the plasmids were cut with restriction enzymes EcoO109, Bst E II, EcoRI and Hind III, and EcoRI and Afe II (Figure 31 and data not shown).

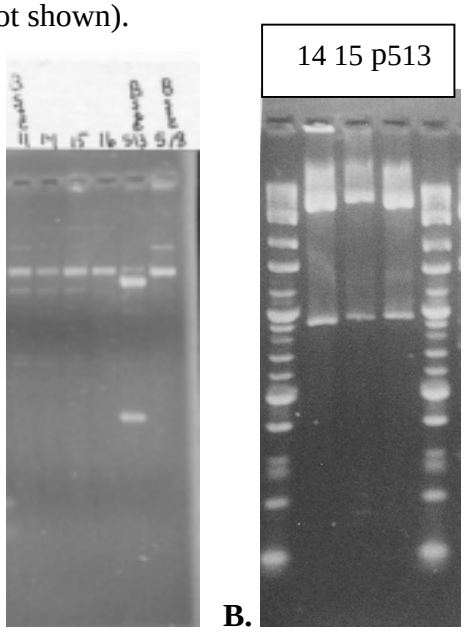

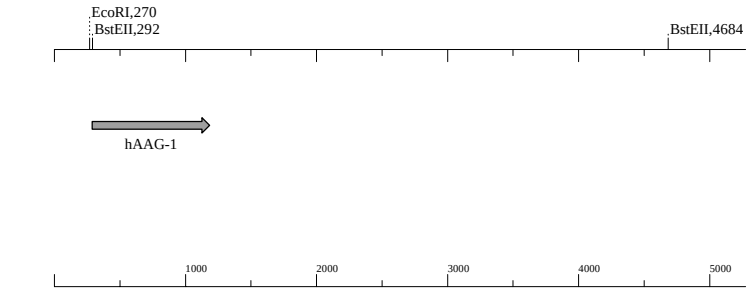

C. **PMV509.TXT** (5274 bps)

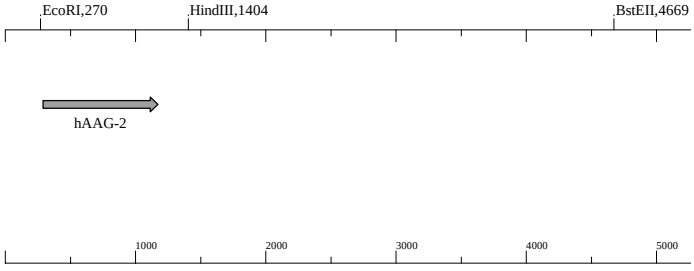

D. **PMV550.TXT** (5259 bps)

Figure 31: Confirmation of Ligation. A) Displays the BstE II restiction digests. Note the lane labeled "BstE 513" shows a band at 882 as "BstE II 518" does. Neither sample labeled 14 nor 15 have this band, showing consistency with pMV518. B) Samples 14 and 15 confer the appropriate insert/vector ratio with this EcoRI-Hind III restriction enzyme cut. C) Restriction map of hAAG-1 and the BstE II cut sites. D). Restriction map of hAAG-2 and the BstE II cut sites. Notice the restriction site at 292bp in hAAG-1 that is not present in hAAG-2. Data in A) confirm the presence of hAAG-2 in samples 14 and 15. C) and D) were created using Clone Manager 4.

These restriction enzymes were selected because clear distinctions could be made to pMV513 versus pMV536 and pMV537, the new form (Figure 31). These digested fragments were run on a 1% TAE agarose gel and the lengths of the bands were analyzed. There is an additional BsteII restriction site in exon 1 of hAAG-1, therefore it would be expected that the restriction map would show two bands, one at 882 and the other at 4.6 Kb. hAAG-2 would show only one band at 5.2 Kb (Figure 31). Two of the plasmids that produced the correct pattern were chosen for DNA sequencing by the University of Massachusetts Nucleic Acid DNA sequencing facility and were later resequenced at the Iowa State University DNA sequencing service facility. The plasmids pMV536 (Figure

31, sample 14) and pMV537 (Figure 31, sample 15) proved to be identical and had the desired DNA sequence. Thus, the Q cells containing plasmid pMV536 was provided the strain number MV4147. The Q cells containing plasmid pMV537 was given the strain number MV4148.

Construction of Expression Plasmids carrying hAAG-2 and hAAG-2-(his)$_6$

The EcoRI-Sal I site from pMV536 and pMV537 plasmids was cloned into the EcoRI-Sal I sites of pMV509 to convert the non his-tagged form of hAAG-1 upstream sequence to that of hAAG-2-his$_6$, thereby creating plasmids expressing the nontagged form of hAAG-2. Two plasmids were retained as pMV550 (hAAG-2 derived from pMV536) and pMV551 (hAAG-2 derived from pMV537) respectively (Figure 32).

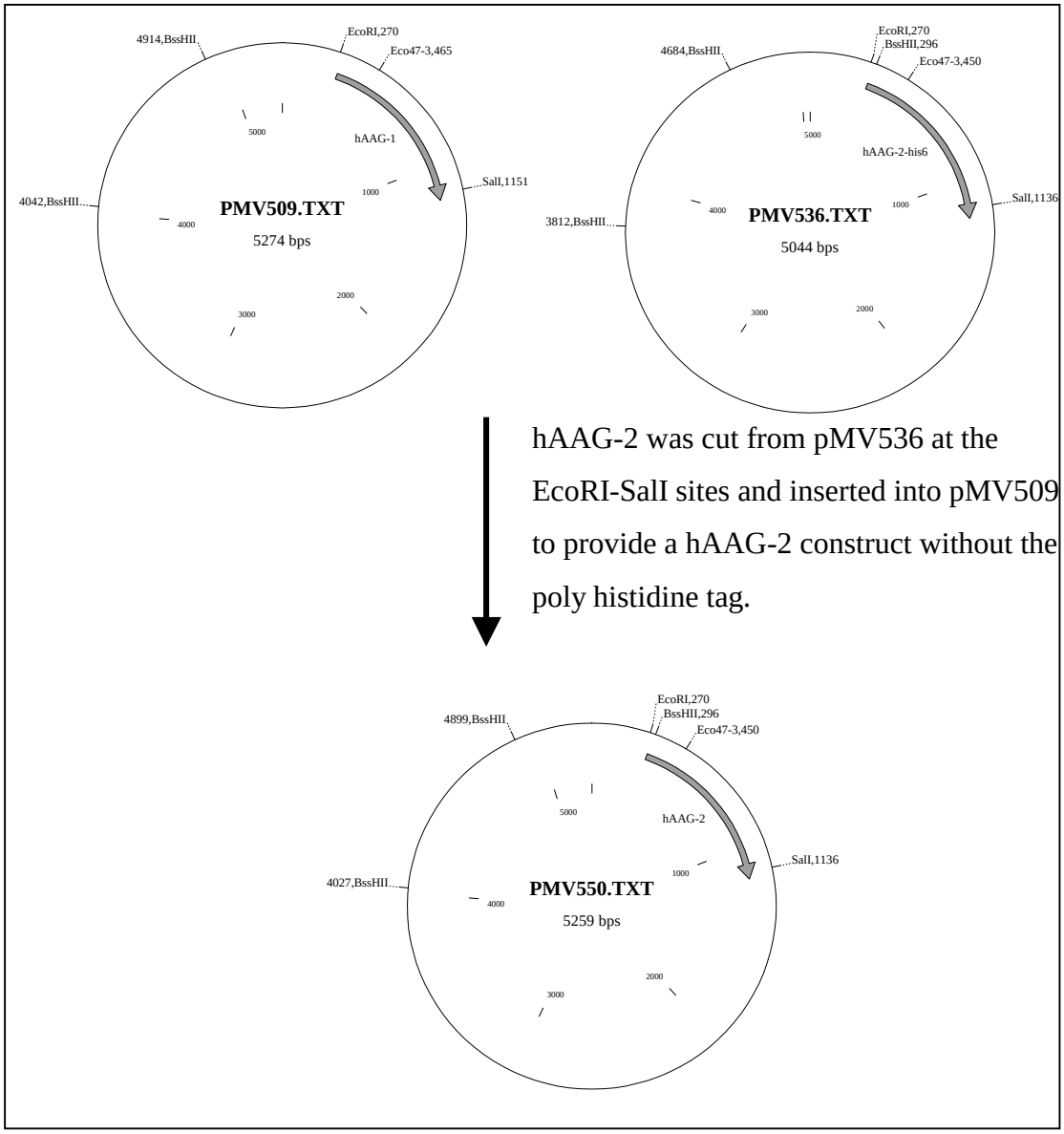

Figure 32: Restriction map showing the construction of hAAG-2. The EcoRI-SalI fragment from pMV536 was inserted into pMV509 lacking its own EcoRI-SalI site to create pMV550 (hAAG-2).

Exon 1 of the hAAG-2 gene has a BssHII site that is lacking in hAAG-1. Therefore, to confirm conversion, the plasmids were digested with Bss HII restriction endonuclease. The expected band sizes for hAAG-1 were 4402 bp and 872 bp and hAAG-2 were 656 bp, 872 bp, and 3.5 kb. Figure 33 demonstrates that the presumptive hAAG-2 bearing plasmids produce the expected BssHII restriction fragments, confirming their structure. Iowa State DNA Sequencing Facility provided further confirmation via sequence analysis. Thus, plasmids expressing hAAG-1, hAAG-1-his_6, hAAG-2, and hAAG-2-his_6 proteins containing identical upstream sequences were made available for future experiments.

A.

B. Top

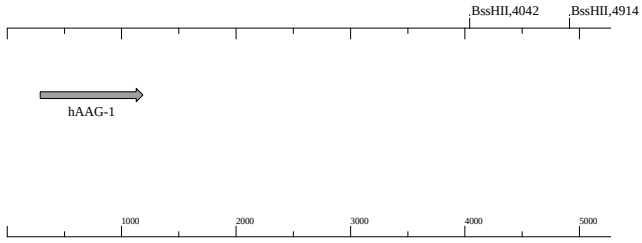

PMV509.TXT (5274 bps)

C.

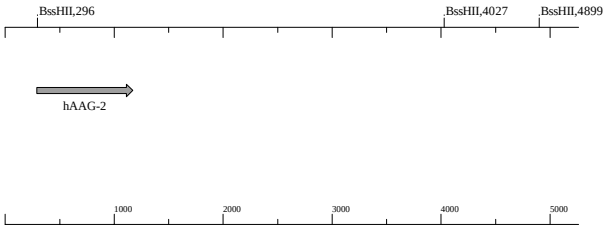

PMV550.TXT (5259 bps)

Figure 33: Confirmation that the EcoRI- Sal I piece from hAAG-2 was correctly inserted into the pMV509 vector. A) Lane 1 contains pMV550 and lane 2 contains pMV551. The expected band sizes are 656 bp, 872 bp,and 3.5 Kb. B). The restriction map of hAAG-1. Note that there are only two BssHII sites. C). The restriction map of hAAG-2. Note that there is an additional BssHII site than in hAAG-1. This additional site allows the performance of restriction analysis to compare each isoform.

Cell Survival Assays

The plasmids bearing hAAG-1, hAAG-1-his$_6$, hAAG-2, hAAG-2-his$_6$, and the vector pTRC99a were transformed into the glycosylase deficient *alkA tag*A *omp*T strain MV4210 to construct strains MV4224, MV4211, MV4232, MV4213, and MV4228. They were also transformed into the glycosylase and excision repair deficient *alkA tag*A *uvr*A strain MV3855 to construct strains MV4237, MV4238, MV4239, MV4240, and MV4236 respectively. These strains were then tested in timed survival experiments to determine if the expression of the human glycosylase genes could protect the cells against killing by alkylating agents and other DNA damaging agents. The survival is expressed as a percentage of untreated control. Data are presented as the Mean ± Standard Error from two to seven independent experiments.

MNNG

The following section displays the effect of the glycosylase activity on cell survival after exposure to MNNG.

MNNG Survival: Effect of the hAAG-1 and hAAG-2 genes

MNNG alkylates DNA by the covalent addition of a methyl group to the oxygen molecules within the phosphates of the DNA backbone and by forming lesions at various positions of the four bases. As explained above, the glycosylase activity of bacterial *alk*A and *tag*A genes are required for normal repair of MNNG damage (Friedberg et al, 1995). The hAAG enzyme has overlapping function with the *alk*A and *tag*A enzymes. This is confirmed in figure 34. The presence of induced hAAG-1 (closed circles) rescues cells deficient in *alk*A and *tag*A repair mechanisms. The IPTG induced hAAG-1 actually causes a higher survival level at higher doses in *E. coli* than the *alk*A *tag*A wild type genes, suggesting it repairs MNNG damage more efficiently than the bacterial glycosylases. This graph shows a dose response of both the hAAG-1 mutant and the wild type strain. At 30 minutes of exposure to 24 ug/ml of MNNG, the repair deficient *alk tag* mutant strain shows a survival level of 0.03%. When hAAG-1 is introduced into this

strain and induced, survival increases to approximately 32%. In contrast, the wild type repair proficient bacterial strain has a survival level of approximately 9%. The uninduced hAAG-1 mutant has approximately a 7% survival level at the same exposure, indicating that hAAG-1 is able to repair methylated lesions created by MNNG in bacteria.

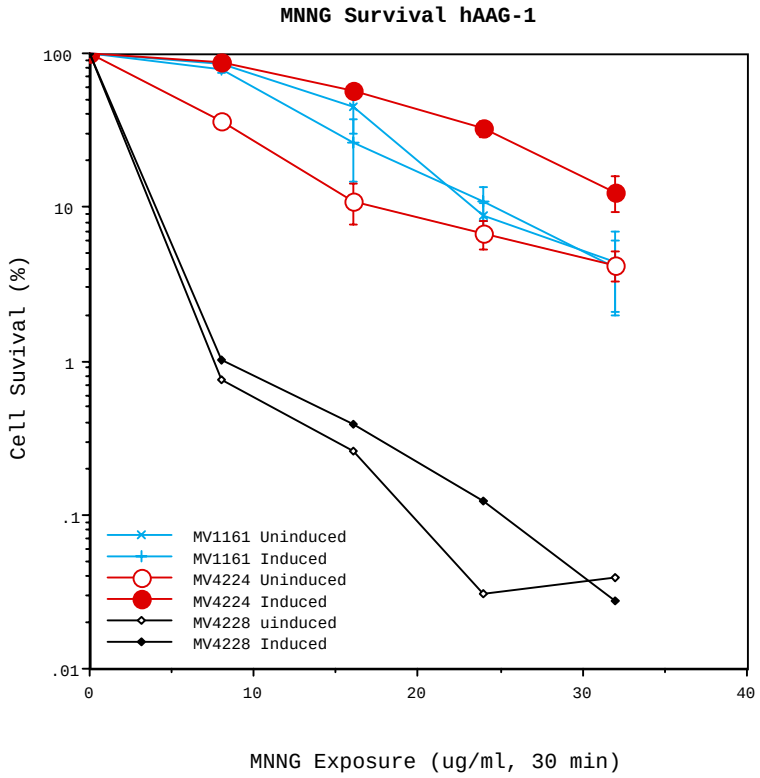

Figure 34: Effect of hAAG-1 on alkylation induced cell killing by MNNG. The induced sample containing hAAG-1 (closed circles) shows increased resistance to MNNG at higher concentrations. The uninduced sample of hAAG-1 remains with the wild type *E. coli* strain (MV1161, x and + symbols). The diamonds represent the vector control deficient in glycosylase acitivity. (MV1161, wild type; MV4224, *alk*A *tag*A/ phAAG-1(plasmid bearing hAAG-1); MV4228, *alk*A *tag* A/pTRC99a vector)

The second isoform of hAAG also confers increased resistance to MNNG in the repair deficient *alk*A *tag* mutant strain. The efficiency of hAAG-2, however, is slightly less than that of the wild type *alk tag* system. At 30 minutes of exposure to 24 ug/ml of MNNG, hAAG-2 induced cells have a 5.2% survival level while wild type cells have a survival level of approximately 9% (Figure 35). The uninduced hAAG-2 cells also

demonstrated approximately 1 log greater rescue than the double mutant control strain (open and closed diamonds).

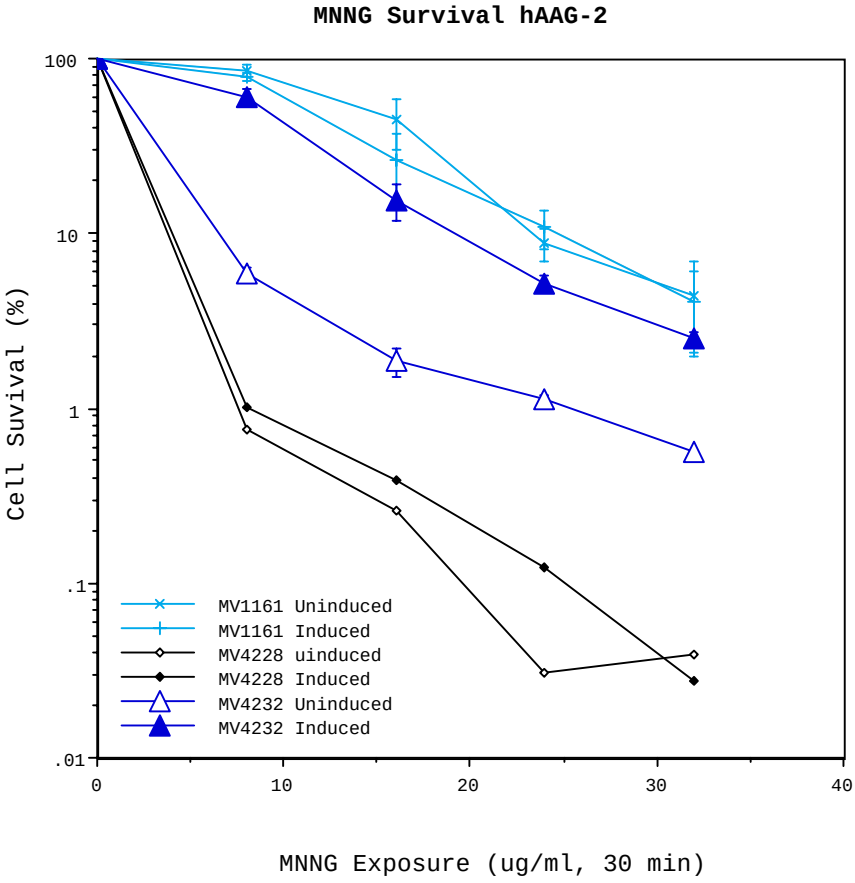

Figure 35: Effect of hAAG-2 on alkylation induced cell killing by MNNG. Closed triangles represent induced glycosylase, open triangles represent the uninduced sample. (MV1161, wild type; MV4228, *alk*A *tag* A/ pTRC99a vector; MV4232, *alk*A *tag*A/ phAAG-2 [plasmid bearing hAAG-2])

When exposed to MNNG, hAAG-2, provides resistance, but does not function as well as hAAG-1. At all doses tested, hAAG-1 increased survival to a greater level than hAAG-2. The survival level attained at an MNNG exposure of 8 ug/ml was 88% when hAAG-1 was expressed, while induced hAAG-2 increased survival to 60%. This difference in survival increased with dose. For example, hAAG-2 increased survival to 2.5% at 30 minutes exposure to 32 ug/ml of MNNG, while hAAG-1 increased survival to12% (Figures 34 and 35).

MNNG Survival: comparison of the hAAG-1 and hAAG-1-his$_6$ genes

The histidine tagged forms of hAAG were constructed for future purification of the enzyme and for use in *in vitro* DNA repair assays. Therefore, it is important to know if the histidine tags affect the repair activity of the hAAG gene products.

The hAAG-1-his$_6$ gene is the hAAG-1 gene with a his tag incorporated onto the end of its fourth exon. Figure 36 shows the rescue of MNNG treated cells by hAAG-1-his$_6$. The level of survival at 24 ug/ml MNNG is approximately 19.8% for the cells induced by IPTG while those uninduced, at the same level of MNNG exposure, were much more sensitive (3.5% survival level). At higher doses, hAAG-1-his$_6$ rescued cells more efficiently than the wild type glycosylases. For example, the level of survival at 24 ug/ml of MNNG exposure of the wild type *E. coli* strain MV1161 is 10% while that of the mutant *alk tag* deficient control is 0.12%.

Since the levels of resistance attained upon induction are similar to those seen with the non-histagged forms of hAAG, it suggests that the addition of the his–tag to hAAG-1 does not alter the ability of hAAG-1 to provide resistance to MNNG.

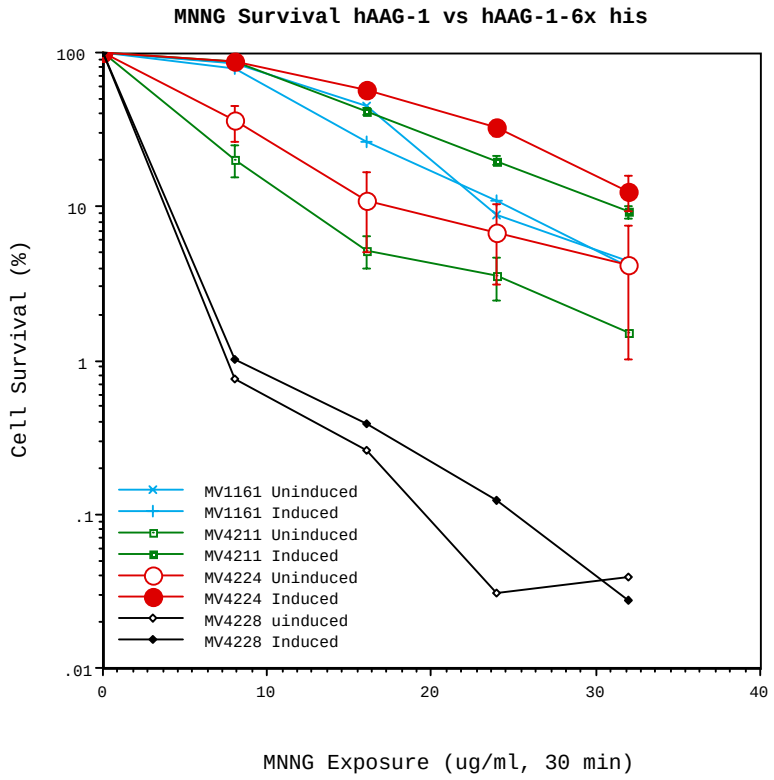

Figure 36: Effect of hAAG-1 (MV4224) and hAAG-1-his6 (MV4211) on alkylation induced cell killing by MNNG. The histidine tag has no effect on the ability of hAAG-1 to function. Closed squares represent induced his–tagged glycosylase, open squares represent uninduced his-tagged sample. (MV1161, wild type; MV4211, *alk*A *tag*A/ phAAG-1-his$_6$ [plasmid bearing hAAG-1-his$_6$]; MV4224, *alk*A *tag*A/ phAAG-1; MV4228, *alk*A *tag* A/ pTRC99a vector)

MNNG Survival: comparison of the hAAG-2 and hAAG-2-his$_6$ genes

The histidine tag to hAAG-2, like that to hAAG-1, also is incorporated on the fourth exon. Figure 37 shows the rescue of MNNG treated cells by hAAG-2-his$_6$. The level of survival at 24 ug/ml MNNG is approximately 5% for the cells induced by IPTG while those uninduced, at the same level of MNNG exposure, were one magnitude more sensitive (0.5% survival level). At higher levels, hAAG-2-his$_6$ resistance equalled that of the wild type *E. coli* proficient in its own *alk*A and *tag* genes. In the *alk tag* deficient mutant, hAAG-2-his$_6$ increased the level of survival quite substantially. At the MNNG

dose of 24 ug/ml, 5% of bacteria survive in the presence of hAAG-2-his$_6$, compared to only 0.12% in its absence. Thus, hAAG-2-his6 functions well against MNNG exposure at the doses tested and the histidine tag has no effect on the function of hAAG-2 when exposed to MNNG. hAAG-2-his$_6$ has similar characteristics to hAAG-2 at all dose levels tested (Figure 37).

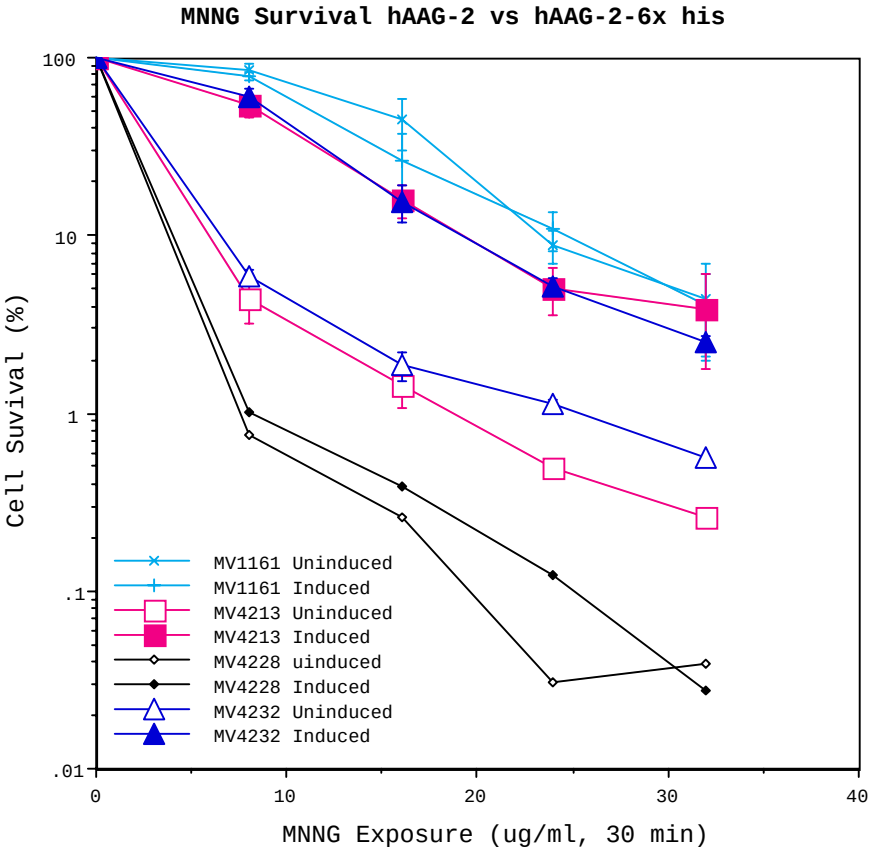

Figure 37: Effect of hAAG-2 (MV4232) and hAAG-2-his$_6$ (MV4213) on alkylation induced cell killing by MNNG. The histidine tag has no effect on the ability of hAAG-2 to function. Closed squares represent induced his–tagged glycosylase, open squares represent uninduced his-tagged sample. (MV1161, wild type; MV4213, *alk*A *tag*A/ phAAG-2-his$_6$ [plasmid bearing hAAG-2-his$_6$]; MV4228, *alk*A *tag* A/ pTRC99a vector; MV4232, *alk*A *tag*A/ phAAG-2)

When induced hAAG-1-his_6 and hAAG-2-his_6 are compared (Figure 36 small closed squares and Figure 37, large closed squares, respectively), hAAG-1-his_6 appears to be more efficient in recovering *e. coli* cells from MNNG killing.

Conclusions for MNNG

Overall, the results from the cell survival tests involving MNNG prove that hAAG-1 and hAAG-2 are able to repair DNA damage produced by the methylating agent MNNG as indicated by the increase in MNNG resistance seen in the repair deficient *alk*A *tag* double mutant strain in the presence of the hAAG forms tested. The results demonstrate that the overexpression of hAAG-1 provides a higher level of resistance than is seen in the repair proficient wild type bacterial strain. The results also show that there are slight differences between hAAG-1 and hAAG-2 and that the his-tagged forms function in a similar manner as their non- tagged forms indicating that the his tags do not affect the activity of either form of hAAG.

MMS

The following section displays the effect of the glycosylase activity on cell survival after exposure.

MMS Survival: Effect of the hAAG-1 and hAAG-2 genes

MMS alkylates DNA by attaching a methyl group to the nitrogen molecules at various positions of the four bases. Glycosylase activity of bacterial *alk*A and *tag*A genes is required for normal repair of MMS damage (Friedberg et al, 1995). The data in Figure 38 further supports the overlapping function of the hAAG enzyme compared to the function of the *alk*A and *tag*A enzymes. The presence of induced hAAG (closed circles) rescues cells deficient in *alk*A and *tag*A repair to the same extent as the *E. coli alk*A *tag*A wild type genes, suggesting human glycosylase repairs MMS damage as efficiently as the bacterial glycosylases. This graph (Figure 38) shows a similar dose response of both the hAAG-1-containing deficient *alk*A *tag* mutant and the wild type strain. At 30 minutes of exposure to 20 mM of MMS, the repair deficient *alk*A *tag*

mutant strain shows a survival level of 0.02%. When hAAG-1 is introduced into this strain and induced, survival increases to approximately 62%. Similarly, the wild type repair proficient bacterial strain has a survival level of approximately 64%. The uninduced hAAG-1 mutant has approximately a 3% survival level at the same exposure, indicating that hAAG-1 is able to repair methylated lesions created by MMS in bacteria.

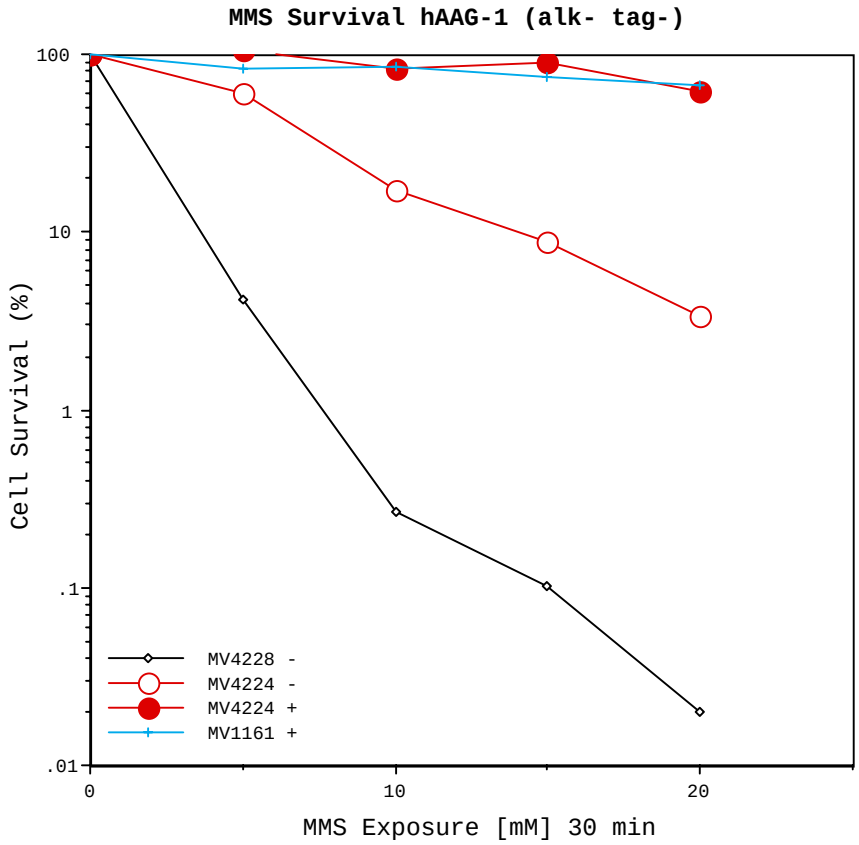

Figure 38: Effect of hAAG-1 on alkylation induced cell killing by MMS. The induced sample containing hAAG-1 (closed circles) shows increased resistance to MMS at higher concentrations. The uninduced sample of hAAG-1 remains with the wild type *E. coli* strain (MV1161, + symbols). (MV1161, wild type; MV4224, *alk*A *tag*A/ phAAG-1; MV4228, *alk*A *tag* A/ pTRC99a vector)

The second isoform of hAAG also confers increased resistance to MMS in the repair deficient *alk*A *tag* mutant strain. The efficiency of hAAG-2, however, is slightly less than that of the wild type *alk tag* system. At 30 minutes of exposure to 20 mM of MMS, hAAG-2 induced cells show 23% survival level while wild type cells have a survival level of approximately 64% (Figure 39). The uninduced hAAG-2 cells (2%

survival level) also demonstrate greater rescue than the double mutant control strain (0.02% survival level, open and closed diamonds) by two orders of magnitude at 20 mM of exposure to MMS, indicating that even low levels of hAAG-2 protein can confer increased MMS resistance. Thus, hAAG-2 effectively rescues bacteria deficient in their own repair mechanism from damage due to exposure to MMS.

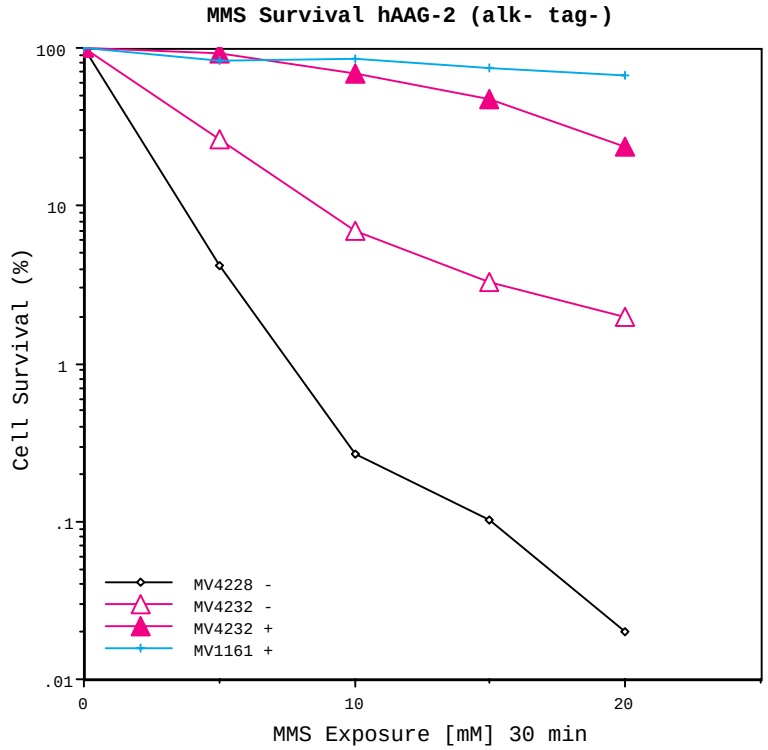

Figure 39: Effect of hAAG-2 on alkylation induced cell killing by MMS. Closed triangles represent induced glycosylase, open triangles represent the uninduced sample. (MV1161, wild type; MV1176, *uvr*A; MV4228, *alk*A *tag* A/ pTRC99a vector; MV4232, *alk*A *tag*A/ phAAG-2)

Comparison of the resluts in Figures 38 and 39 sugguest that hAAG-2 protect *E. coli* cells to somewhate lesser extent than the hAAG-1 form from MMS toxicity. However, this difference in survival level is narrower compared to that of MNNG (Figures 34 and 35).

MMS Survival: comparison of hAAG-1 and hAAG-2 activity in uvr*A deficient and proficient strains*

The *uvr*A mutation inactivates the nucleotide excision repair (NER) pathway in *E. coli* (see: Friedberg et al., 1995). The results in Figure 40 (star symbols, MV1176) show that the *uvr*A mutation in a base excision repair wild type background does not sensitize cells to MMS. In addition, the *uvr*A mutation does not increase sensitivity to MMS of *alk*A *tag* glycosylase deficient *E. coli* cells (compare Figure 38 and 40, diamonds). The results in Figure 40 however suggest that the presence of functional *E. coli* nucleotide excision repair slightly increases, a protection provided by human AAG-2 against MMS toxicity.

The NER pathway may be more important for the repair of DNA adducts bulkier than a methyl group. DNA lesions that have adducts greater in size than methyl groups, such as the ethyl group or mitomycin crosslinks, are repaired by the *uvr*ABC nucleotide excision repair system (Van Hauten, 1990). Since bulky adducts are introduced by other agents in this study, and since such repair activity could mask the effect of the human DNA glycosylase activity, the remaining cell survival experiments were performed in the *alk*A *tag*A *uvr*A triple mutant background.

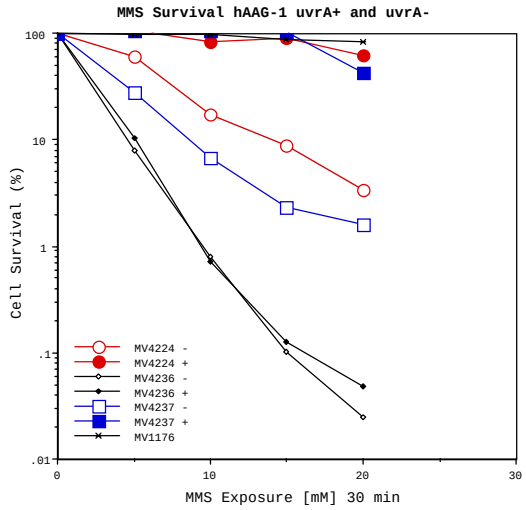

Figure 40: Effect of hAAG-1 on alkylation induced cell killing by MMS in the presence and absence of the uvrA gene. hAAG-1 *alk*A *tag* (closed circles) and hAAG-1 *alk*A *tag uvr*A (closed squares) rescue cells from MMS damage to the same extent. The alk+ tag+ uvrA- control also rescues cells quite efficiently (star symbol). (MV1176, *uvr*A; MV4224, *alk*A *tag*A/ phAAG-1; MV4236, *alk*A *tag* A *uvr*A pTRC99a vector; MV4237, *alk*A *tag*A *uvr*A/ phAAG-1)

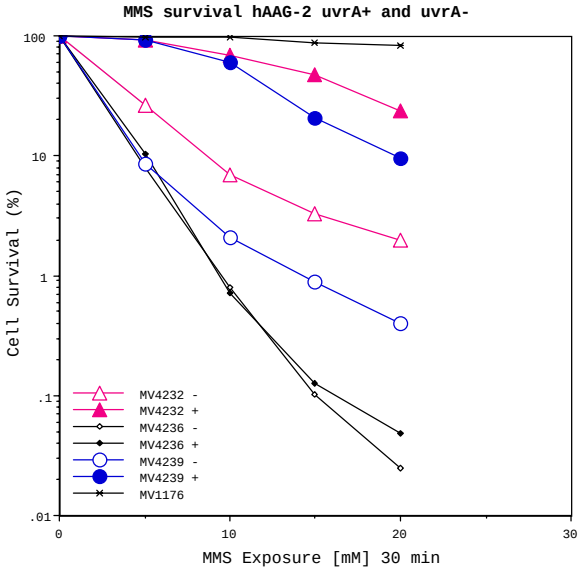

Figure 41: Effect of hAAG-2 on alkylation induced cell killing by MMS in the presence and absence of the uvrA gene. hAAG-2 rescues cells from MMS damage to a greater extent in the *alk*A *tag* (closed triangles) than in the *alk*A *tag uvr*A background (closed circles). The *uvr*A mutation in the *alk*A^{+} *tag*$^{+}$ background (star symbols) does not sensitize cells to MMS. (MV1176, *uvr*A; MV4232, *alk*A *tag*A/ phAAG-2; MV4236, *alk*A *tag* A *uvr*A pTRC99a vector; MV4239, *alk*A *tag*A *uvr*A/ phAAG-2)

MMS Survival: comparison of the hAAG-1 and hAAG-1-his$_6$ genes

Figure 42 shows the rescue of MMS treated cells by hAAG-1-his$_6$. The level of survival at 20 mM MMS is approximately 43% for the cells induced by IPTG while those uninduced, at the same level of MMS exposure, were much more sensitive (0.5% survival level). hAAG-1-his$_6$ and hAAG-1 have extremely similar survival patterns, suggesting that the addition of the his–tag to hAAG-1 does not alter the ability of hAAG-1 to provide resistance to MMS. hAAG-1-his$_6$ rescues cells just as efficiently as the *uvr*A deficient *E. coli* strain MV1176. The level of survival at 15 mM of MMS exposure of the *uvr*A deficient *E. coli* strain MV1176 is 87% while that of hAAG-1-his$_6$ is 64%. The mutant *alk tag uvr*A deficient control is 0.11% (Figure 42).

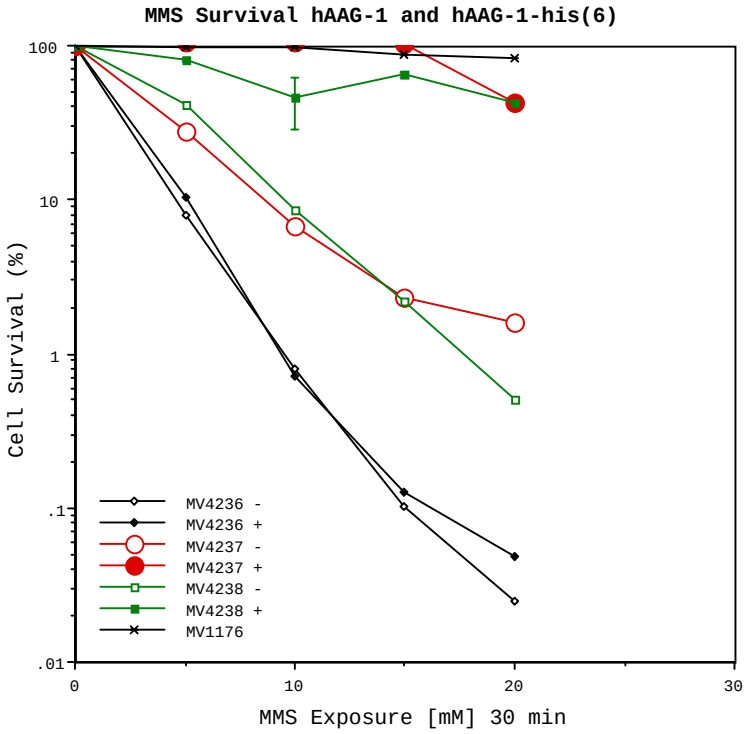

Figure 42: Effect of hAAG-1 (MV4237) and hAAG-1-his6 (MV4238) on alkylation induced cell killing by MMS. The histidine tag has no effect on the ability of hAAG-1 to function. Closed squares represent induced his–tagged glycosylase, open squares represent uninduced his-tagged sample. (MV1176, *uvr*A; MV4236, *alk*A *tag* A *uvr*A pTRC99a vector; MV4237, *alk*A *tag*A *uvr*A/ phAAG-1; MV4238, *alk*A *tag*A *uvr*A/ phAAG-1-his$_6$)

MMS Survival: comparison of the hAAG-2 and hAAG-2-his$_6$ genes

The addition of the histidine tag to hAAG-2, like that of hAAG-1, has little effect on the ability of hAAG to function (Figure 43). The rescue of MMS treated cells by hAAG-2-his$_6$, when induced, obtains survival levels approaching those of hAAG-2. The level of survival at 20 mM MMS is approximately 4.1% for the cells bearing the hAAG-2-his$_6$ plasmid. At the same level of MMS exposure, hAAG-2 has a 9.5% survival level. While the level of hAAG-2-his$_6$ survival at 20 mM MMS provides resistance to cells induced by IPTG, uninduced cells, at the same level of MMS exposure, were just as sensitive as the triple mutant strain (0.03% survival level). hAAG-2-his$_6$ and hAAG-2 have similar survival levels when induced, suggesting that the addition of the his–tag to hAAG-2 does not alter the ability of hAAG-2 to rescue cells from DNA damage caused by exposure to MMS.

Compared to the *alk tag uvr*A deficient mutant, hAAG-2-his$_6$ increased the level of survival dramatically at exposure to 20 mM of MMS when induced. hAAG-2-his$_6$ has a survival level of 4.1% at 20 mM MMS exposure while the triple mutant has a survival level of 0.25%, a decrease of more than two orders of magnitude Thus, hAAG-2-his$_6$ functions well against MMS exposure at the doses tested.

In the induced sample, the histidine tag has no effect on the function of hAAG-2 when exposed to MMS. However, uninduced samples showed no basal level activity. This deviates from results obtained by MNNG expsoure, albiet in the double mutant strain (Figure 35, above). Nonetheless, induced hAAG-2-his$_6$ has similar characteristics to induced hAAG-2 at all dose levels tested, thus the histidine tag does not affect hAAG-2 activity (Figure 43).

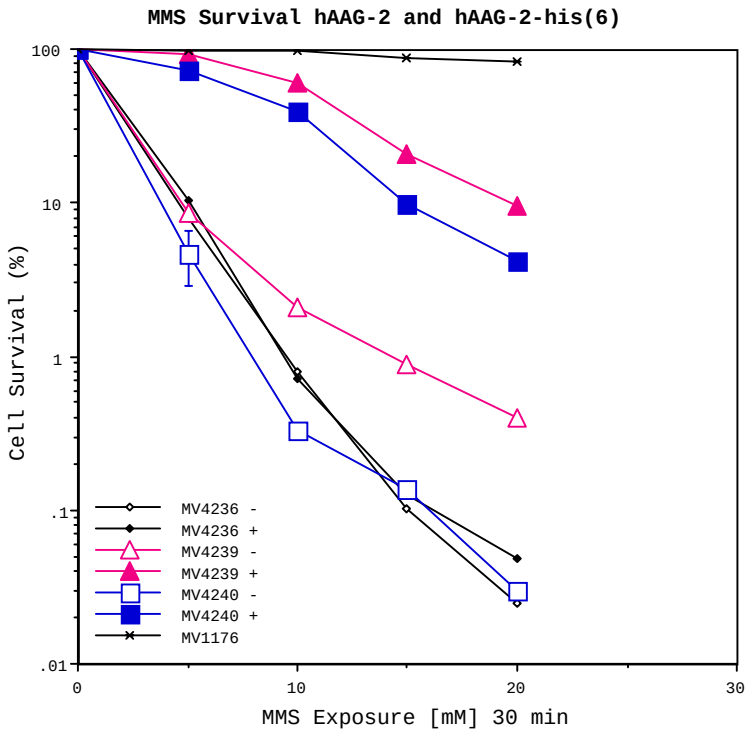

Figure 43: Effect of hAAG-2 (MV4239) and hAAG-2-his6 (MV4240) on alkylation induced cell killing by MMS. The histidine tag has no effect on the ability of hAAG-2 to function, however uninduced hAAG-2-his(6) show no basal level expression. Closed squares represent induced his–tagged glycosylase, open squares represent uninduced his-tagged sample. (MV1176, *uvr*A; MV4236, *alk*A *tag* A *uvr*A pTRC99a vector; MV4239, *alk*A *tag*A *uvr*A/ phAAG-2; MV4240, *alk*A *tag*A *uvr*A/phAAG-2-his$_6$)

Each histidine tagged form of hAAG has a similar ability to restore MMS resistance to that of the non-tagged forms. The levels of survival, however, for each form, were slightly lower than that of their non-tagged forms. This difference, however, was not statistically significant due to statistical analysis of experimental error. As was the case for the nontagged gene products, hAAG-1-his$_6$ functioned more efficiently than hAAG-2-his$_6$ (Figures 42 and 43).

Conclusions for MMS

Overall, the results from the cell survival tests involving MMS support those obtained from exposure to MNNG and prove that hAAG-1 and hAAG-2 are able to

rescue DNA from the damage produced by the methylating agent MMS. This is indicated by the large increase in MMS resistance observed when *alk*A *tag*A cells expressing any of the forms of the hAAG are exposed to MMS. The results of the *alk*A *tag uvr*A triple mutant strain further show that nucleotide excision repair is not needed to fix methylated lesions and that hAAG complementation is as effective as the *alk*A *tag*A *uvr*A^+ strain. These results demonstrate that the overexpression of hAAG-1 functions as well as the wild type *E. coli* glycosylases in the *uvr*A proficient and deficient strains.

The results also show that there are slight differences between hAAG-1 and hAAG-2, consistant with the results from MNNG exposure. hAAG-1-his_6 and hAAG-2-his_6 function in a similar manner as their non- tagged forms. Thus, differences between hAAG-1 and hAAG-2 are also present in the his-tagged forms.

The Nitrosoureas

Cells expressing each form of hAAG in the triple mutant background were exposed to two members of the nitrosourea family of DNA damaging agents: CNU and BCNU.

CNU

The following section displays the effect of human glycosylase on survival of *E. coli* cells after exposure to CNU.

CNU Survival: Effect of the hAAG-1 and hAAG-2 genes

CNU is known to crosslink DNA from cytosine to guanine residues. Glycosylase activity of bacterial *alk*A and *tag*A genes does not normally repair lesions created by CNU damage because the adducts created are beyond the substrate specificity of the bacterial glycosylases (Friedberg et al, 1995). The function of the hAAG enzyme may differ from that of its *E. coli* homologs in this type of DNA repair. In mouse cells, the absence of hAAG has been shown to sensitize cells to BCNU and Mitomycin C exposure suggesting that hAAG is required for repair of BCNU and Mitomycin C damage (Engleward et al, 1997). However, the presence of induced hAAG (closed circles) does

not rescue cells deficient in *alk*A *tag*A and *uvr*A repair mechanisms (Figure 44). This suggests that hAAG-1 does not repair CNU damage as efficiently as methylation damage. In fact, the presence of hAAG at the higher dose ranges actually is slightly toxic to the cells. At 30 minutes of exposure to 0.5 mM of CNU, the repair deficient *alk tag uvr*A mutant strain shows a survival level of 0.17%. When hAAG-1 is introduced into this strain and induced, sensitivity increases to an approximately survival level of 0.023%. The wild type repair proficient bacterial strain has a survival level of approximately 18.5% at 0.5 mM CNU exposure for 30 minutes. At the same exposure, the uninduced hAAG-1 mutant has approximately an 0.18% survival level, indicating that strain lacking *alk*A *tag* and *uvr*A is more sensitive by two orders of magnitude than the wild type strain. Also displayed in this figure, is the *E. coli* mutant deficient in the *uvr*A gene. This strain is also sensitive to CNU exposure. The level of survival is comparable with that of the triple mutant, suggesting that the *alk*A and *tag* genes have a small role in the repair of CNU generated damage to the *E. coli* genome. Thus, comparing the wild type to the *uvr*A deficient strain provides evidence that the nucleotide excision repair mechanism is needed for the repair of CNU damaged lesions. These data indicate that hAAG-1 is not able to repair lesions created by CNU in bacteria and that the nucelotide excision repair system is used on DNA damage created by CNU exposure (Figure 44).

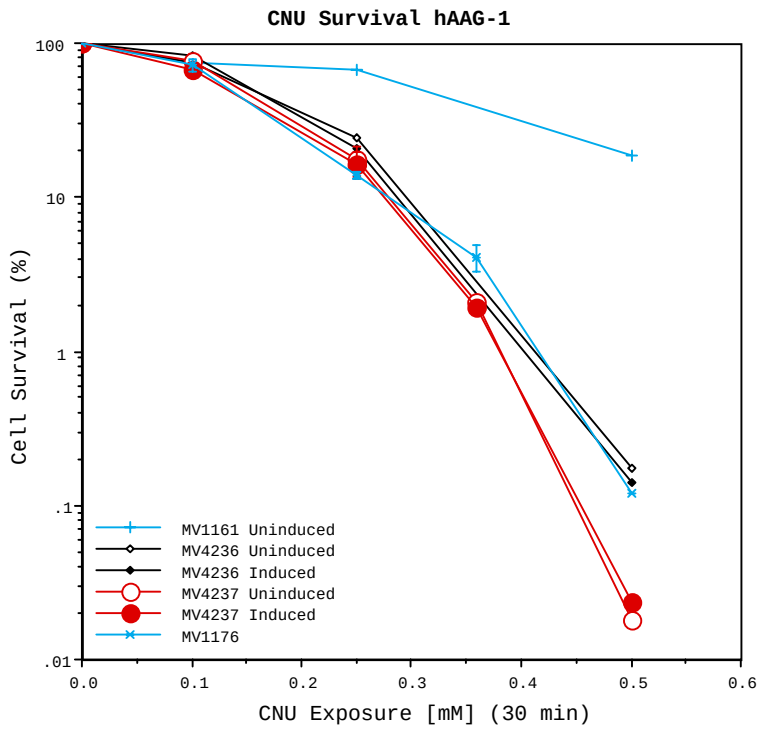

Figure 44: Effect of hAAG-1 on induced cell killing by CNU. The induced sample containing hAAG-1 (closed circles) shows increased sensitivity to CNU at higher concentrations. Interestingly, the wild type *E.coli* shows some resistance to CNU exposure, but once the *uvr*A gene is removed, the bacterial glycosylases alone are not able to rescue the cells, thus the survival level drops to that of the triple mutant strain. The uninduced sample of hAAG-1 remains as sensitive as the *alk*A$^+$ *tag*$^+$ *uvr*A deficient *E. coli* strain (MV1176, star symbols) and becomes more sensitive at higher doses. (MV1161, wild type; MV1176, *uvr*A; MV4236, *alk*A *tag* A *uvr*A pTRC99a vector; MV4237, *alk*A *tag*A *uvr*A/ phAAG-1)

The second isoform of hAAG also confers increased sensitivity to high CNU dose in the repair deficient *alk*A *tag uvr*A mutant strain. hAAG-2, like hAAG-1, is more toxic than the glycosylases of the wild type *alk tag* system. At 30 minutes of exposure to 0.5 mM of CNU, hAAG-2 induced cells have a 0.021% survival level, while wild type cells have a survival level of approximately 18.5% (Figure 45, closed triangles). The uninduced hAAG-2 cells (0.028% survival level at 0.5 mM of CNU exposure) also demonstrate greater cellular toxicity than the triple mutant control strain (0.17% survival level at 0.5 mM of CNU exposure, open and closed diamonds). This increased sensitivity of strains bearing the hAAG-2 plasmid is nearly an order of magnitude at 0.5 mM of

exposure to CNU. Thus, hAAG-2 does not rescue bacteria deficient in their own repair mechanism from damage due to exposure to CNU, but actually increases sensitivity to the DNA damaging agent.

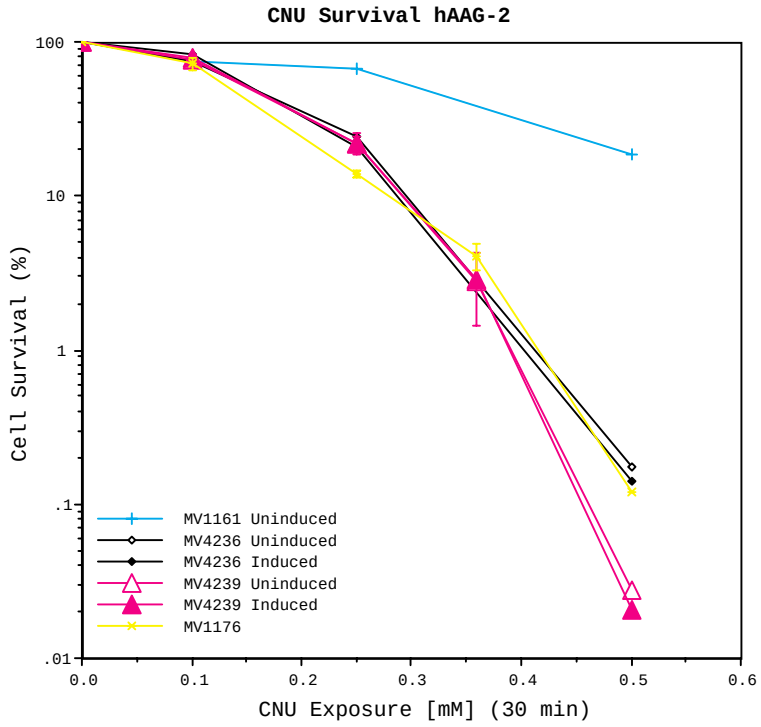

Figure 45: Effect of hAAG-2 on DNA damage induced cell killing by CNU. Closed triangles represent induced glycosylase in the *alk*A *tag* *uvr*A deficient background, open triangles represent the uninduced sample in the same background. (MV1161, wild type; MV1176, *uvr*A; MV4236, *alk*A *tag* A *uvr*A pTRC99a vector; MV4239, *alk*A *tag*A *uvr*A/ phAAG-2)

When exposed to a high dose of CNU, the presence of hAAG-1 and hAAG-2 make the cells more sensitive. Both isoforms function in a similar manner. At low levels of CNU exposure, hAAG-1 and hAAG-2 both have similar survival levels, which are actually analogous to the triple gene, *alk*A *tag*, and *uvr*A deficient mutant. For example, at 0.25mM of CNU exposure for 30 minutes, hAAG-1 has a survival level of 16%, hAAG-2 has a survival level of 21.8%, and the triple mutant has a survival level of 21%. However, as the dose concentration increases, so too does the separation in sensitivity until the presence of hAAG increases sensitivity of the *alk*A, *tag* proficient strain (Figure 45).

CNU Survival comparison of the hAAG-1 and hAAG-1-his$_6$ genes

Figure 46 shows the sensitivity of hAAG-1-his$_6$ to CNU treatment. The level of survival at 0.5 mM CNU is approximately 0.048% for the cells induced by IPTG while those uninduced, at the same level of CNU exposure, were equally as sensitive (0.040% survival level). hAAG-1-his$_6$ and hAAG-1 have extremely similar survival levels, suggesting that the addition of the his–tag to hAAG-1 does not resistance to CNU. hAAG-1-his$_6$ does not affect sensitivity of the *uvr*A deficient *E. coli* strain MV1176 until it is treated at the highest dose of 0.5 mM CNU for 30 minutes. Thus, hAAG-1-his$_6$ increases sensitivity of the *uvr*A deficient *E. coli* strain MV1176 at the highest doses. The level of survival at 0.36 mM of CNU exposure of the *uvr*A deficient *E. coli* strain MV1176 is 4% while that of hAAG-1-his$_6$ is 2.4%, a relatively similar level of survival. However, at 0.5 mM CNU exposure, the *uvr*A deficient bacteria have a 0.12% survival level while the strain bearing the plasmid containing hAAG-1-his$_6$ has a 0.048% survival. The same pattern is seen for the strain bearing the plasmid containing hAAG-1. At 0.5 mM CNU exposure, the strain containing the plasmid bearing hAAG-1 has a 0.023% survival level. Thus, the presence of hAAG-1, whether his-tagged or normal, increases sensitivity with respect to the mutant *alk tag uvr*A deficient control (0.14% survival level at 0.5 mM CNU exposure) and the *uvr*A deficient strain (Figure 46).

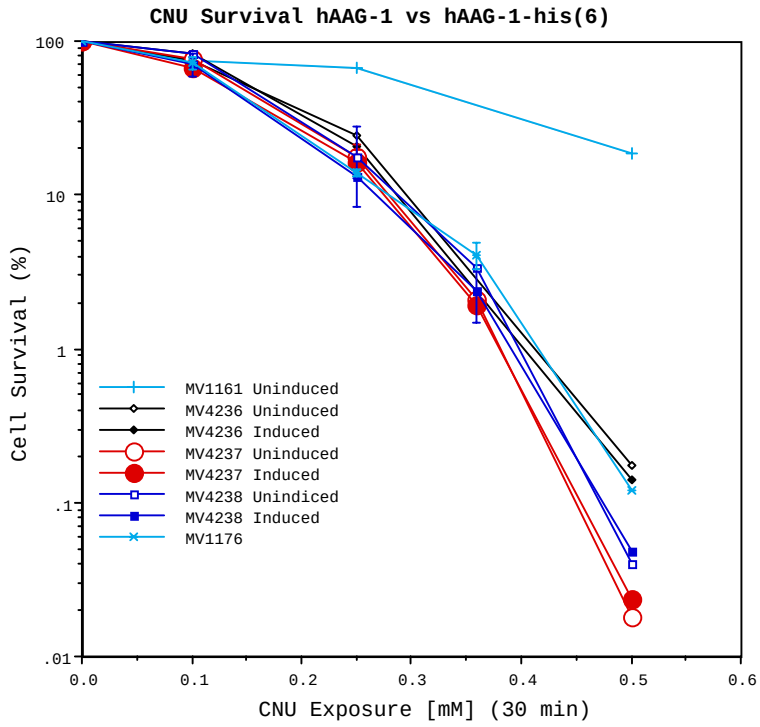

Figure 46: Effect of hAAG-1 (MV4237) and hAAG-1-his6 (MV4238) on induced cell killing by CNU. The histidine tag has no effect on the ability of hAAG-1 to function, although when hAAG-1 functions, greater levels of sensitivity are achieved at higher doses. Closed squares represent induced his–tagged glycosylase in the *alk*A *tag* *uvr*A triple mutant background, open squares represent uninduced his-tagged sample in the same triple mutant background. (MV1161, wild type; MV1176, *uvr*A; MV4236, *alk*A *tag* A *uvr*A pTRC99a vector; MV4237, *alk*A *tag*A *uvr*A/ phAAG-1; MV4238, *alk*A *tag*A *uvr*A/ phAAG-1-his$_6$)

CNU Survival comparison of the hAAG-2 and hAAG-2-his$_6$ genes

The addition of the histidine tag to hAAG-2, like that of hAAG-1, has little effect on the ability of hAAG to function (Figure 47). hAAG-2-his$_6$ is sensitive to CNU treatment and becomes more sensitive at higher concentrations. The level of survival at 0.5 mM CNU is approximately 0.025% for the cells induced by IPTG while those uninduced, at the same level of CNU exposure, were equally as sensitive (0.018% survival level). hAAG-2-his$_6$ and hAAG-2 have extremely similar survival levels, suggesting that the addition of the his–tag to hAAG-2 does not alter the ability of hAAG-2 to provide resistance to CNU. The survival of hAAG-2-his$_6$ is equal to that of the *uvr*A

deficient *E. coli* strain MV1176 until it is treated at the highest dose of 0.5mM CNU for 30 minutes. Thus, hAAG-2-his$_6$ is more sensitive at this dose than the *uvr*A deficient *E. coli* strain MV1176. The level of survival at 0.36 mM of CNU exposure of the *uvr*A deficient *E. coli* strain MV1176 is 4% while that of hAAG-2-his$_6$ is 3.7%, a relatively similar level of survival. However, at 0.5 mM CNU exposure, the *uvr*A deficient bacteria have a 0.12% survival level while the strain bearing the plasmid containing hAAG-1-his$_6$ has a 0.025% survival. The same survival level occurs for the strain bearing the plasmid containing hAAG-2. At 0.5 mM CNU exposure, the strain containing the plasmid bearing hAAG-2 has a 0.021% survival level. Therefore, the presence of hAAG-2, like hAAG-1, whether his-tagged or normal, increases sensitivity with respect to the mutant *alk tag uvr*A deficient control, which has a survival level of 0.14% at 0.5 mM CNU exposure, and the *uvr*A deficient strain (Figure 47).

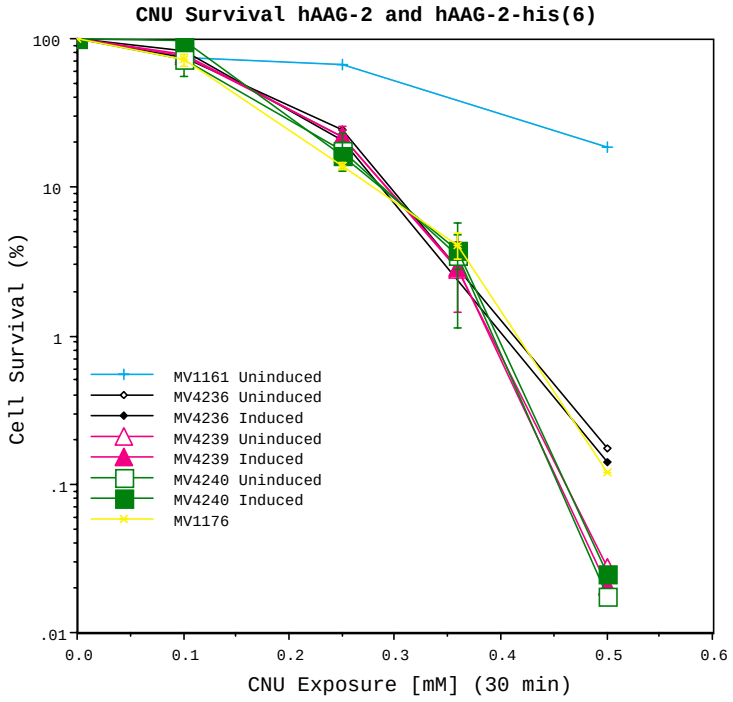

Figure 47: Effect of hAAG-2 (MV4239) and hAAG-2-his6 (MV4240) on induced cell killing by CNU. The histidine tag has no effect on the ability of hAAG-2 to function, although when hAAG-1 functions, greater levels of sensitivity are achieved at higher doses. Closed squares represent induced his–tagged glycosylase in the *alk*A *tag* *uvr*A triple mutant background, open squares represent uninduced his-tagged sample in the same background. (MV1161, wild type; MV1176, *uvr*A; MV4236, *alk*A *tag* A *uvr*A pTRC99a vector; MV4239, *alk*A *tag*A *uvr*A/ phAAG-2; MV4240, *alk*A *tag*A *uvr*A/phAAG-2-his$_6$)

Conclusions for CNU

Overall, the results from the cell survival tests involving CNU are quite different from those observed from exposure to MNNG and MMS. These data prove that hAAG-1 and hAAG-2 are not able to rescue *E. coli* cells from the damage produced by the DNA crosslinking agent CNU. This is based on the lack of increased resistance when strains expressing any of the forms of the hAAG forms are exposed to CNU in the repair deficient *alk*A *tag uvr*A triple mutant strain. A deleterious role of hAAG is suggested by the increased sensitivity seen at high CNU doses when hAAG is expressed. The results of the two control strains (wild type strain and glycosylase proficient, excision repair deficient strain) show that, in *E. coli*, nucleotide excision repair is needed to fix lesions created by CNU exposure (Figure 47, above).

The results also show that the only noticeable differences between hAAG-1 and hAAG-2 involves the level of sensitivity at the 0.5 mM dose. hAAG-2 is slightly more sensitve than hAAG-1 at this dose (Figure 48). hAAG-1-his$_6$ and hAAG-2-his$_6$ function in a similar manner as their non- tagged forms. Thus, the differences between hAAG-1 and hAAG-2 are also present in the his-tagged forms.

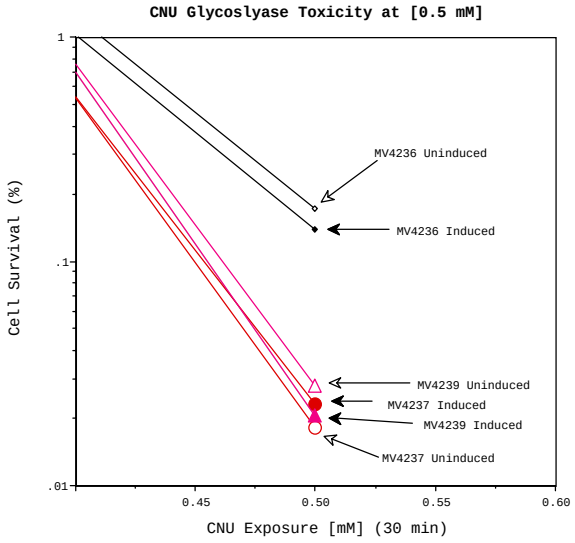

Figure 48: Toxic Effect of hAAG-1 and hAAG-2 on induced cell killing by CNU at 0.5mM. hAAG-1 *alk*A *tag uvr*A strain (closed circles) and hAAG-2 *alk*A *tag uvr*A strain are more sensitive to the cell than the strain deficient in *alk*A *tag uvr*A (diamond symbols) when exposed to CNU at 0.5mM for 30 minutes. (MV4236, *alk*A *tag* A *uvr*A pTRC99a vector; MV4237, *alk*A *tag*A *uvr*A/ phAAG-1; MV4239, *alk*A *tag*A *uvr*A/ phAAG-2)

BCNU

The following section describes the effect of the human glycosylase on the survival of *E. coli* cells exposed to BCNU.

BCNU Survival: Effect of the hAAG-1 and hAAG-2 genes

BCNU is a DNA damaging agent that crosslinks DNA. Glycosylase activity of bacterial *alk*A and *tag*A genes does not normally repair lesions created by BCNU damage, for similar reasons to CNU, because the adducts created by BCNU are beyond the substrate specificity of the bacterial glycosylases (see: Friedberg et al, 1995). The function of the hAAG enzyme may differ from that of its *E. coli* homologs in the repair of BCNU lesions. The absence of mouse AAG has been shown to sensitize cells to BCNU and Mitomycin C exposure, thus mouse AAG protects against cell killing by BCNU and Mitomycin C (Engleward et al, 1996, Engleward et al, 1998). However, the presence of induced hAAG (closed circles) does not rescue cells deficient in *alk*A *tag*A and *uvr*A repair mechanisms (Figure 49). This suggests that hAAG-1 does not repair BCNU damage as efficiently as methylation damage. The wild type *E.coli* shows some resistance to BCNU exposure, but once the *uvr*A gene is removed, the bacterial glycosylases alone are not able to rescue the cells, thus the survival level of the *uvr*A strain is identical to that of the *alk*A *tag uvr*A triple mutant strain. In fact, the presence of hAAG-1 at the higher dose ranges actually increases sensitivity. At 30 minutes of exposure to 3 mM of BCNU, the repair deficient *alk tag uvr*A mutant strain shows a survival level of 0.353%. When hAAG-1 is introduced into this strain and induced, sensitivity increases one order of magnitude to the survival level of 0.030%. The wild type repair proficient bacterial strain has a survival level of approximately 31% at 3 mM BCNU exposure for 30 minutes. Thus, the wild type bacterium is better suited to maintain cellular survival than those strains bearing the hAAG-1 plasmid. The uninduced hAAG-1 cells have approximately a 0.104% survival level at the same exposure. These data indicate that cells with induced hAAG-1 are more sensitive by two orders of magnitude compared to wild type *E. coli* cells (Figure 49). Also displayed in this figure is the *E. coli* mutant deficient in the *uvr*A gene. This strain is also sensitive to BCNU exposure. The level of survival is comparable with that of the triple mutant,

suggesting that the *alk*A and *tag* genes have a small role in the repair of BCNU generated damage to the *E. coli* genome. Thus, comparing the wild type to the *uvr*A deficient strain provides evidence that the nucleotide excision repair mechanism is needed for the repair of BCNU damaged lesions. These data indicate that hAAG-1 is not able to repair lesions created by BCNU in bacteria (Figure 49).

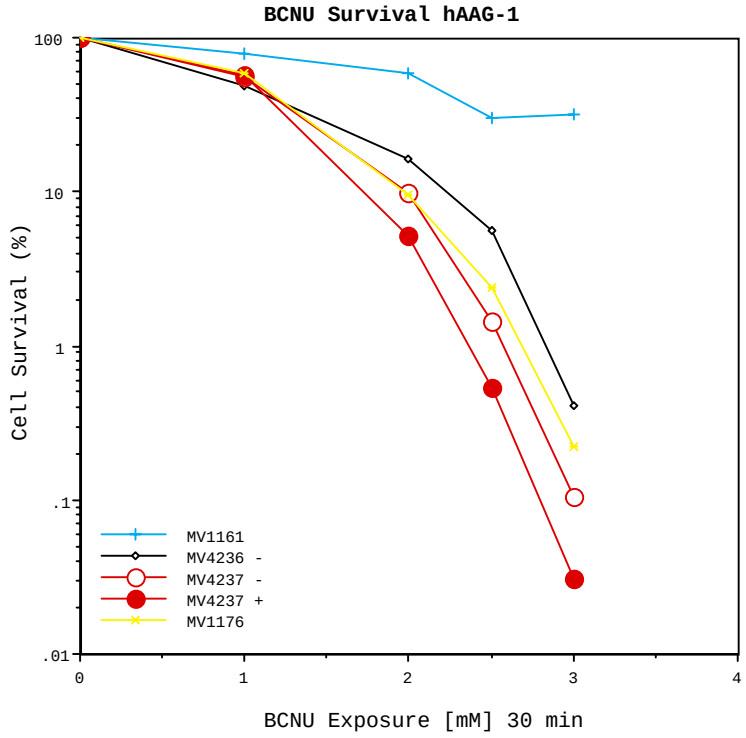

Figure 49: Effect of hAAG-1 on induced cell killing by BCNU. The induced sample containing hAAG-1 (closed circles) in the *alk*A *tag* *uvr*A triple mutant background shows increased sensitivity to BCNU at all concentrations. The uninduced sample of hAAG-1 remains with the *uvr*A deficient *E. coli* strain (MV1176, star symbol). (MV1161, wild type; MV1176, *uvr*A; MV4236, *alk*A *tag* A *uvr*A pTRC99a vector; MV4237, *alk*A *tag*A *uvr*A/ phAAG-1)

The second isoform of hAAG does not confer increased sensitivity to BCNU in the repair deficient *alk*A *tag* *uvr*A mutant strain. At 30 minutes of exposure to 3 mM of BCNU, hAAG-2 induced cells have a 0.65% survival level (Figure 50, closed triangles), while wild type cells have a survival level of approximately 31%. The uninduced hAAG-2 cells (2.5% survival level at 3 mM of BCNU exposure) show greater resistance than the deficient *alk*A *tag* *uvr*A triple mutant control strain (0.41% survival level at 3 mM of

BCNU exposure, open and closed diamonds). hAAG-2 does not rescue bacteria deficient in their own repair mechanism from damage due to exposure to BCNU (Figure 50).

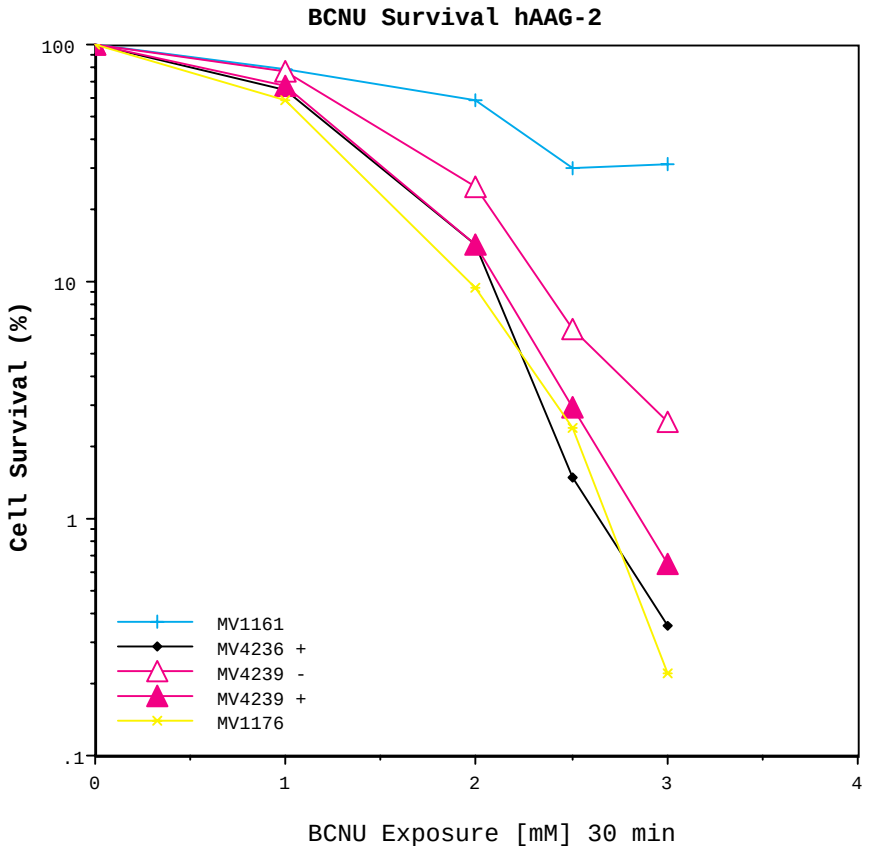

Figure 50: Effect of hAAG-2 on DNA damage induced cell killing by BCNU. Closed triangles represent induced glycosylase in the *alk*A *tag uvr*A deficient background, open triangles represent the uninduced sample in the same background. (MV1161, wild type; MV1176, *uvr*A; MV4236, *alk*A *tag* A *uvr*A pTRC99a vector; MV4239, *alk*A *tag*A *uvr*A/ phAAG-2)

Neither hAAG-1 nor hAAG-2 assist in the repair of lesions created by BCNU. However, hAAG-1 increased sensitivity of the bacteria at higher doses, while hAAG-2 had no effect on the survival of the *alk*A *tag uvr*A triple mutant strain. At low levels of BCNU exposure, hAAG-1 and hAAG-2 both were similar and had no measurable affect on the *alk*A *tag*, and *uvr*A deficient mutant and the wild type strain (Figures 49 and 50).

BCNU Survival: Effects of the his_6 tag on each isoform of hAAG

Each histidine tagged form of hAAG is as sensitive to BCNU exposure as the *alk*A *tag uvr*A triple mutant strain and the *uvr*A deficient strain. hAAG-1-his_6 functions similar to hAAG-1, but hAAG-2-his_6 is more sensitive than hAAG-2 at higher doses. The levels of survival, however, for each form, were only slightly lower than that of the *alk*A *tag uvr*A triple mutant strain and the *uvr*A deficient strain at 3 mM of BCNU exposure (Figure 51 and 52).

Figure 51 shows the sensitivity of hAAG-1-his_6 to BCNU treatment. The level of survival at 3 mM BCNU is approximately 0.10% for the cells induced by IPTG while those uninduced, at the same level of BCNU exposure, were equally sensitive (0.093% survival level). hAAG-1-his_6 and hAAG-1 have extremely similar survival levels, indicating that the addition of the his–tag to hAAG-1 does not alter the ability of hAAG-1 to provide resistance to BCNU. Expression of hAAG-1-his_6 has no effect on the *uvr*A deficient *E. coli* strain MV1176. At the highest dose of 3 mM BCNU for 30 minutes, hAAG-1-his_6 is more sensitive than the *uvr*A deficient *E. coli* strain MV1176. The level of survival at 2.5 mM of BCNU exposure of the *uvr*A deficient *E. coli* strain MV1176 is 2.4% while that of hAAG-1-his_6 is 1.8%, a relatively similar level of survival. However, at 3 mM BCNU exposure, the *uvr*A deficient bacteria have a 0.22% survival level while the strain bearing the plasmid containing hAAG-1-his_6 has a 0.1% survival. At 3 mM BCNU exposure, the strain containing the plasmid bearing hAAG-1 has a 0.030% survival level compared to 0.40% for the control. Thus, the presence of hAAG-1, whether his-tagged or normal, increases sensitivity of the *alk tag uvr*A strain. The *uvr*A deficient strain is also less sensitive than those expressing hAAG at high concentrations of BCNU (Figure 51).

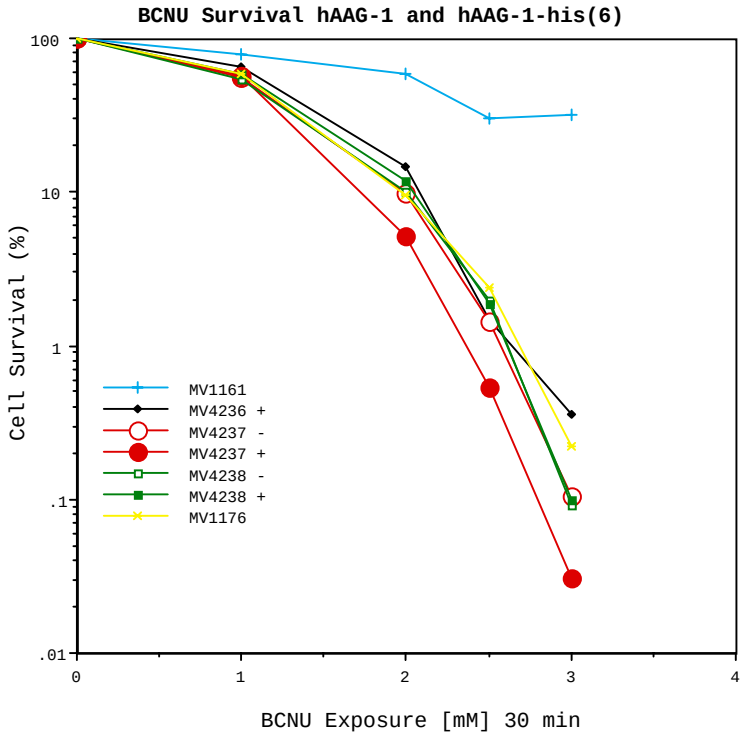

Figure 51: Effect of hAAG-1 (MV4237) and hAAG-1-his$_6$ (MV4238) on induced cell killing by BCNU. The histidine tag has little effect on the ability of hAAG-1 to function, as the presence of the his-tag makes hAAG-1 less toxic at high doses. Closed squares represent induced his–tagged glycosylase in the *alk*A *tag* *uvr*A triple mutant background, open squares represent uninduced his-tagged sample in the same triple mutant background. (MV1161, wild type; MV1176, *uvr*A; MV4236, *alk*A *tag* A *uvr*A pTRC99a vector; MV4237, *alk*A *tag*A *uvr*A/ phAAG-1; MV4238, *alk*A *tag*A *uvr*A/ phAAG-1-his$_6$)

The addition of the histidine tag to hAAG-2, has a more toxic effect on the ability of hAAG to function (Figure 52). hAAG-2-his$_6$ is sensitive to BCNU treatment, more so than hAAG-2, and becomes increasingly sensitive at higher concentrations. The level of survival at 3 mM BCNU is approximately 0.178% for the cells induced by IPTG while those uninduced, at the same level of BCNU exposure, were equally as sensitive (0.2% survival level). hAAG-2-his$_6$ and hAAG-2 have diverse levels of survival, suggesting that the addition of the his–tag to hAAG-2 alter the ability of hAAG-2 by increasing the sensitivity of strains expressing hAAG-2-his$_6$. hAAG-2-his$_6$ is as sensitive as the *uvr*A deficient *E. coli* strain MV1176. The level of survival at 2.5 mM of BCNU exposure of

the *uvr*A deficient *E. coli* strain MV1176 is 2.4% while that of hAAG-2-his$_6$ is 1.2%, a relatively small difference in the level of survival. At 3 mM BCNU exposure, the *uvr*A deficient bacteria have a 0.22% survival level while the strain bearing the plasmid containing hAAG-2-his$_6$ has a 0.17% survival. A different survival level occurs for the strain bearing the plasmid containing hAAG-2. At 3 mM BCNU exposure, the strain containing the plasmid bearing hAAG-2 has a 0.65% survival level. The presence of hAAG-2-his$_6$ increases sensitivity of the mutant *alk tag uvr*A deficient control, which has a survival level of 0.14% at 3 mM BCNU exposure, and has a similar survival level as the *uvr*A deficient strain (Figure 52). Thus, the his-tag has a toxic effect on the hAAG-2 gene.

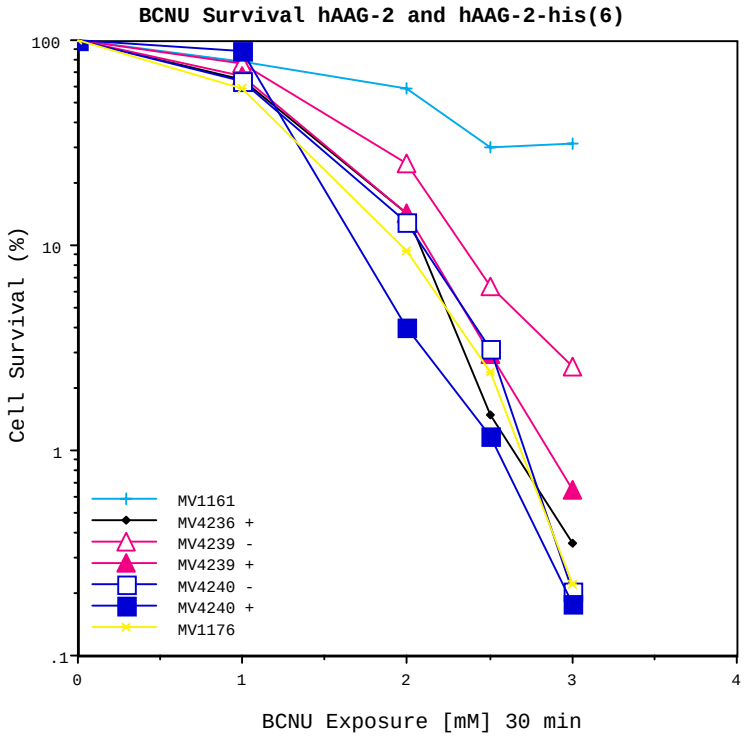

Figure 52: Effect of hAAG-2 (MV4239) and hAAG-2-his6 (MV4240) on induced cell killing by BCNU. The histidine tag has a toxic effect on the sensitivity of hAAG-2, but may not effect the ability of hAAG-2 to function, although when hAAG-2-his(6) is induced, greater levels of sensitivity are achieved at higher doses. Closed squares represent induced his–tagged glycosylase in the *alk*A *tag uvr*A triple mutant background, open squares represent uninduced his-tagged sample in the same background. (MV1161, wild type; MV1176, *uvr*A; MV4236, *alk*A *tag* A *uvr*A pTRC99a vector; MV4239, *alk*A *tag*A *uvr*A/ phAAG-2; MV4240, *alk*A *tag*A *uvr*A/phAAG-2-his$_6$)

Conclusions for BCNU

Overall, the results from the cell survival tests involving BCNU are quite different from those observed from exposure to MNNG and MMS, but similar to CNU. The BCNU survival results contradict published data (Engleward et al, 1996). Engleward showed that loss of AAG activity in mouse cells caused BCNU sensitivity, indicating a role for hAAG in BCNU damage repair. The data from this study indicate that hAAG-1 and hAAG-2 are not able to repair DNA damaged by the crosslinking DNA damaging agent BCNU in a deficient *alk*A *tag uvr*A mutant strain. The results of the two control bacterial strains show that nucleotide excision repair is needed to fix lesions created by BCNU exposure. These results demonstrate that the overexpression of hAAG-1 and hAAG-2 are toxic to the bacteria at 3 mM BCNU exposure compared to the *alk*A *tag uvr*A triple mutant strain (Figure 53).

The results also show that the only noticeable differences between hAAG-1 and hAAG-2 involves the level of sensitivity at the 3 mM dose. hAAG-2 is less sensitve than hAAG-1 at this dose by more than one order of magnitude (Figure 53). hAAG-1-his_6 and hAAG-2-his_6 function in a similar manner as their non- tagged forms, however hAAG-2-his_6 is slightly more toxic at higher doses than hAAG-2.

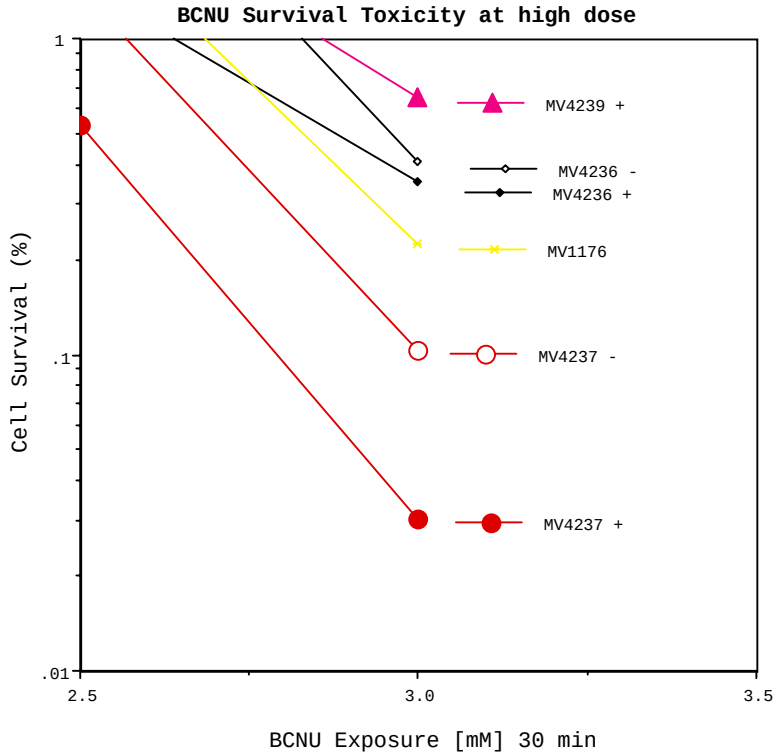

Figure 53: Toxic Effect of hAAG-1 compared to hAAG-2 on induced cell killing by BCNU at 3 mM. hAAG-1 *alk*A *tag uvr*A strain (closed circles) is more sensitive to the cell than the hAAG-2 *alk*A *tag uvr*A strain and the strain deficient in *alk*A *tag uvr*A (diamond symbols) when exposed to BCNU at 3 mM for 30 minutes. (MV1176, *uvr*A; MV4236, *alk*A *tag* A *uvr*A pTRC99a vector; MV4237, *alk*A *tag*A *uvr*A/ phAAG-1; MV4239, *alk*A *tag*A *uvr*A/ phAAG-2)

Mitomycin C (MMC)

The following section displays the effect of human glycosylase activity on the survival after exposure of *E. coli* cells to the crosslinking agent Mitomycin C (MMC).

MMC Survival tests for the hAAG-1 gene

Mitomycin C is a DNA damaging agent that creates interstrand crosslinks in double stranded DNA, thus preventing it from replicating. Prior studies show increased Mitomycin C sensitivity in mammalian cells lacking a functional hAAG gene (Engleward et al, 1996), suggesting that hAAG may play a role in the rescue of DNA damage produced by Mitomycin C.

Mitomycin C creates bulky adducts to the DNA that may cause bending or kinking of the DNA strand when it intercalates into the helix. Since uvrABC excises bulky lesions during repair as a part of the nucleotide excision system, it became important to observe the functional differences between *E. coli* strains deficient in *alk*A and *tag* and *E. coli* strains deficient in *alk*A, *tag*, and *uvr*A. Therefore, two hAAG-1 strains were tested for resistance to Mitomycin C. One is the strain deficient in *alk*A and *tag* and the other is deficient in *alk*A, *tag*,and *uvr*A. Each strain demonstrated unique results, which may suggest the role of the *uvr*ABC system on the repair of Mitomycin C created adducts.

The *alk*A *tag* double mutant strain was less sensitive than the *alk*A *tag uvr*A triple mutant to Mitomycin C exposure (Figure 54).

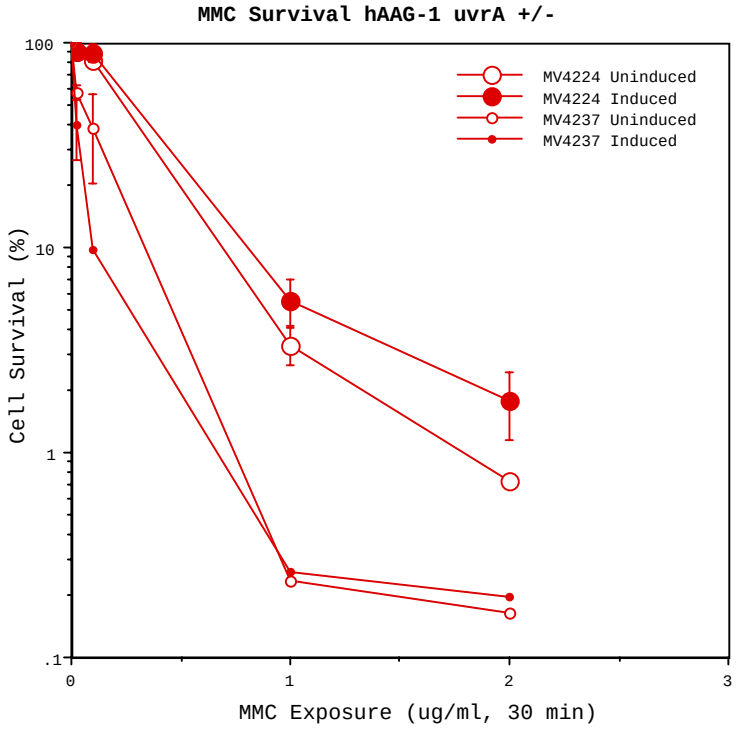

Figure 54: Effect of hAAG-1 activity on cell killing by Mitomycin C. The induced sample containing hAAG-1 (closed circles) in the *alk*A *tag* background and the uninduced sample of hAAG-1 (open circles) are more resistant than those of the hAAG-1 in the *alk*A *tag* *uvr*A deficient mutant (small circles). (MV4224, *alk*A *tag*A/ phAAG-1; MV4228, *alk*A *tag* A/ pTRC99a vector; MV4237, *alk*A *tag*A *uvr*A/ phAAG-1)

There are two genetic differences between these two strains. The first is the absence of the *omp*T outer membrane protease from the *alk*A *tag* double mutant. Prior data for MNNG showed that this mutation does not have any effect on the ability of the glycosylase to function *in vivo* (data not shown). The second genetic difference between the two strains is the absence of the *uvr*A gene from the *alk*A *tag uvr*A triple mutant. Since the *uvr*A gene encodes a protein needed for the function of the nucleotide excision repair system, by knocking out the *uvr*A gene, the entire nucleotide excision repair pathway is not able to function. This may explain the reason for the differences obtained.

To further examine the role of hAAG-1, a comparison was made based on the survival of *E. coli* proficient in *uvr*A, but deficient in *alk*A and *tag*. The level of survival of these strains is similar to that of its hAAG-1 bearing derivative (Figures 54 and 55).

An interesting note, however, is the increased resistance of the plasmid bearing *alk*A *tag* deficient strains, regardless of the presence of hAAG-1. The *alk*A *tag* double mutant containing the plasmid vector pTR99a shows equal resistance as that strain deficient in *alk*A and *tag* containing hAAG-1 (Figure 55). Thus, the *alk*A *tag* double mutant strains are less sensitive than the wild type glycosylase strain suggesting that bacterial glycosylase(s) sensitize cells for MMC killing. On the other hand, human glycosylase expressed in *E. coli* has little or no effect on MMC cytotoxicity (Figure 55).

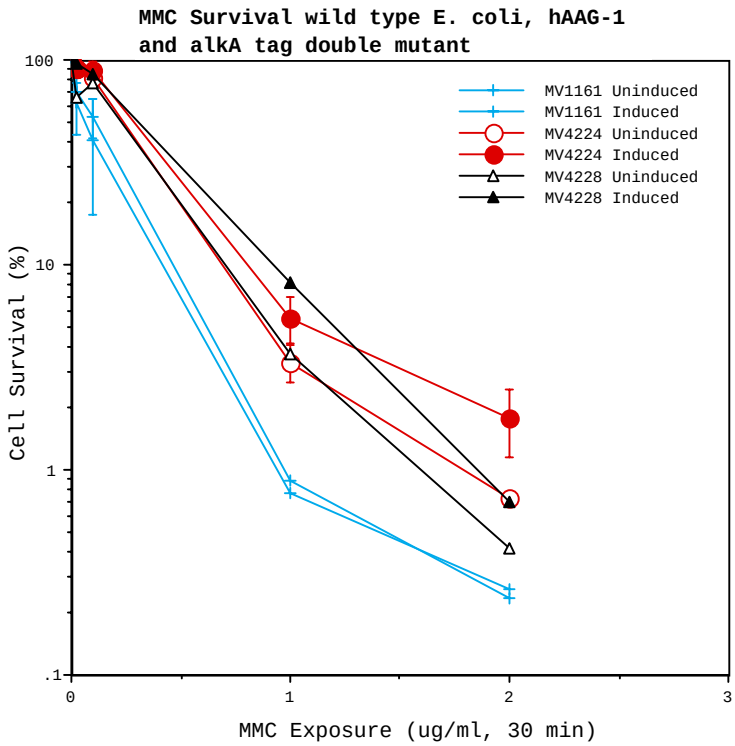

Figure 55: Effect of hAAG-1 activity on cell killing by MMC. The induced sample containing hAAG-1 (closed circles) in the *alk*A *tag* background and the uninduced sample of hAAG-1 (open circles) show levels of survival similar to those of the *alk*A *tag* deficient double mutant (small triangles), yet greater than those of the wild type *E. coli* strain (+ symbol). (MV1161, wild type; MV4224, *alk*A *tag*A/ phAAG-1; MV4228, *alk*A *tag* A/ pTRC99a vector)

An interesting finding was seen when the *alk*A *tag uvr*A triple mutant strain containing hAAG-1 was analyzed. This strain, unlike the double mutant, showed great sensitivy to Mitomycin C, especially at lower dose levels. Thus, the role of *uvr*A may be a factor in these differences. The effect of hAAG-1 in the *alk*A *tag uvr*A triple mutant background was to increase Mitomycin C sensitivity at low levels (Figure 56).

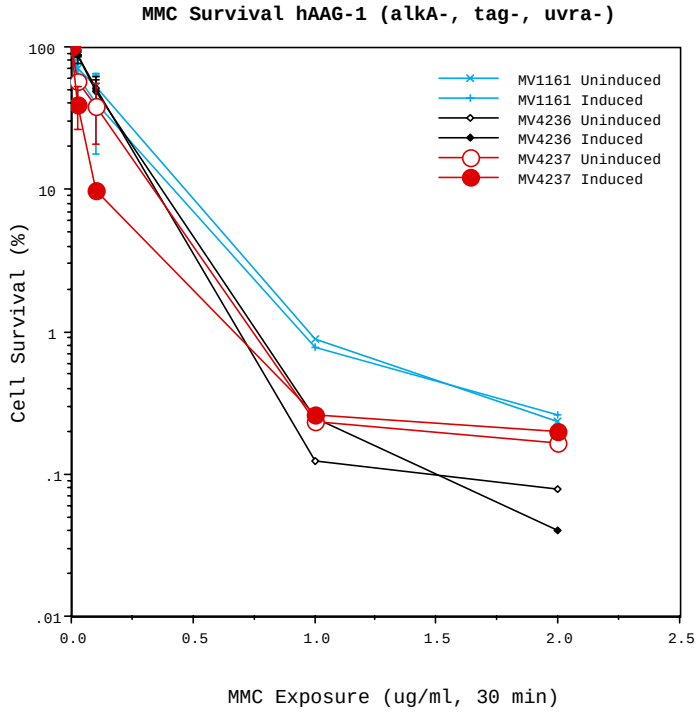

Figure 56: Effect of hAAG-1 on cell killing by Mitomycin C. The induced sample containing hAAG-1 (closed circles) in a *alk*A *tag* *uvr*A mutant background and the uninduced sample of hAAG-1 in the same background show toxic levels of survival at lower doses yet regain resistance similar to that of the wild type *E. coli* strain at higher doses (MV1161, + symbols). The diamond represents the *alk*A *tag* *uvr*A vector control, which was used in the comparison of hAAG-1 toxicity. (MV1161, wild type; MV4236, *alk*A *tag* A *uvr*A pTRC99a vector; MV4237, *alk*A *tag*A *uvr*A/ phAAG-1)

MMC Conclusions for hAAG-1 Survival in uvrA + and uvrA - backgrounds

Comparing the two strains containing hAAG-1, one can clearly see diversity between the sensitivity of the two strains. Figures 57 revisits the activity displayed by the two strains with respect to the wild type mutant and the *uvr*A deficient mutant. Panel B of figure 57 uses a logarithmic scale to expand the lower levels of exposure.

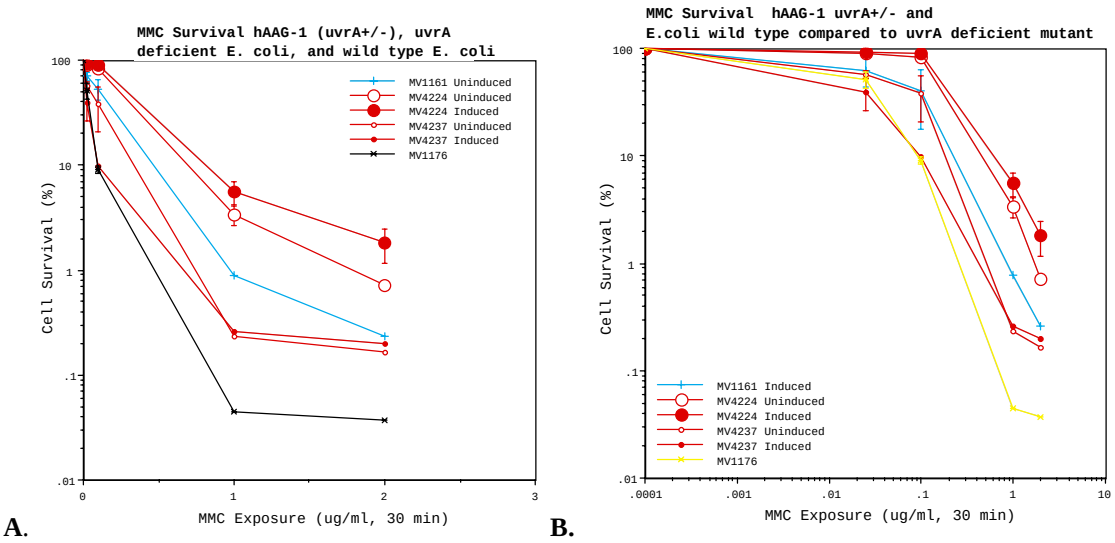

Figure 57: Effect of hAAG-1 against MMC cell killing in the *alk*A *tag* background and in the *alk*A *tag uvr*A background. A). The induced sample containing hAAG-1 in the *alk*A- *tag*- *uvr*A+ strain (closed red circles) and the uninduced sample of hAAG-1 show levels of survival greater than those of the wild type *E. coli* strain (MV1161, cyan color). The induced sample of the *alk*A- *tag*- *uvr*A- strain (closed purple squares) and uninduced sample (open purple squares) show more sensitivity to MMC than the double mutant strain. B). Using a logarithmic x-axis to amplify the exposure at low doses, one can compare the differences observed between strains containing and lacking the uvrA gene. The induced sample containing hAAG-1 (closed circles) in the *alk*A *tag* double mutant show greater resistance at low levels of Mitomycin C exposure. The induced sample of hAAG-1 in the *alk*A *tag uvr*A triple mutant background show levels of survival equal to the *uvr*A deficient bacterial strain at low levels. (MV1161, wild type; MV1176, *uvr*A; MV4224, *alk*A *tag*A/phAAG-1; MV4237, *alk*A *tag*A *uvr*A/phAAG-1)

General conclusions about the function of hAAG-1 can be drawn from the difference in hAAG-1 function in these survival assays between the *alk*A *tag* background and the *alk*A *tag uvr*A backgrounds. First, the presence of *uvr*A greatly increases the performance of hAAG-1. In the absence of *uvr*A, hAAG-1 expression increased Mitomycin C sensitivity at the low dose levels of 0.025 ug/ml and 0.1ug.ml. The survival levels at these dose ranges can be summarized in Table 5. hAAG-1 expression in the *alk*A *tag uvr*A deficient background sensitizes to the greatest degree at low doses, however the *alk*A *tag* proficient *uvr*A deficient strain becomes more sensitive than hAAG-1 as the dose increases (Table 5).

Table 5: Percent survival comparison among various dose levels of Mitomycin C exposure for 30 minutes.

Sample	Dose (ug/ml)			
	0.025	0.1	1	2
hAAG-1 uvrA^{+} alkA^{--} tag^{--}	91 %	89%	5.5%	1.8%
Wild type E. coli	70%	53%	0.88%	0.25%
hAAG-1 uvrA^{--} alkA^{--} tag^{--}	39.5%	9.8%	0.26%	0.19%
E. coli uvrA^{--} alkA^{+} tag^{+}	51.3%	9.2%	0.04%	0.03%

MMC Survival: Effects of the hAAG-2 gene

The second isoform of hAAG confers increased sensitivity to Mitomycin C exposure in the repair deficient *alk*A *tag uvr*A mutant strain. In the *alk*A *tag uvr*A deficient background, hAAG-2, like hAAG-1, is more toxic than the glycosylases of the wild type *alk tag uvr*A proficient system. hAAG-2 is also slightly more resistant than the *uvr*A deficient bacteria mutant. At 30 minutes of exposure to 2 ug/ml of Mitomycin C, hAAG-2 induced cells (Figure 58, closed triangles) have a 0.061% survival level, while wild type cells have a survival level of approximately 0.25%. The uninduced hAAG-2 cells (0.093% survival level at 2 ug/ml of Mitomycin C exposure) also demonstrate equal sensitivity to that of the triple mutant control strain (0.04% survival level at 2 ug/ml of Mitomycin C exposure (Figure 58, diamonds). Thus, hAAG-2 does not rescue bacteria deficient in their own repair mechanisms from damage due to exposure to Mitomycin C, but actually increases sensitivity to the DNA damaging agent to the survival level of the *alk*A *tag uvr*A triple mutant.

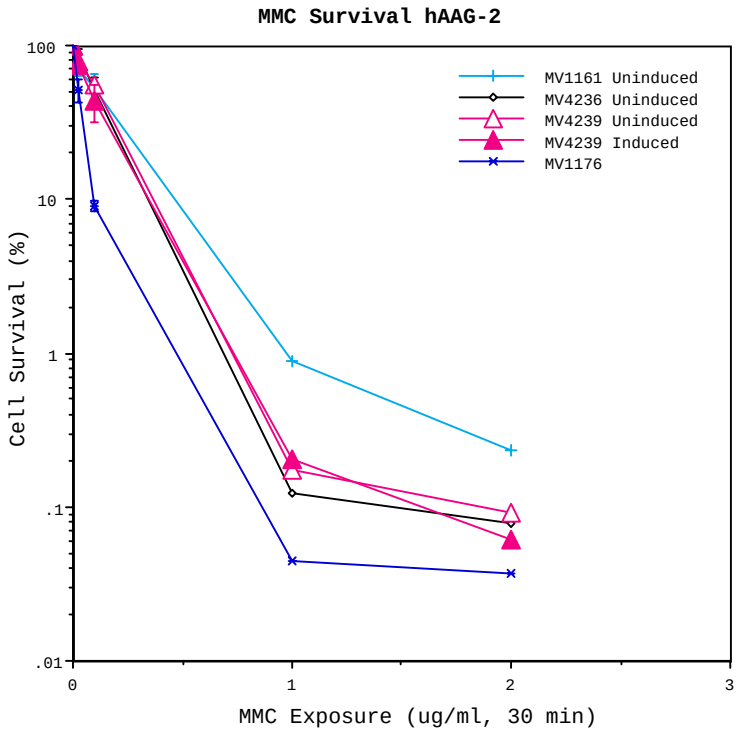

Figure 58: Effect of hAAG-2 on cell killing by Mitomycin C. The induced sample containing hAAG-2 (closed triangles) in a *alk*A *tag* *uvr*A mutant background and the uninduced sample of hAAG-2 in the same background show equal sensitivity as those expressed by the *alk*A *tag* *uvr*A vector control. Levels of survival are lower than those of the *alk*A *tag* *uvr*A proficient *E.coli* (+ symbols). However, survival levels are slightly more resistant than the *uvr*A deficient *E. coli* strain (star symbols). (MV1161, wild type; MV1176, *uvr*A; MV4236, *alk*A *tag* A *uvr*A pTRC99a vector; MV4239, *alk*A *tag*A *uvr*A/ phAAG-2)

When exposed to Mitomycin C, the presence of hAAG-1 and hAAG-2 make the cells just as sensitive as the *alk*A *tag*, and *uvr*A deficient mutant. The strain proficient in all repair pathways showed less sensitivity than those strains containing plasmids bearing hAAG. At lower doses of Mitomycin C exposure, hAAG-1 was more toxic than hAAG-2. However, at higher doses, hAAG-2 was actually slightly more sensitive than hAAG-1. This data indicates that hAAG-1 is toxic in cells when exposed to low levels of Mitomycin C whereas hAAG-2 is not as toxic to this low exposure of Mitomycin C. At 0.1 ug/ml Mitomycin C exposure, hAAG-1 is more sensitive than hAAG-2 by a full order of magnitude (Figures 57 and 58). At high levels of Mitomycin C exposure, hAAG-1 and hAAG-2 both have similar survival levels, which are actually similar to the *alk*A *tag*,

*uvr*A deficient mutant. For example, at 1 ug/ml of Mitomycin C exposure for 30 minutes, hAAG-1 has a survival level of 0.26%, hAAG-2 has a survival level of 0.20%, and the triple mutant has a survival level of 0.24%. However, as the dose concentration increases, so too does the separation in sensitivity. hAAG-2 increases the sensitivity to Mitomycin C to a greater extent than hAAG-1 (Figure 58).

MMC Survival: comparisons of the his_6 tagged forms of hAAG

hAAG-1-his_6 and hAAG-2-his_6 have both similarities and differences. hAAG-2-his_6 shows more sensitivity than hAAG-1-his_6, however both were sensitive at the lower doses (Figure 59). A logarithmic scale was needed to clearly see the sensitivity to low concentrations of Mitomycin C. Induction increased toxicity, suggesting that the greater amount of his-tagged glycosylase, the more sensitive the cells were to Mitomycin C exposure.

The hAAG-1-his$_6$ gene showed similar sensitivity to Mitomycin C as hAAG-1 in the same background (*alk*A- *tag*- *uvr*A triple mutant). At lower levels, toxicity was very high, yet as the doses increased, so did the level of survival (Figure 59). Thus, the his-tag has no effect on sensitivity to MMC.

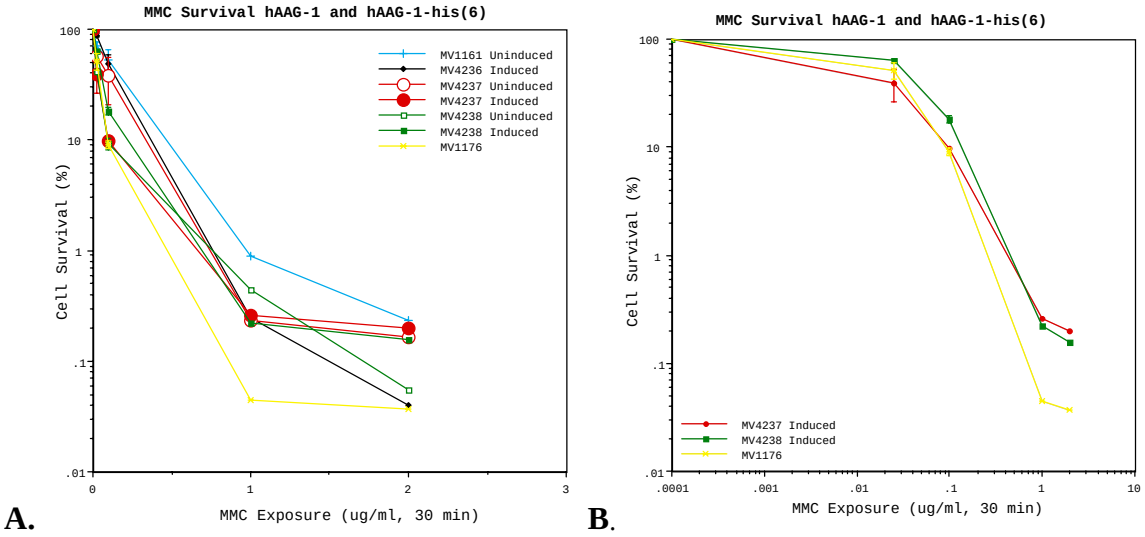

Figure 59: Effect of hAAG-1 and hAAG-1-his$_6$ on cell killing by MMC. The induced sample containing hAAG-1 (closed circles) in the *alk*A- *tag*- *uvr*A background and the uninduced sample of hAAG-1 in the same background show levels of survival lower than those of the wild type *E. coli* strain (MV1161, + symbols). The induced sample of hAAG-1-his$_6$ also reacts very similar to hAAG-1. B). The induced sample containing hAAG-1 (closed circles) in the *alk*A- *tag*- *uvr*A background shows a level of survival higher than those of the *uvr*A deficient *E. coli* strain (MV1176, star symbols). The induced sample of hAAG-1-his$_6$ in the same background also react very similar to hAAG-1. This figure represents the data from panel A, however using a logarithmic scale for the x-axis in order to see more clearly the sensitivity at lower levels. (MV1176, *uvr*A; MV4237, *alk*A *tag*A *uvr*A/ phAAG-1; MV4238, *alk*A *tag*A *uvr*A/ phAAG-1-his$_6$)

The histidine tag attached to hAAG-2 posed a great variation to that on the hAAG-1, similar to that seen in the BCNU treatments. This is very strange due to the fact that hAAG-2-his$_6$ was created from hAAG-1-his$_6$. However, it is obvious from this data that hAAG-2-his$_6$ shows great sensitivity to Mitomycin C by over three orders of magnitude at the low doses of 0.025 ug/ml and 0.1 ug/ml (Figure 60). The hAAG-2-his$_6$ was very toxic when induced by IPTG at lower dose levels, however as the dose

increased, the toxicity decreased. hAAG-2-his$_6$ actually displayed sensitivity equal to the control *alk*A- *tag*- *uvr*A triple mutant at the higher doses (Figure 60).

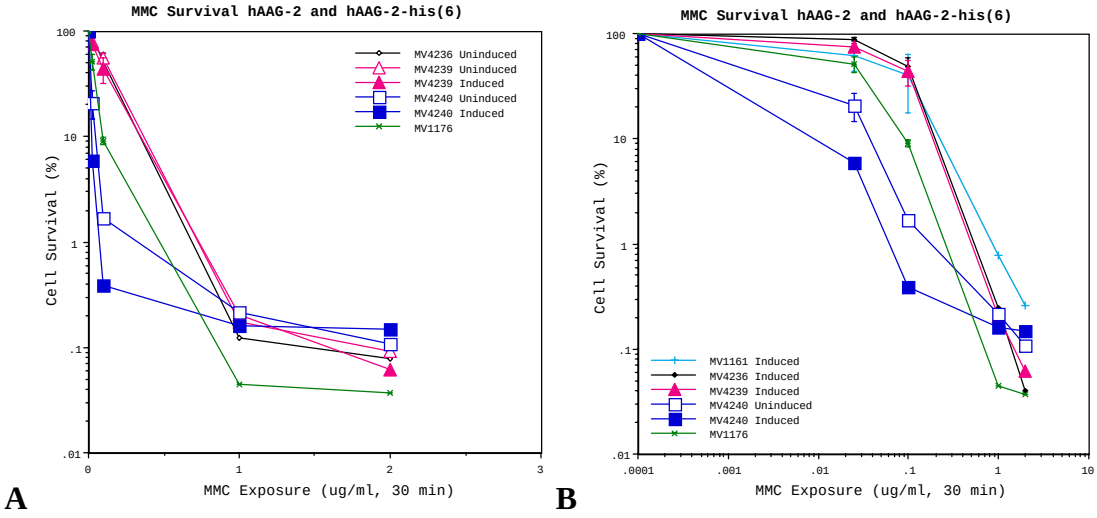

Figure 60: A)Effect of hAAG-2 and hAAG-2-his$_6$ on cell killing by MMC. The induced sample containing hAAG-2 (closed triangles) in the *alk*A- *tag*- *uvr*A background and the uninduced sample of hAAG-2 in the same background show levels of survival lower than those of the wild type *E. coli* strain (MV1161, + symbols). The induced sample of hAAG-2-his$_6$ reacts in a very sensitive manner compared to hAAG-2 sensitivity at low doses. B). The induced sample containing hAAG-2 (closed triangles) in the *alk*A- *tag*- *uvr*A background shows a level of survival higher than those of the *uvr*A deficient *E. coli* strain (MV1176, star symbols). The induced sample of hAAG-2-his$_6$ in the same background, shows a survival level much lower than those of hAAG-2 and of the *uvr*A deficient *E. coli* strain. This figure represents the data from panel A, however using a logarithmic scale for the x-axis in order to see more clearly the sensitivity at lower levels. (MV1176, *uvr*A; MV4236, *alk*A *tag* A *uvr*A pTRC99a vector; MV4239, *alk*A *tag*A *uvr*A/ phAAG-2; MV4240, *alk*A *tag*A *uvr*A/ phAAG-2-his$_6$)

hAAG-2-his$_6$ shows extreme sensitivity at low levels of MMC exposure, suggesting that the histidine tag may alter the function of the hAAG-2 isoform (Figure 61).

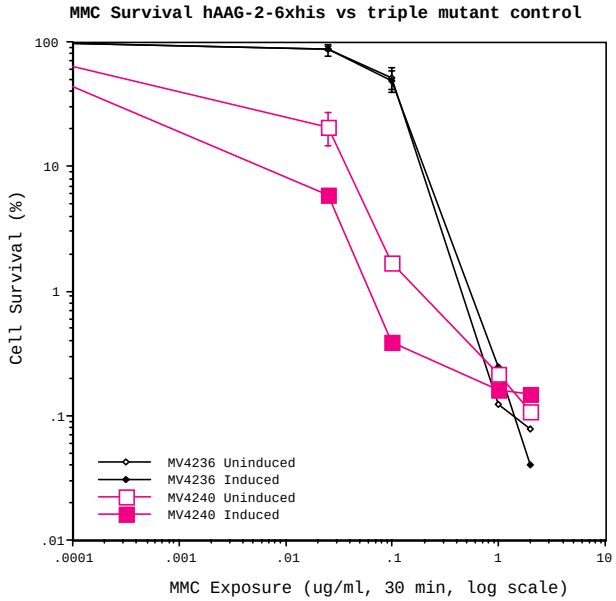

Figure 61: Cell Killing by MMC. hAAG-2-his$_6$ (large squares) in an *alk*A *tag uvr*A background proves to be very toxic at low levels of Mitomycin C exposure. (MV4236, *alk*A *tag* A *uvr*A pTRC99a vector; MV4240, *alk*A *tag*A *uvr*A/ phAAG-2-his$_6$)

Conclusions for MMC Survival Assays

Mitomycin C displayed interesting results. hAAG-1 was more sensitive to Mitomycin C exposure than hAAG-2 at lower doses, but as the dose increased, a reversal in sensitivity occurred. hAAG-2-his$_6$ was more sensitive to Mitomycin C exposure at lower dose levels than hAAG-1-his$_6$, suggesting the possibility that the alternative exon 1 of hAAG-2 may present the increased sensitivity to Mitomycin C. The possibility of a poor dilution to obtain the lower level concentrations can be ruled out due to the daily consistency obtained in the results.

A result worth pursuing is the effect of the *uvr*A gene to Mitomycin C exposure. When hAAG-1 was in the *uvr*A proficient background, it increased Mitomycin C resistance relative to the control. When it was in the *uvr*A deficient background, it caused sensitivity. The presence and absence of *uvr*A function had the same effect in the *alk*A *tag* double mutant (Figure 62).

A general hypothesis for the relationship between the glycosylase activity and the nucleotide excision repair system is that glycosylase needed to create perform initial repair to DNA in order to produce recognizable adducts for the excision repair system to excise. Therefore, strains containing both the presence of glycosylase genes and the *uvr*A gene should be more resistant than strains lacking either of those repair systems. This is not the case, however, when exposed to Mitomycin C. The level of survival for the *alk*A *tag* double mutant is very comparative to that of the its derivative expressing hAAG-1, which suggests that the presence of glycosylase may not be relevant to the recovery of cells exposed to Mitomycin C. However, the *alk*A *tag uvr*A strain is more resistant than the *uvr*A deficient strain at 1 ug/ml of Mitomycin C exposure, suggesting that glycosylase activity sensitizes the cells in the absence of the *uvr*A gene (Figure 62).

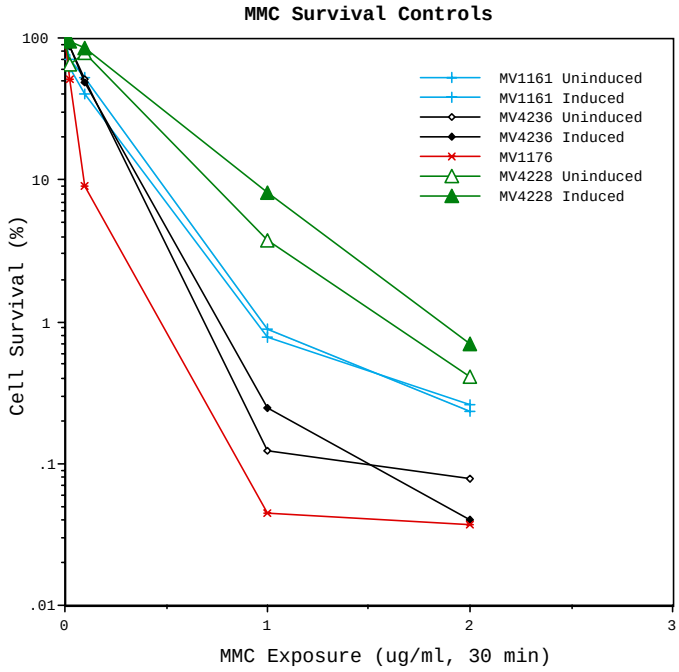

Figure 62: Effect of cell killing by Mitomycin C. This graph shows Mitomycin C's effect on strains without hAAG. Most sensitive is the *uvr*A deficient strain (star symbols). Then, the *alk*A- *tag*- *uvr*A triple mutant (diamonds) was next sensitive. More resistant than this was the proficient strain (+ symbols). The most resistant was the *alk*A- *tag*- double mutant strain (small triangles). (MV1161, wild type; MV1176, *uvr*A; MV4228, *alk*A *tag*A/ pTRC99a vector; MV4236, *alk*A *tag* A *uvr*A pTRC99a vector)

hAAG-1-his$_6$ and hAAG-2-his$_6$ Protein Analysis

The first step in conducting the protein analysis of hAAG-1-his$_6$ and hAAG-2-his$_6$ was to provide a system in which the maximum level of production would be achieved. The system chosen knocked out the protease activity of the *omp*T protein. Then, protein analysis to determine expression levels and time assays were conducted.

Constructing a Strain Carrying an alkA1 tagA1 ompT Mutant Gene

The goal of this series of experiments was to create an ompT::Kan^R mutant strain to control the function of ompT allowing bacterial expression of hAAG protein. *Omp*T is an outer membrane protein that cleaves proteins upon their release from cells between two basic amino acid residues (Henderson, 1994). Therefore, this protease causes cleaveage of hAAG during purification by cleaving hAAG between two arginine residues. Based on the results of amino terminal protein sequencing it was found that the hAAG-1-His$_6$ protein was cleaved at a site between two Arginine residues (S. Wright, Q. Li and D. Ludlum, Personal Communication). Since this is the prefered clevage site of the OmpT protease (Sugimura and Higashi 1988), we decided to construct an *ompT::kanR* mutant of our *alkA tag*A mutant strain MV2157 or derivative, using P1 transduction to block the Arginine cleavage. In doing so, we prevent cleavage of full-length proteins, allowing us to perform further testing on the protein's function. Since this strain was already kanamycin resistant, it was first necessary to place the *ompT*::*kanR* gene next to a selectable marker for genetic transfer in MV4137. I tested three strains known to carry Tn 10 (tetracycline resistance) insertions located near *omp*T for linkage in order to find the one that is closest.

Properties of the ompT *Mutant Strain*

Since the *alk*A *tag*A strain MV2157 carried a kanamycin resistance element and was, therefore, *alk*A, it was necessary to construct an ompT::Kan^R derivative by transferring ompT::Kan^R from strain AD202 into a strain that carries a Tn10-Tet^R marker tightly linked to *omp*T, using P1 transduction and selecting for Kan^R Tet^R transductants (Volkert, 1999).

Choosing a Recipient Cell Strain

Three strains, CAG12149, CAG12021, and CAG12171 were tested for linkage of Tn10-tet^R to *omp*T::Kan using the strain P1-MV4137 ompT::Kan^R as a donor. The P1-MV4137 packages random 90 kilobase DNA piece approximately 2% the size of a chromosome and transfersthe desired fragment at a frequency of about 10^{-5} transductants (Miller, 1972). It also lacks the Tet^R marker of the strain and is Tet^S (see figure 63a).

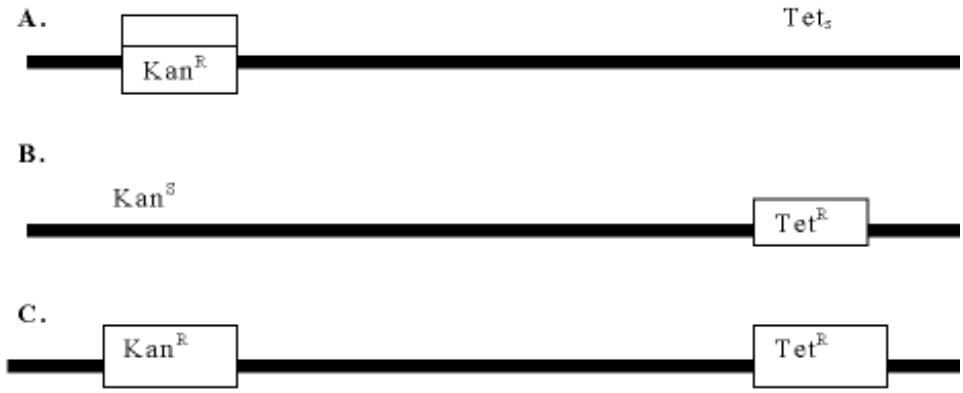

Figure 63: A Crude genetic map of A). the P1-MV4137 ompT::Kan^R strain B). the CAG Recipient Strain Kan^S Tet^R orientation. C). the Kan^R and Tet^R cells, the Desired Recombinant.

The recipient strains have just the opposite resistance and suppressor sites as the P1-MV4137. Figure 63b displays the orientation of the kan and tet antibiotics in these cell lines. This experiment was accomplished to detect the presence of the desired Kan^R and Tet^R recombinant (Figure 63c).

Prior to obtaining this *omp*T resistance, a test cross was completed to provide accuracy in our determination that the strain had accepted the Kan^R and was not expressing its unlinked Kan^R marker downstream from the gene. Therefore, the test cross was done to determine which tet^R marker was closest to the *omp*T::Tn10Kan. This is indicated in this cross by the one yielding the lowest ration of Tet^R Kan^R to Tet^S Kan ^{R} recombinants, the Tet^S Kan^R recombinants are those inheriting both donor markers. Table 6 shows this ratio was lowest in the P1-MV4137 to CAG12171 cross.

Table 6: Ratio of P1-MV4137 with CAG recipient crosses

	Kan^R cell count	Kan^R—Tet^R cell count
CAG12021	69	52
CAG12149	20	13
CAG12171	44	10
P-1 only (control)	0	0

A Tet^R::*omp*T Kan^R recombinant was then picked , purified, and subsequently used as a P1-donor strain in a second cross in which P1-MV1161 was used and MV4139 and MV4140 were used as recipients. P1 was grown on MV4139 and it was used to transduce MV2157, MV4122, MV4126, and MV4137. Four colonies of each were picked and purified, then tested for coinheritance of *omp*T::Kan^R by backcrossing into strain Q and selecting for Tet^R::Kan^R in order to determine which backcross donors carried the Kan^R allele linked to the Tet^R allele. Table 7 shows that strains MV2157, MV4126, and MV4137 inherited both markers and stain MV4122 did not.

Table 7: Percentage yield of backcrosses in each of the four *alk*A *tag*A strains

Strain	Number of dual cells	Number of Streaked Cells	Percentage
MV2157	20	50	40
MV4122	0	50	0
MV4126	14	50	28
MV4137	15	50	30

Once the *omp*T *alk*A *tag*A strain carrying the hAAG-1-his_6 expressing plasmid was constructed, it was grown and its hAAG-1-his_6 protein purified and subjected to polyacrylamide gel electrophoresis. The purified protein was found to be about 1 kDa larger than the protein previously purified from the *omp*T^+ strain, suggesting it was intact. Amino terminal sequencing confirmed that that *ompT::kanR alkA tag*A mutant strain yielded an intact hAAG protein (S. Wright, Q. Li and D. Ludlum, Personal Communication).

Transfer of hAAG-2- 6x his to a pBluescript vector

One of the focuses of this project, and as an ongoing project in the Ludlum laboratory was the protein production and purification of the hAAG genes. The his-tagged versions of each gene were incorporated into the plasmid pBluescript KS- so that the T7 promoter could regulate hAAG. The plasmid construction of hAAG-1-his_6 was engineered previously, so only hAAG-2-his_6 was constructed in this work. pBluescript and pMV536 were each cut at the EcoRI and Hind III sites. The restriction product was purified using the gene clean kit (Bio101, Inc.) and ligated using T4 DNA ligase at 16 degrees C. The product was then transformed into competent Q cells and colonies were picked and the plasmids purified using the Qiagen plasmid miniprep kit. Restriction digests were perfomed to determine that the ligation occurred correclty. The plasmids were cut with EcoRI-HindIII, and EcoRI-Afe II (data not shown). Figure 64 shows a restriction digest by BsteII. This enzyme was used because of its unique single site in pBluescript and because with the hAAG-2-his_6 site added to the pBluescript, the sites mapped to 2.8 kb, 884 bp, and 114 bp- an ideal distance to distinguish easily on a gel if the correct fragment had been ligated. The lane labeled 552 displays these three fragments, thus restriction analysis has provided the conclusion that hAAG-2-his_6 was transfered to pBluescript correctly.

Figure 64: Restriction Digestion of Ligation product of hAAG-2-6x his insert and pBluescript Vector. The lane labeled 552 displays the BstE II restriction digest. Bands corresponding to 114 bp, 884 bp, and 2.8 kb were observed.

Plasmids containing the hAAG-2-his_6 were erroneously transformed into MV4210 because it was thought that the absence of the OmpT protease could be used to benefit increased protein production. However, plasmid pMV552 must be transferred into strains BL21 (DE3) and BL21 (DE3) lysS so that expression can be achieved from the T7 promoter located within the pBluescript plasmid. Expression from the T7 promoter should yield increased protein production.

Protein Synthesis and Production Time Assay

The first time assay was successful, however the protein produced did not yield high enough levels to be detected on a Western blot. Therefore, longer incubation time in the presence of IPTG will occur in the next Western blot assay.

Western Blot Analysis

Currently, attempts at observing the his-tagged protein via chemiluminescense have not been completed successfully. In these Western Blot experiments, transfer to the membrane had occurred. Therefore, it is believed that higher concentrations are needed in order to observe the histidine tagged hAAG proteins. This will be accomplished in the next protein synthesis time study.

DISCUSSION

Construction of hAAG-2 and hAAG-2-his$_6$

The second isoform of hAAG present in the plasmid pMV518 was reconstructed to provide an identical upstream sequence to that of hAAG-1 by incorporating it into a 5' primer (MV20) to be used in a PCR reaction. The addition of this sequence, containing a ribosomal binding site and key restriction endonuclease, and the incorporation of the PCR fragment into the plasmids containing hAAG-1 and hAAG-1-his$_6$ provided the lab with a gene that functioned similarly to hAAG-1.

PCR primers must be very close in melting temperature in order for the reaction to occur properly. Once a 3' primer was constructed with a similar melting temperature to that of the 5' primer, the PCR proceeded as expected. After the plasmids bearing hAAG-2 and hAAG-2-his$_6$ were constructed, they expressed phenotypically similar properties to their alternately spliced isoform. Thus, the original hAAG-2-his$_6$ within pMV518 was not being expressed properly, possibly due to transcriptional and/or translational problems.

The only biological difference between the two isoforms of hAAG is the first exon. Exon 1 of hAAG-2 is 15 base pairs greater in length than exon 1 of hAAG-1. In addition to this size difference, hAAG-1 and hAAG-2 have an altered amino acid sequence in the first exon. This may create slightly different protein structures when the amino acids conform into the tiertiary and quartinery protein structures. It may also result in different stabilities and/or subcellular localization in mammalian cells.

Survival Data

The information collected and observed from the cell survival assays provide insight to the biological function of each isoform of hAAG when cells are exposed to various chemical DNA damaging agents. This section presents key insight specific to

each drug used and then is followed by a section dedicated to a general discussion involving all the data collected.

MNNG and MMS Survival tests

The human AAG-1 is able to function in an *alk*A *tag* bacterium to increase resistance to MNNG. At higher doses, this increase in resistance is greater than that seen in a wild type bacterium that expresses its own *alk* and *tag* encoded glycosylases. This suggests that hAAG-1 functions more efficiently in the *E. coli* system than *alk*A and *tag*A. Even basal level production of hAAG-1 substantially increases resistance to MNNG opposed to cells deficient in glycosylase activity (Figure 34). The hAAG-1 bearing strain shows IPTG induction of hAAG-dependent MNNG resistance.

The addition of the histidine tag does not alter the performance of hAAG-1 when cells are exposed to MNNG (Figure 36). The survival of both the induced and uninduced cells carrying the plasmid bearing hAAG-1-his_6, at all doses, is similar to the survival of induced and uninduced cells carrying the plasmid bearing hAAG-1. Therefore, the addition of the histidine tag has no effect on the ability of hAAG-1 to function in repair of MNNG damage to DNA.

Both MNNG and MMS methylate DNA to cause damage. The wild type *E. coli* is able to repair this damage at very high levels of survival. Induced hAAG-1 has provided resistance comparable with that of wild type when introduced into the MMS sensitive *alk*A *tag* double mutant and the *alk*A *tag uvr*A triple mutant strains. As is the case with MNNG, uninduced hAAG-1 and hAAG-2 show some basal level rescue, however neither show the level of resistance of the induced cells.

The presence of hAAG-2 also increases the cellular resistance to MNNG and MMS. This increase in resistance, however, is not as great as that of the presence of hAAG-1 when exposed to equal doses of drug. This data suggests a possible difference between the two isoforms, since cells containing the plasmid bearing hAAG-1 are more resistant than those containing the plasmid bearing hAAG-2. hAAG-1 performs more efficiently than the wild type glycosylases; hAAG-2 functions equal to *alk*A and *tag*

glycosylase activity of the wild type cells. The maximum survival rate of hAAG-2 corresponds to the level seen in uninduced cells bearing the hAAG-1 expressing plasmids (Figures 37, 43). This suggests hAAG-1 is more effective than hAAG-2 for repair of methyl damage.

There is a difference in the survival level of cells expressing the different isoforms of hAAG. There are several reasons why this may occur. Since it is not yet known why there are two known isoforms of hAAG, these differences are interesting to analyze because they may provide insight to the reason(s) for the two isoforms of hAAG.

The first possibility for the different survival levels provided by each isoform is the activity of each isoform of hAAG. hAAG-1 may be more active in cells than hAAG-2, thus it functions in a more efficient manner. There may also be more hAAG-1 protein than hAAG-2 protein present in the strains due to stability of their enzyme products under the given conditions or there may be differences in their expression. The stability of each protein may explain why survival levels of hAAG-1 expressing strains are greater than those of strains expressing hAAG-2. hAAG-1 protein may be produced in greater amount than hAAG-2 or hAAG-2 expression may never quite reach its optimal expression levels inside the *E. coli* system used. Thus, hAAG-1 may be more readily available than hAAG-2 to repair methyl lesions. Protein analysis using an immunoblot detection system may be able to determine if the level of expression is greater for one isoform over the other.

A second reason for the difference in survival levels between each isoform may be a difference in activity. hAAG-2 may correct methylated lesions less efficiently than hAAG-1. Thus, hAAG-1 may have a greater specific activity or a higher affinity for methylated lesions than hAAG-2.

The differences between hAAG-1 and hAAG-2 in the repair of methylation damage produced by MNNG and MMS exposure show similarities between the two methylating agents. Each isoform of hAAG is able to repair lesions quite efficiently, however hAAG-1 provides more resistance than hAAG-2. The histidine tagged versions of each isoform function in a similar manner to their non-his tagged counterparts.

Nitrosourea Survival Tests

The hAAG-1 and hAAG-2 genes both function in a similar manner when cells containing a plasmid bearing each isoform are exposed to CNU. Addition of the histidine tag does not effect survival after exposure to CNU. Both the induced and uninduced curves result in toxicity at a high dose ([0.5mM]). This toxicity, compared to a triple mutant genotype, provides evidence that the presence of no glycosylase is better than the expression of glycosylase at either induced levels or basal level expression. This evidence may be explained through the same phenomenon as another crosslinking agent tested: MMC. The glycosylase creates lesions that may be repaired by the nucleotide excision repair pathway, however in the absence of *uvr*A, the NER pathway does not exist, thus the abasic site created by the glycosylase becomes lethal.

Another possibility is that the glycosylase is dependent on the presence of another protein or protein complex. This protein or protein complex may serve as a chaperone or may recruit hAAG to the lesion. Present in human cells, this protein or complex may not be present in bacteria, or may be present in an unrecognizable or incompatible form. Thus, hAAG is not able to function properly because it is not recognized, or does not recognize, this helper protein.

BCNU reacts analogous to CNU in the experiments except that hAAG-2 is not any more sensitive than the *alk*A *tag uvr*A triple mutant at high doses, whereas hAAG-1 is more toxic than the triple mutant strain. Even though hAAG-1 is more toxic than hAAG-2 when exposed to BCNU, both isoforms display a similar response at each dose. The induced sample is more sensitive than the uninduced sample. In this instance, the presence of induced glycosylase is worse for (hAAG-1) or equal to (hAAG-2) no glycosylase activity at all in the cell. hAAG-2 follows the same dose response as the bacterial mutant deficient in *uvr*A, showing that neither hAAG-2 nor bacterial *alk*A and *tag* glycosylase activities function without *uvr*A present. The wild type *E. coli*, proficient in all repair genes, has a survival level of about 2.5 orders of magnitude greater than the *uvr*A deficient mutant strains at the 3 mM dose.

The histidine tagged versions of hAAG-1 has a different effects than its non his-tagged counterpart when exposed to BCNU. hAAG-1-his_6 becomes slightly less sensitive than the non his-tagged version as the induced sample retains the sensitivity of

the *alk*A *tag uvr*A deficient triple mutant. hAAG-2-his_6 on the other hand becomes more sensitive than hAAG-2 by about 0.5 greater magnitude.

The data collected display a different result than those data published by the Samson laboratory involving the activity of AAG in a knockout mouse (Engleward et al, 1996, Engleward et al, 1998). Their data predicts that AAG is capable of repairing BCNU and Mitomycin C damage. Thus, there may either be an apparent difference between the mammalian and bacterial systems, a difference between the human and mouse genes, or a component may be missing in the bacterial system that is present in the mammalian system. This component may indeed be nucleotide excision repair function since hAAG enhances excision repair of Mitomycin C. However, to date, neither CNU nor BCNU have been tested to determine if hAAG proteins enhance their excision repair, and these experiments need to be performed.

MMC Survival Tests

The survival of hAAG-1 expressing cells upon exposure to Mitomycin C proved to be very interesting. Two strains were used in the MMC experiments, a double mutant deficient in *alk*A and *tag* and a triple mutant deficient in *alk*A, *tag*, and *uvr*A. The *uvr*A mutation was added to the double mutant strain because MMC damage is a substrate for nucleotide excision repair and that efficient repair by the bacterial excision system might mask a low level of repair by the hAAG proteins. The result that the loss of excision repair, as an effect of the *uvr*A mutation, greatly increases MMC sensitivity of the *alk*A *tag* strain (Figure 62), confirms a role for excision in the repair of MMC damage to DNA. Because hAAG knockout mouse cells are sensitive to MMC damage when compared to their hAAG + controls, Engleward et al suggested that mammalian glycosylases are able to repair crosslinks in DNA (Engleward et al, 1996). This conclusion predicts that hAAG-1 expression alone should increase resistance to MMC. This is not the case, since hAAG-1 does not increase MMC resistance of the *alk*A *tag uvr*A strain. In fact, a small, but reproducible increase in sensitivity is seen upon hAAG-1 expression. Interestingly, hAAG expression does increase MMC resistance in the excision repair proficient *alk*A

tag mutant strain (figure 57), suggesting both repair systems may be required. Thus, it is possible that hAAG-1 enhances excision repair by the bacterial *uvr*ABC excision system.

One model to explain this result is based on a similar phenomenon seen when photolyase is over expressed in excision proficient strains. This enzyme binds UV lesions in the dark but requires white light for activation of its repair activity. However binding of lesions by photolyase in the dark stimulates lesion recognition by *uvr*A protein and enhances repair and UV survival. As is the case with hAAG-1, this enhanced repair is seen only in *uvr*A+ strains and is abolished by *uvr* mutations (Sancar, 1994). Thus, hAAG may play a similar role and is itself unable to repair MMC damage, but may enhance excision repair of MMC lesions. Thus, hAAG-1 may not itself repair damage produced by complex alkylators such as MMC, BCNU, and CNU; however, it may be required for efficient repair by other repair systems. Alternatively, it is possible that hAAG does repair these lesions in mammalian cells, but that other cofactors, not present in *E. coli,* are required for this repair, or that the protein requires post-translational processing not functional in *E. coli* for this repair activity.

The base excision repair system assisting other repair systems model is speculative and more studies have to be performed to confirm it. The role of nucleotide excision repair is able to function as well as hAAG-1 in the *alk*A *tag* double mutant background. Thus, the role of excision repair is present in the absence of glycosylase to levels greater than wild type *E. coli* repair systems (Figure 55). Testing the non hAAG expressing *uvr*A strain shows great sensitivity relative to the proficient *uvr*A strain. Thus, *uvr*A is vital to the protection of *E. coli* from damage caused by Mitomycin C. While the nucleotide repair system is able to repair some of the damage created by Mitomycin C exposure, it is not able to rescue a large percentage of cells (Figure 62). For example, at 0.1 ug/ml of Mitomycin C exposure, the survival level of wild type cells is 53% while that of the *uvr*A deficient strain is 9.2%, roughly a half order of magnitude difference. Therefore, *uvr*ABC repairs some damage created by Mitomycin C exposure.

Another interesting aspect of the Mitomycin C curves was the toxicity of hAAG-2-his_6 at lower doses. The presence of glycosylase in these instances makes the cells more sensitive than those with no glycosylase activity at all (Figure 61). This suggests that the histidine tag effects the ability of the hAAG-2-his_6 protein to function.

It is interesting to observe the effect of Mitomycin C exposure on the 4 strains without a plasmid bearing hAAG. Surprisingly, the *alk*A *tag* deficient double mutant is more resistant than the wild type *E. coli* strain at 1ug/ml of Mitomycin C exposure. (Figure 62). At 2 ug/ml, these two strains are relatively similar in surivival level. This suggests that glycosylase activity is not involved in the repair of Mitomycin C lesions and in the absence of such activity, repair is slightly more efficient. This is further supported by the *uvr*A deficient strain and the *alk*A *tag uvr*A deficient triple mutant control. The most sensitive strain is the *uvr*A deficient strain. This strain has glycosylase activity in the form of the *alk*A and *tag* gene products. The *alk*A *tag uvr*A triple mutant is more resistant than the *uvr*A deficient strain at 1ug/ml Mitomycin C exposure, but is equally sensitive at 2ug/ml of exposure to Mitomycin C (Figure 62). These data suggest that the presence of glycosylase is toxic to cells in the absence of *uvr*A and that merely the presence of *uvr*A accounts for increased resistance to Mitomycin C exposure.

The relationship between Glycosylase activity and Nucleotide Excision Repair

It may be possible that nucleotide excision repair and glycosylase activity have a partnership. If these two systems jointly function, then the presence of glycosylase may effect the activity of nucleotide excision repair by providing it a substrate. Preliminary studies of hAAG-1 in the *alk*A *tag* double mutant background exposed to Mitomycin C show an increased resistance than that of hAAG-1 in the *alk*A *tag uvr*A triple mutant background. The only caveat is that initial experiments involving the *alk*A *tag* deficient mutant strain shows similar resistance. Therefore, the activity of hAAG-1 may not be important to the function of *uvr*A, but maybe simply the presence of *uvr*A is needed to repair lesions created by Mitomycin C damage as the absence of glycosylase activity and the presence of hAAG-1 have similar effects in the *uvr*A proficient strain. Since this data is in its preliminary stages, strong conclusions may not be made at this time. However, it is apparent that there is a relationship between glycosylase activity and nucleotide excision repair since hAAG functions at toxic levels when exposed to high doses of DNA damaging agents in the absence of *uvr*A.

Protein Analysis

At the current time, no progress has been made analyzing the hAAG protein products. However, once this data has been collected, we will be able to determine the level of protein produced by each his-tagged isoform of hAAG. Since the his-tagged versions of both hAAG-1 and hAAG-2 displayed very similar quantitative properties as their non his-tagged counterparts in the cell survival assays, we will assume that the protein production between the tagged and non-tagged versions of each isoform is relatively similar. One worry, however is the increase in toxicity that hAAG-2-his_6 displayed for the crosslinking agents with respect to hAAG-2. This toxicity may be directly due to the presence of the histidine tag. A modification or change may need to occur for hAAG-2 to function properly, and the histidine tag may prevent this change from taking place. This is unlikely, however, since hAAG-2-his_6 functions very similar to hAAG-2 when exposed to MNNG and MMS.

If the protein levels detected by the Western blot show a greater level of hAAG-1 product than hAAG-2, then it provides a possible explanation for the difference in methylation rescue from MNNG or MMS exposure.

Future Experiments

There are several experiments that can be conducted to provide additional information to this study. Many involve the relationship of base excision repair glycosylases such as hAAG, *alk*A, and *tag* to nucleotide excision repair mechanisms such as the *uvr*ABC system of *E. coli.* First, additional cell survival analysis to compare the survival levels of the *alk*A *tag* double mutant strains to exposure of BCNU, CNU, and Mitomycin C. Since BCNU and Mitomycin C are clinically used, understanding how glycosylase activity is involved in the repair process, if even at all, is important. Knowledge obtained from these cell survival assays may allow scientists to better understand the relationship of the two excision repair systems and how they affect the repair of certain drugs such as BCNU and Mitomycin C. Not only would doctors be able to use these treatments more efficiently, but the increased knowledge of these repair systems are valuable for molecular biologists.

Therefore, proposed experiments include testing the survival of hAAG-1 and hAAG-2 in the *alk*A *tag* background to exposure of CNU, BCNU, and Mitomycin C. It would also be interesting to observe if the toxicity of the hAAG-2-his_6 in the *uvr*A proficient background is maintained or rescued. By conducting these tests, we will learn more about the ability of glycosylase activity, of nucleotide excision repair, and of the DNA damaging agents.

The toxicity of induced hAAG at high doses of the nitrosoureas is also an interesting discovery. It would be curious to determine if this toxicity is due to the presence of the glycosylase, the absence of the *uvr*ABC system, or caused by increased base pairing mutations. Experiments to determine the mutational frequency at high concentrations of DNA damaging agent exposure may be an effort well worthwhile.

The differences between the two isoforms of hAAG may be consistent with exposure to DNA damaging agents. Experiments may be conducted in which induced versions of hAAG are exposed to DNA damaging agents for an extended period of time in order to observe if resistance is created over this period of time. For example, it is known that induced hAAG-1 exposed to 32 ug/ml of MNNG for 30 minutes has a survival level of about 13%. Similar to how the immune system combats an infection, (but without the use of antibodies), it may be possible that increased exposure to chemical agents allow the cell to increase their survival level. For example, if the cells are incubated for an extended period of time, possibly, as future replications occur, increased resistance to MNNG damage may also occur because one, or both, of the isoforms may protect the DNA from lesions formed by MNNG more efficiently in the presence of constant exposure to the chemical agent.

REFERENCES

Allan JM, et al. (1994) The use of purified DNA repair proteins to detect DNA damage. *Mutation Research* **313:** 165-174.

Allan, JM et al (1998) Mammalian 3-Methyladenine DNA Glycosylase Protects against the Toxicity and Clastogenicity of Certain Chemotherapeutic DNA Cross-Linking Agents. *Cancer Research* **58**: 3965-3973

Birboim, H. C. and Doly, J. (1979) A rapid alkaline lysis procedure for screening recombinant plasmid. DNA. *Nucleic. Acids Research.* **7**, 1513-1522.

Bodell, WJ. et al (1988) Differences in DNA Alkylation Products Formed in Sensitive and Resistant Human Glioma Cells Treated with N-(2-Chloroethyl)-N-nitrosourea. *Cancer Research* **48**: 4489-4492

Caradonna SJ, et al. (1982) DNA glycosylases. *Molecular and Cellular Biochemistry* **46:** 49-63

Cavard, D and C. Lazdunski (1990) Colicin Cleavage by OmpT Protease during Both Entry into and Release from *Escherichia coli* Cells *Journal of Bacteriology* **172**: 648-652

Chen et al (1994) The *Escherichia coli* AlkB Protein Protects Human Cells against Alkylation-Induced Toxicity *Journal of Bacteriology* **176:** 6255-6261.

Croteau et al (1999) Mitochondrial DNA repair pathways *Mutat Research* **434:** 137-148.

Cunningham RP. (1997) DNA glycosylases. *Mutation Research* **383:** 189-196.

Cuolotta, E and DE Koshland, Jr. (1994) DNA Repair Works Its Way to the Top *Science* **266:** 1926-1929.

Davis, L, Kuehl, M, and J Battey (1994) *Basic methods in molecular biology*. Appleton & Lange. **2,** 1-304.

Day, RS. III, et al. (1980) Defective repair of alkylated DNA by human tumour and SV40-transformed human cell strains. *Nature* **288**: 724-727

Dosanjh, M.K. et al (1994) 1,N^6-Ethenoadenine Is Preferred over 3-Methyladenine as Substrate by a Cloned Human N-Methylpurine-DNA Glycosylase (3-Methyladenine-DNA Glycosylase) *Biochemistry* **33**: 1624-1628

Ducore, JM. and BS. Rosenstein (1985) Theophylline release of replicon initiation inhibition by nitrosoureas correlates with the synergistic killing in L1210 leukemia in vitro. *Mutation Research* **146**: 1-8

Eisenbrand G et al (1986) DNA Adducts and DNA Damage by Antineoplastic and Carcinogenic N-nitrosocompounds. *Journal of Cancer Research and Clinical Oncology* **112(3):** 196-204.

Elder et al (1998) Alkylpurine-DNA-N-glycosylase Knockout Mice Show Increased Susceptibility to Induction of Mutations by Methyl Methanesulfonate. *Molecular and Cellular Biology* **18 (10):** 5828-37.

Engelward BP et al (1998) A Chemical and Genetic Approach Together Define the Biological Consequences of 3-Methyladenine Lesions in the Mammalian Genome*Journal of Biological Chemistry* **273:** 5412-5418.

Engelward, BP et al (1996) Repair-deficient 3-methyladenine DNA glycosylase homozygous mutant mouse cells have increased sensitivity to alkylation-induced chromosome damage and cell killing. *The EMBO Journal* **15**: 945-952

Engelward, BP et al (1997) Base excision repair deficient mice lacking the Aag alkyladenine *Proc. Natl. Acad. Sci. USA* **94**: 13087-13092

Engleward, BP et al. (1993) Cloning and characterization of a mouse 3-methyladenine/7-methylguanine/3-methylguanine DNA glycosylase cDNA whose gene maps to chromosome 11. *Carsinogenesis* **14**: 175-181

Erickson, LC. et al. (1980) DNA cross-linking and monoadduct repair in nitrosourea-treated human tumour cells. *Nature* **288**: 727-729

Friedberg EC, et al. (1981) The repair of DNA damage: recent developments and new insights. *Journal of Supramolecular Structure and Cellular Biochemistry* **16:** 91-103.

Friedberg EC et al (1995) DNA Repair and Mutagenesis. Washington DC: ASM Press.

Gichner and Veleminsky (1982) Genetic effects of the N-methyl-N'nitro-N-nitrosoguanidine and its homologs. *Mutational Research* **99:** 129-242.

Glassner et al (1998) Generation of a strong mutator penotype in yeast by imbalanced base excision repair *Proceedings of the National Academy of Science* **95:** 9997-10002.

Glassner et al (1998) The influence of DNA glycosylases on spontaneous mutation *Mutat Research* **400:** 33-44.

Gonzaga, PE. et al (1992) Identification of the Cross-Link between Human O^6-Methylguanine-DNA Methyltransferase and Chloroethylnitrosourea-treated DNA. *Cancer Research* **52**: 6052-6058

Goodman and Gilman (1996) *The Pharmacological Basis of Therapeutics,* 9th edition McGraw-Hill Co., New York

Green MO and Greenberg J (1960) The activity of nitrosoguanidines against ascites tumors in mice. *Cancer Research* **44:** 1166-1171.

Grossman L. (1981) Enzymes involved in the repair of damaged DNA. *Archives of Biochemistry and Biophysics* **211:** 511-522.

Grossman, L et al (1988) Repair of DNA-containing pyrimidine dimers *FASEB J* **2:** 2696-2701.

Hanawalt, PC. (1994) Transcription-Coupled Repair and Human Disease *Science* **266:** 1957-1958.

Hang, B. et al (1996)1,N^6-Ethenoadenine and 3,N^4-ethenocytosine are excised by separate human DNA glycosylases *Carcinogenesis* **17**: 155-157

Hang, B. et al (1997) Targeted deletion of alkylpurine-DNA-N-glycosylase in mice eliminates repair of 1,N^6-ethenoadenine and hypoxanthine but not of 3,N^4-ethenocytosine or 8-oxoguanine. *Proc. Natl. Acad. Sci. USA* **94**: 12869-12874

Henderson, TA. et al. (1994) Artifactual Processing of Penicillin-Binding Proteins 7 and 1b by the OmpT Protease of *Escherichia coli*. *Journal of Bacteriology* **176**:256-259

Holmquist GP (1998) Endogenous lesions, S-phase-independent spontaneous mutations, and evolutionary strategies for base excision repair. *Mutation Research* **400:** 59-168.

Izumi, T et al (1997) Molecular cloning and characterization of the promoter of the human N-methylpurine-DNA glycosylase (MPG) gene. *Carcinogenesis* **18**: 1837-1839

Jacobs et al (1998) Hypermutation of immunoglbulin genes in memory B cels of DNA repair-deficient mice *Journal of Experimental Medicine* **187:** 1735-1743.

Jeggo, P et al (1977) An adaptive response of E. coli to low levels of alkylating agent: comparison with previously characterized DNA repair pathways *Molecular General Genetics* **157**: 1-9.

Kacinski BM, et al. (1985) Repair of Haloethylnitrosourea-induced DNA Damage in Mutant and Adapted Bacteria. *Cancer Research* **December; 45 (12 Part 1):** 6471-4.

Kaufmann, A et al. (1994) New Outer Membrane-Associated Protease of *Escherichia coli* K-12. *Journal of Bacteriology* **176**: 359-367

Koshland, DE. Jr. (1994) Molecule of the Year: The DNA Repair Enzyme *Science* **266:** 1925.

Kow YW (1994) Base excision repair in *E. coli*: an overview. *Annual N Y Academy of Science* **726:** 178-180.

Krokan, HE. et al (1997) DNA glycosylase in the base excision repair of DNA. *Biochemistry. Journal* **325**: 1-16

Lau, AY. et al (1998) Crystal Structure of a Human Alkylbase-DNA Repair Enzyme Complexed to DNA: Mechanisms for Nucleotide Flipping and Base Excision. *Cell* **95**: 249-258

Laval J, et al (1998) Antimutagenic role of base-excision repair enzymes upon free radical-induced DNA damage. *Mutation Research* **402:** 93-102

Laval J. (1996) Role of DNA repair enxymes in the cellular resistance to oxidative stress. *Pathological Biology* **44:** 14-24.

Lewin B (1997) Genes VI. Oxford, England: Oxford Press

Lindahl, T (1976) New class of enzymes acting on damaged DNA *Nature* **259:** 64-66.

Lindahl, T (1979) DNA Glycosylases, Endonucleases for Apuric/Apyrimidinic Sites, and Base Excision Repair *Prog in Nucleic Acid Research Molecular Biology* **22:** 135-192.

Lindahl, T (1982) DNA Repair Enzymes *Annual Review of Biochemistry* **51**: 61-87.

Lindahl, T (1990) Repair of intrinic DNA lesions. *Mutation Research* **238:** 305-311.

Lloyd RS (1998) Base excision repair of cyclobutane pyrimidine dimers. *Mutation Research* **408:** 159-170

Loeb LA, et al. (1986) Mutagenesis by apurinic/apyrimidinic sites. *Annual Review of Genetics* **20:** 201-230.

Ludlum, D (1997) The Chloroethylnitrosoureas: Sensitivity and Resistance to Cancer Chemotherapy at the Molecular Level. *Cancer Investigation* **15 (6)**: 588-598

Ludlum, D (1997) Development of the Nitrosoureas *Cancer Therapeutics: Experimental and Clinical Agents.* New Jersey: B. Teicher Humana Press Inc. **Ch. 3:** 81-92.

Mackay et al (1994) DNA Alkylation Repair Limits Spontaneous Base Substitution Mutation in *Escherichia coli. Journal of Bacteriology* **176:** ***3324-3230.***

Matijasevic, Z et al. (1993) Protection against chloroethylnitrosourea cytotoxicity by eukaryotic 3-methyladenine DNA glycosylase. *Proceedings of the National Academy of Scientists, USA* **90**: 11855-11859.

Maze et al (1996) Increasing DNA repair methyltransferase levels via bone marrow stem cell transduction rescues mice from the toxic effects of 1,3-bis(2-chloroethyl)-1-nitrosourea, a chemotherapeutic alkylating agent *Proceedings of the National Academy of Scientists* **93:** 206-210.

Memisoglu, A and L Samson (1996) DNA Repair Function in Heterologous Cells. *Critical Reivews in Biochemistry and Molecular Biology* **31**: 405-447.

Mitra, S, et al. (1993) Regulation of repair of alkylation damage in mammalian genomes. *Prog Nucleic Acid Research Molecular Biology* **44:** 109-142.

Opperman, T et al (1999) A model for a *umu*DC-dependent prokaryotic DNA damage checkpoint. *The Proceedings of the National Academy of Science* **96:** 9218-9223.

Oren, M (1999) Regulation of the p53 Tumor Suppressor Protein. *The Journal of Biological Chemistry.* **274:** 36031-36034.

Pendlebury, A et. al (1994) Evidence for the simultaneous expression of alternatively spliced alkylpurine N-glycosylase transcripts in human tissues and cells. *Carcinogenesis* **15**: 2957-2960

Rangaswamy, V. et al (1998) Analysis of Genes Involved in Biosynthesis of Coronafacic Acid, the Polyketide Component of the Phytotoxin Coronatine. *Journal of Bacteriology*. **180**, 3330-3338.

Rauth, AM et al (1998) Bioreductive Therapies: an Overview of Drugs and Their Mechanisms of Action. *International Journal of Radiation Oncology Biological Physics* **42**(4): 755-762

Reuven, NB et al (1999) The Mutagenesis Protein UmuC Is a DNA Polymerase Activated by UmuD', RecA, and SSB and Is Specialized for Translesion Replication. *The Journal of Biological Chemistry* **274(45):** 31763-31766.

Roy, R et al. (1996) Distinct substrate preference of human and mouse N-methylpurine-DNA glycosylases. *Carcinogenesis* **17**: 2177-2182

Roy, R et al. (1998) Specific Interaction of Wild-Type and Truncated Mouse N-Methylpurine-DNA Glycosylase with Ethenoadeninie-Containing DNA. *Biochemistry* **37**: 580-589

Sakumi K, and M Sekiguchi. (1990) Structures and functions of DNA glycosylases. *Mutation Research* **236:** 161-172.

Samson L et al (1986) Suppression of human DNA alkylation-repair defects by *Escherichia coli* DNA-repair genes *Proceedings of the National Academy of Science* **83:** 5607-5610.

Samson L and J Cairns (1977) A new pathway for DNA repair in Escherichia coli. *Nature* **267:** 281-283.

Samson, L (1992) The repair of DNA alkylation damage by methytransferases and glycosylases *Essays Biochemistry* **27:** 69-78

Samson, L (1992) The suicidal DNA repair methyltransferases of microbes *Molecular Microbiology* **6**: 825-831.

Samson, L et. al (1991) Cloning and characterization of a 3-methyladenine DNA glycosylase cDNA from human cells whose gene maps to chromosome 16. *Proc. Natl. Acad. Sci. USA* **88:** 9127-9131

Sancar, A (1994) Mechanisms of DNA Excision Repair *Science* **266:** 1954-1956.

Saparbaev, M et al. (1995) *Escherichia coli*, *Saccharomyces cerevisiae*, rat and human 3-methyladenine DNA glycosylases repair 1,N^6-ethenoadenine when present in DNA. *Nucleic Acids Research* **23**: 3750-3755

Sedgwick, B (1989) In Vitro Proteolytic Cleavage of the *Escherichia coli* Ada Protein by the *omp*T Gene Product. *Journal of Bacteriology* **171**: 2249-2251

Sellers WR and DE Fisher (1999) Apoptosis and cancer drug treatment. *Journal of Clinical Investigation* **104:** 1655-1661.

Sheikh, MS and AJ Fornance, Jr. (2000) Role of p53 Family Members in Apoptosis. *Journal of Cellular Physiology* **182:** 171-181.

Silverman, RB. (1992) *The Organic Chemistry of Drug Design and Drug Action*, Academic Press, New York

Singer, B (1996) DNA Damage: Chemistry, Repair, and Mutagenic Potential. *Regulatory Toxicology and Pharmacology* **23**: 2-13

Singer, B and B. Hang (1997) What Structural Features Determine Repair Enzyme Specificity and Mechanism in Chemically Modified DNA? *Chemical Research in Toxicology* **10**: 713-732

Smith GJ and JW Grisham (1983) Cytotoxicity of monofunctional alkylating agents Methyl methanesulfonate and methyl-N'-nitro-N-nitrosoguanidine have different mechanisms of toxicity for 10T1/2 cells. *Mutational Research* **111(3):** 405-417.

Smith KC (1978) Multiple pathways of DNA repair and their possible roles in mutagenesis. *National Cancer Institute Monogram* **50:** 107-114.

Smith, MT. (1985) Quinones as Mutagens, Carcinogens, and Anticancer Agents: Introduciton and Overview *Journal of Toxicology and Enviromental Health* **16**: 665-672

Studier FW and BA. Moffatt (1986) Use of Bacteriophage T7 RNA Polymerase to Direct Selective High-level Expression of Cloned Genes. *Molecular Biology* **189:** 113-130.

Studier, et al (1990) Use of T7 RNA Polymerase to Direct Expression of Cloned Genes. *Methods in Enzymology* **185:** 60-89.

Sugimura and Higashi (1988) *Journal of Bacteriology***170**:3650-3654

Tang et al (1999) UmuD'$_2$C is an error-prone DNA polymerase, *Escherichia coli* pol V. *The Proceedings of the National Academy of Science* **96:** 8919-8924.

Tong WP et al (1982) Modifications of DNA by different haloethylnitrosoureas. *Cancer Research* **42:** 4460-4464.

Verly WG (1980) Prereplicative error-free DNA repair. *Biochemical Pharmacology* **29:** 977-982.

Verweij, J. et al, (1995) Antitumor antibiotics. *Cancer Chemotherapy: Principles and Practice*, 2nd edition J. B. Lippincott Co., Philadelphia.

Vickers, MA et al (1993) Structure of the human 3-methyladenine DNA glycosylase gene and localization close to the 16p telomere. *Proceedings of the National Academy of Science USA* **90**: 3437-3341

Voet and Voet (1995) Biochemistry. New York: John and Wiley Press.

Weinkam, RJ and ME Dolan (1983) An Analysis of 1-(2-Chloroethyl)-1-nitrosourea Activity at the Cellular Level. *Journal of Medicinal Chemistry* **26**: 1656-1659

White, CB et al. (1995) A Novel Activity of OmptT Proteolysis Under Extreme Denaturing Conditions. *Journal of Biological Chemistry* **270**: 12990-12994

Wilson, D III and LH. Thompson (1997) Life without DNA repair. *Proceedings of the National Academy of Science USA* **94**: 12754-12757

Wolffe et al (1999) DNA demethlation *Proceedings of the National Academy of Science* **96:** 5894-5896.

Wyatt et al (1999) 3-methyladenine DNA glycosylases: structure, function, and biological importance *Bioessays* **21.8:** 668-676.

Yu Z, et al. (1999) Human DNA repair systems: an overview. *Environmental and Molecular Mutagenesis* **33:** 3-20.

Zhao, GP and RL Somerville (1993) An Amino Acid Switch (Gly^{281} → Arg) within the "Hinge" Region of the Tryptophan Synthase B Subunit Creates a Novel Cleavage Site for the OmpT Protease and Selectively Diminishes Affinity toward a Specific Monoclonal Antibody. *The Journal of Biological Chemistry* **268**: 14912-14920